UNIVERSITÄT OSNABRÜCK

The role of the M_{2C} region of the K^+ translocating subunit KtrB of the Ktr system of *Vibrio alginolyticus*

Dissertation
zur Erlangung des Grades eines

Doctor rerum naturalium
(Dr. rer. nat.)

eingereicht am Fachbereich
Biologie / Chemie
der Universität Osnabrück

von
Inga Hänelt

Osnabrück, April 2010

„Der höchste Lohn für unsere Bemühungen ist nicht das, was wir dafür bekommen, sondern das, was wir dadurch werden."

John Ruskin

TABLE OF CONTENTS

PREFACE

This work was financially supported by the Deutsche Forschungsgemeinschaft (SFB431: “Membranproteine: Funktionelle Dynamik und Kopplung an Reaktionsketten“ (Teilprojekt P6). Collaborations with the research groups of Prof. Dr. Heinz-Jürgen Steinhoff (Department of Physics, University of Osnabrück) and of Prof. Dr. Bert Poolman (Department of Biochemistry, University of Groningen, The Netherlands) contributed to the success of this thesis.

The results are presented in three chapters. Chapter 2 reveals results which served as preparations for the research of chapters 3 and 4. Chapter 3 has already been published (Hänelt et al. 2010). The fourth chapter is currently in preparation for publication. These three chapters represent the results of this thesis, which provides new insights into the structural and functional role of subregion M_{2C2} of the KtrB subunit of the Ktr system of *Vibrio alginolyticus.*

ABBREVIATIONS

Amp	ampicillin
A_X	absorbance at a certain wavelength X
Cam	chloramphenicol
CMC	critical micelle concentration
cw	continuous wave
DDM	β-D-dodecylmaltoside
DEER	double electron electron resonance
dry wt	dry weight
EPR	electron paramagnetic resonance
Ery	erythromycin
GFP	green fluorescence protein
His_{10}-KtrA	KtrA with a tenfold N-terminal his-tag
His_{10}-KtrAB	KtrAB with a tenfold his-tag N-terminal of KtrA
K	Kelvin
Kan	kanamycin
kDa	kilo dalton
KTN	K^+ transport nucleotide binding
KtrB-His_6	KtrB with a six-fold C-terminal his-tag
LS	light scattering
M_W	molecular weight
MTSSL	(1-oxyl-2,2,5,5-tetramethylpyrroline-3-methyl) methanethiosulfonate spin label
ND	not determined
NMG	N-methyl-D-glucamine
OD_X	optical density at a certain wavelength X
PhoA	alkaline phosphatase
R1	spin-labeled residue
RCK	regulation of K^+ channel (activity)
RI	refractive index
SEC	size exclusion chromatography
SKT	superfamily of K^+ transporters
*Va*KtrB	KtrB of *Vibrio alginolyticus*
WT-KtrB	wildtype KtrB
X^R	antibiotic resistance against X

S

SUMMARY

Summary

The Na^+-dependent high affinity K^+-transport system Ktr from the bacterium *Vibrio alginolyticus* consists of two types of subunits. The membrane-associated, regulatory subunit KtrA, which is supposed to be regulated by the binding of ATP, confers velocity, Na^+-dependency, and cation selectivity to the system. The KtrB subunit transports K^+ but looses transport velocity and Na^+-dependence in the absence of KtrA. This observation, however, indicates that KtrB remains actively folded even when KtrA is absent. In addition, it transports also sodium but with a lower affinity than that for potassium. KtrB is a member of the superfamily of K^+ transporters (SKT), which are proposed to have evolved by multiple gene duplication and gene fusion from simple KcsA-like potassium channels. Since the crystal structure of KcsA is well known, it can serve as a reasonable model for structural predictions of SKT proteins in general. The main structure of KcsA as well as that of the SKT proteins consists of four M_1PM_2 motifs. M_1 and M_2 are transmembrane stretches and P indicates a P-loop that folds halfway back into the membrane and contains the potassium selectivity filter. However, whereas KcsA is formed by four identical, individual subunits, the four M_1PM_2 motifs of the SKT proteins are covalently linked via cytoplasmic loops and differ in their amino acid sequences. In KtrB, especially helix M_{2C} shows a strikingly different amino acid sequence compared to KcsA. While the first (M_{2C1}) and the third (M_{2C3}) part of this helix can be modeled as α-helices, M_{2C2} with its small and polar amino acids rather forms a random coil or β-turn structure. According to these structural predictions, two models of KtrB have been proposed. In the first model, M_{2C1} and M_{2C3} span the membrane as α-helices, while M_{2C2} forms a loop that fills the cavity just beneath the selectivity filter. In the second model, M_{2C1} and M_{2C2} span the membrane with M_{2C2} adopting a coiled conformation. According to its partial amphipathic character M_{2C3} lies on the inner surface of the membrane. However, so far neither model has been experimentally confirmed. Initial PhoA fusion studies on M_{2C}, which were performed in order to analyze the orientation of single amino acids point towards a flexible structure of M_{2C2}. Other data appeared to argue in favor of the second structural model.

Chapter III and IV of this thesis highlight the role of M_{2C2}, whereas chapter III mainly concentrates on its function and chapter IV on its structure. In the context of the analysis of the role of M_{2C2} in purified and reconstituted KtrB by biophysical and biochemical approaches, chapter II describes a protocol for the overproduction, purification and reconstitution of natively folded, active protein. In addition, results obtained from static light scattering measurements are shown in order to gain information about the oligomeric state of the single subunits as well as of the assembled KtrAB complex. A short outlook completes this thesis.

Based on existing overproduction and purification protocols a procedure was established, to ensure the activity of KtrB at the different purification steps. The activity of KtrB during its overproduction was guaranteed by using *Escherichia coli* strain LB2003, which is defective in its endogenous potassium uptake systems. Since the strain was shown to grow at low potassium concentrations in the presence of KtrB, the protein must have been synthesized in an active form. After membrane preparation, $^{86}Rb^+$ uptake into membrane vesicles further demonstrated the function of KtrB. The solubilized, His-tagged KtrB subunit was isolated via affinity and size exclusion chromatography to homogeneity. Subsequently, the protein was reconstituted into liposomes. Finally, an $^{86}Rb^+$-influx assay proved the activity of KtrB in proteoliposomes.

The stoichiometry of KtrA, KtrB and KtrAB was analyzed by static light scattering measurements on purified proteins. KtrA was found to form an octamer whereas detergent-solubilized KtrB occurred as a dimer. These findings are in accord with former data. In contrast, for solubilized KtrAB, a still preliminary 16:2 composition was estimated from the light scattering analyses. This result is contradictory

to a previously proposed 8:2 stoichiometry, raising doubt on the latter conclusion.

In order to investigate the function of subregion M_{2C2}, extensive point and deletion mutations have been carried out. The effect of these exchanges and deletions was analyzed by complementation studies as well as by potassium and sodium uptake assays into *E. coli* strains LB2003 and TO114. Several point mutations as well as partial to complete deletions led to increased V_{max} values for K^+ uptake via KtrB. The affinity for potassium was found to be decreased only for some deletion variants. Sodium uptake was increased for at least deletion variant $KtrB_{\Delta 326\text{-}328}$ but was uneffected by all point mutations. By the expression of *ktrAB*, the presence of KtrA did not suppress any of these gain of function effects in corresponding experiments. However, for some deletion variants the binding of KtrA to KtrB was found to be diminished as shown by Ni^{2+}-NTA affinity chromatography. Extended PhoA studies confirmed former suggestions that M_{2C2} forms a flexible structure within the membrane, thus allowing M_{2C3} to be directed either to the cytoplasm or (artificially) to the periplasm. These data were interpreted to mean that M_{2C2} forms a flexible gate controlling K^+ translocation at the cytoplasmic side of KtrB. In addition, M_{2C2} was shown to be required for the interaction between KtrA and KtrB.

The gain of function effects of the mutations in M_{2C2} raised further question concerning the structure of this region. In order to obtain such information, continuous wave and pulsed EPR measurements on reconstituted, spin-labeled single and double cysteine mutants were performed. The activity of spin-labeled KtrB mutants was shown with an $^{86}Rb^+$-influx assay with proteoliposomes. From the analysis of side chain mobility and polarity of singly labeled residues, region M_{2C2} could be modeled as a flexible loop positioned in the cavity of the protein. Distance measurements of double labeled proteins in the presence and absence of potassium displayed conformational changes in region M_{2C2}. By summarizing all distances obtained and by performing rotamer library analyses two structural models of KtrB in an open and a closed conformation are proposed. The already existing models of KtrB could be excluded by these modelings. In the open conformation, M_{2C2} is oriented alongside the cavity, while it blocks the cavity in the closed conformation. We propose a downward movement of the linker region M_{2C2} in the presence of potassium, thus enabling its passage through the KtrB protein. Since such a flexible gate is missing in the KcsA potassium channel, this sorting mechanism is interpreted as a transporter-specific feature.

Chapter I

I

GENERAL INTRODUCTION

GENERAL INTRODUCTION

I. Hänelt
Department of Microbiology, University of Osnabrück

The role of potassium in prokaryotes

Potassium is the prevalent cellular cation in all kingdoms of life. It plays a central role in osmoregulation (1-3) and pH homeostasis (4). In addition, cytoplasmic K^+ is required for the activation of some enzymes (5). Thus, the controlled accumulation of K^+ in the cytoplasm is of major importance for the cell physiology under different conditions. In prokaryotes the uptake and release of K^+ occurs via channels, pumps and transporters (1;6). In *Escherichia coli* the first response to changes in external osmolality is water movement across the cell membrane, followed by uptake or release of potassium. Upon an increase in external molality the intracellular concentration of K^+ rises from 200-500 mM up to a molar range and, thus, reverses water efflux (3;7;8). Concomitantly, organic anions like glutamate are synthesized in order to counterbalance K^+ in the cells. Since high concentrations of K^+-glutamate inhibit enzyme activity, compatible solutes like the zwitterionic proline, glycine or betaine as well as uncharged carbohydrates like trehalose are synthesized or accumulated in a second response. Under these conditions K^+ is again excreted from the cells and glutamate is degraded (3). A decrease in external osmolality causes a complete loss of K^+-glutamate and trehalose from the cells. The efflux of potassium occurs via mechanosensitive channels (4;9). It is not yet known why potassium is the main osmolyte in the cell and why it is preferred above Na^+ in this function. In bacteria, K^+ might modulate the activity and correct folding of some enzymes better than Na^+. Another explanation for the accumulation of K^+ and the concommittant active extrusion of Na^+ is that this situation enables the cells to develop an inwardly directed electrochemical transmembrane Na^+ gradient. This gradient can then be used for energy-consuming processes like secondary transport or flagella movement (10). As mentioned above potassium is also involved in pH and pmf homeostasis. Upon cytoplasmic acidification, internal pH is increased by an active, electrogenic K^+ or Na^+ uptake coupled to the antiport of H^+ out of the cell. The same principle applies vice versa. K^+/H^+- and Na^+/H^+ antiporters in combination with ion channels and transporters are held responsible for this regulatory function (4;11).

The superfamily of K^+ transporters

Several potassium transporters/ symporters involved in the uptake of K^+ belong to a superfamily of potassium transporters (termed SKT proteins) (12;13). This enzyme family includes the potassium-translocating subunits of the Trk (1), Ktr (14;15) and Kdp (12) systems from prokaryotes, Trk1,2 from fungi (16;17) and HKT1,2 from plants (18;19) (Fig. 1). In a recent publication a Trk/HKT-type K^+ transporter was also described for *Trypanosoma brucei*, a member of eukaryotic kinetoplastids (20). In addition, a phylogenetic tree of a representative selection of so far identified or hypothesized

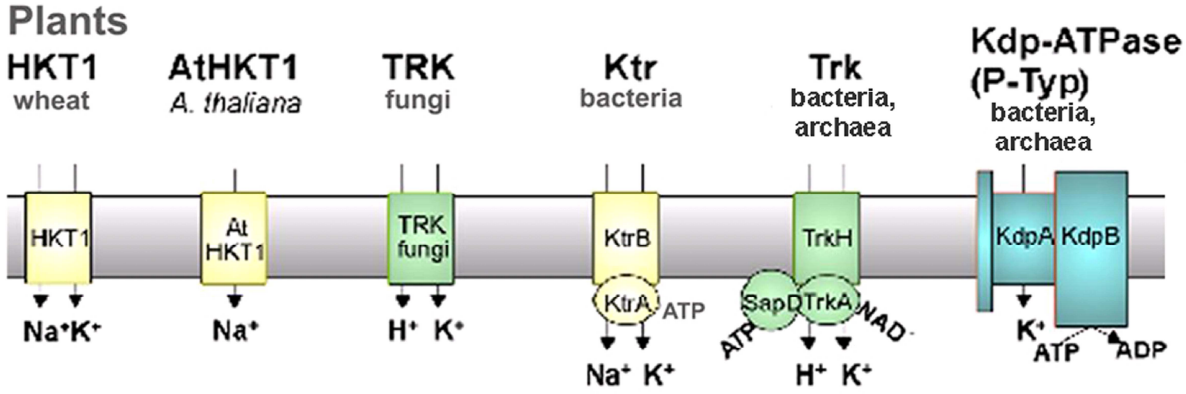

Figure 1. **Overview of the SKT protein superfamily.** Similar transport systems are given the following colors: yellow= sodium-dependent, green= proton-dependent, blue= P-type ATPase (according to Durell et al., 1999 (12); Durell et al., 2000 (13) and Tholema, 2002 (43), figure taken from (43)).

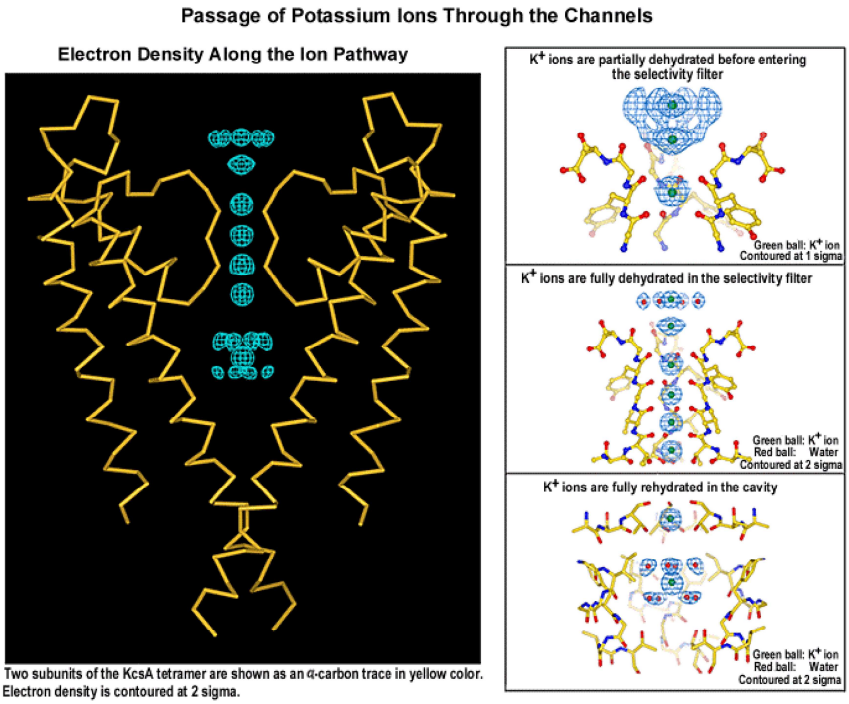

Figure 2. **KcsA crystal structure of *Streptomyces lividans*.** Left: cross-section comprising two subunits of the KcsA tetramer, right: passage of a potassium ion through the selectivity filter with its dehydration and rehydration steps. Figure taken from http://www.hhmi.org/research/investigators/mackinnon.html, image by Yufeng Zhou, HHMI, Chevy Chase according to Zhou et al. (26).

SKT proteins (appendix, figure 1) proposes further eukaryotic members from kinetoplastids, *Entamoeba*, cellular slime molds and cercozoans. All SKT proteins contain four M_1PM_2 motifs, in which M_1 and M_2 designate transmembrane helices and P stands for a P-loop, which folds back from the external side into the cell membrane and connects M_1 with M_2 (12;13;21-23). It is hypothesized that all these proteins have evolved from simple K^+-channels of the M_1PM_2 type, like KcsA or Kir, by means of gene duplication and gene fusion events (13). In 1998, the crystal structure of the KcsA channel of *Streptomyces lividans* was solved. This structure has provided major insights in the molecular function of K^+ channels (24) and as a template it allows the prediction of the structures of SKT proteins.

The KcsA channel of *S. lividans* is formed by a tetramer of four identical 18 kDa M_1PM_2 subunits. The central pore is formed by the four pore (P) loops, which comprise the K^+ selectivity filter with the highly conserved sequence TVGYG (25). This filter contains four binding sites for dehydrated potassium ions. In each binding site eight carbonyl oxygen atoms serve as binding partner for the K^+ ion (Fig. 2). During the channeling process, only positions 1 and 3 or positions 2 and 4 are occupied by K^+ simultaneously. In the cavity just below the selectivity filter, the potassium ion becomes rehydrated with eight water molecules and finally enters the cytoplasm (26). In a recent publication (27), crystal structures of the KcsA channel were shown in both, an open and a closed state. It reveals that upon the transition from the close to the open state the selectivity filter undergoes only small changes, whereas the C-terminal helix bundle on the cytoplasmic side of the channel opens considerably (27;28).

Compared to KcsA, the SKT members show several striking differences. First, four non-identical M_1PM_2 domains are covalently linked via cytoplasmic loops of different length and sequence. They are designated as MPM_A, MPM_B, MPM_C and MPM_D, respectively (13;23). Secondly, the selectivity filter sequences of SKT proteins are less conserved. In most transporters the selectivity filter is formed by only a single glycine residue in each P-loop (14;29-31). In KdpA, the K^+ translocating subunit of the P-type-ATPase KdpFABC, there is a glutamine instead of the glycine in P_A (22). However, this change does not alter the ion selectivity of Kdp. In contrast, in plant HKT1 a serine substitution in P_A is held responsible for a change in ion selectivity from potassium to sodium (18;19). Finally, compared to KcsA, the various MPM sequences have changed to different extents. By use of extensive sequence alignments, an evolutionary relationship between K^+ channels and different SKT proteins has been predicted ((12;13); Fig. 3). KtrB, the K^+-translocating subunit of the Ktr system, is most closely related to simple MPM channels, but especially M_{2C} and M_{2D} differ considerably from M_2 in KcsA. In

addition to the potassium-translocating subunits, the prokaryotic systems Ktr, Trk, and Kdp contain at least one regulatory subunit. The ATP-binding KtrA subunit of the Ktr system (32-34) may have evolved by the seperation of a dinucleotide binding domain of a K^+ channel ancestor (13). Such a domain is absent in most eukaryotic and some prokaryotic K^+ channels (like KcsA) but is present in several others like in some 6TM type K^+ channels, e.g. Kch from *E. coli* (35) or the 2TM K^+ channel MthK from *Methanobacterium thermoautotrophicum* (36; see below). TrkH proteins contain two additional transmembrane helices at their N-terminus and also differ with several other respects (37). However, regions M_{2C} and M_{2D} are quite similar to KtrB, thus TrkH might have evolved from KtrB. The regulatory NAD^+/NADH-binding bacterial subunit TrkA (1;32;35) also could have originated from a covalently linked nucleotid binding domain but probably underwent subsequent internal gene duplication. The Trk1,2 family of fungi has diverged more, displaying an extensive cytoplasmic loop between MPM_A and MPM_B and a smaller linker-like insert between MPM_C and MPM_D (13). HKT1,2 from plants is slightly closer related to Trk1,2 than to KtrB. None of the eukaryotic symporters comprises a yet known regulatory, dinucleotide-binding subunit. In addition, these symporters are lacking an extension of small and polar amino acids in membrane region M_{2C} (13). The KdpA proteins differ the most from all other proteins. They comprise two additional transmembrane regions, each one flanking the four consecutive MPM-motifs. However, a high degree of conservation exists within the KdpA sub-family, even between members from bacteria and archaea (12;38).

Despite of all the differences between the different sub-families of SKT proteins, the middle part of the M_{2C} region from KdpA, KtrB and TrkH all contain a number of small, partially polar residues, like A, G, S, and T. Usually, these residues occur in random coil structures. The regions may have evolved independently of each other but may have the same function. The absence of such regions in eukaryotic SKT proteins suggests that this structure is not essential for the K^+ transport process itself (12;13;23). An alignment of M_{2C} regions of different SKT proteins is shown in the appendix, figure 2 to clarify the differences between the several sub-families. Since the M_{2C} region with its small and polar amino acids is only present in systems containing additional regulatory subunits, Durell and Guy proposed that this region might be important for subunit interaction (12).

In contrast, positively charged amino acids in M_{2D} are present in all transporters/ symporters. An arginine residue is the most conserved charged residue among all SKT proteins. It is proposed to function as an energy barrier to prevent the free diffusion of K^+ ions through the

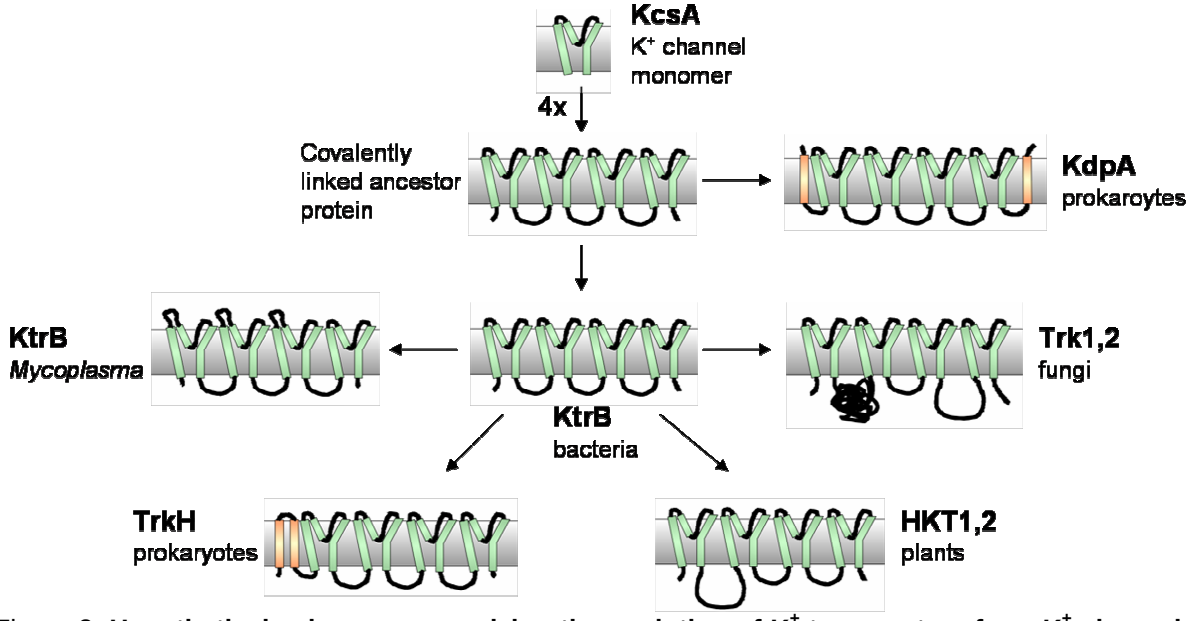

Figure 3. **Hypothetical scheme summarizing the evolution of K^+ transporters from K^+ channels.** According to Durell et al, 1999 and 2000 (12,13), modified from Tholema, 2002 (47). The scheme shows the development of K^+ transporters from K^+ channels like KcsA by gene duplication and fusion events. Transmembrane helices coloured in orange have developed independently of the fourfold M_1PM_2 motif (green).

pore (23). For plant HKT, fungal Trk and bacterial KtrB these positively charged residues are essential for transport activity (39).

The role and regulation of K^+ in *Vibrio alginolyticus*

V. alginolyticus is a Gram-negative, marine organism of the family of Vibrionaceae, which belong to the class of Gammaproteobacteria (40). Vibrionaceae are mobile rods, mesophilic and chemoorganotroph. Best known is the human pathogen *V. cholera*, but also *V. alginolyticus* as a weak human pathogen is of special interest. As a fish and seafood spoiler it is causing major problems in fishing industry (41;42). In addition, *V. alginolyticus* is important in biotechnology where it is used for the production of proteolytic enzymes, antibiotics and proteases.

As all other microorganisms, *Vibrio* needs to react rapidly upon any changes in the environment with respect to nutrient, temperature, oxygen, osmolality and pH. For osmoadaptation and pH homeostasis the regulation of internal K^+ is important. *V. alginolyticus* possesses two systems for K^+ uptake and several for K^+-efflux. The first uptake system, a Trk system, is constitutive and possesses a low affinity for potassium (K_m= 3 mM) (32;43). The second system, KtrAB, shows a higher affinity (K_m= 0.3 mM), and its synthesis is induced only if necessary (32). Together with a less well defined K^+/H^+-antiporter these systems keep the cytoplasmic pH stable at 7.8 at external pH values between 6 and 9 (44). In addition, *Vibrio* can generate an electrochemical Na^+ gradient by combining the activity of a Na^+/H^+-antiporter (44;45) with that of the sodium-pumping NADH/ coenzyme Q reductase (46). This Na^+ gradient enables Na^+-dependent proton transport under alkaline conditions, a condition at which it is hard to establish a proton gradient. A steady proton gradient is important for flagella rotation and amino acid uptake in cotransport with Na^+. As described in section 1.1. for *E. coli*, K^+ is transported into the cell via the Trk and Ktr systems in rapid response to an increase in external osmolality and it is excreted via mechanosensitive channels upon a decrease in external osmolality.

The KtrAB system

The KtrAB system of *V. alginolyticus* was first described by Nakamura et al. in 1998. Its genes are arranged on the chromosome in the order *ktrA, ktrB* and overlap by one nucleotide. The Ktr system was functionally cloned and expressed in *E. coli*. In this bacterium it is constitutive and exhibits K^+ transport activity with a K_m value of 25 µM and a V_{max} of 200 $nmol.min^{-1}.mg^{-1}$ dry wt (47). In addition, it depends on the presence of sodium ions. It is not yet known whether the two cations are symported or Na^+ only acts as an activating ligand for KtrB. KtrB alone was functionally expressed in *E. coli*, but thereby lost its sodium dependency, transport velocity (by factor of 100) and ion specificity (transport of Na^+ as well). However, its affinity for K^+ was not altered.

The KtrA subunit

The membrane-associated, cytoplasmic subunit KtrA is the regulatory component of the Ktr system, has a molecular weight of 28 kDa, and contains a nucleotide binding site as already mentioned in a previous section. This binding site is formed by the so called "Rossman fold" comprising the conserved, glycine-rich sequence GxGxxG...(D/E) at its N-terminal β-α-domain (1;35;48;49). Due to this structural motif, KtrA is assigned as family member of the KTN ($\underline{K}^+$ transport nucleotide binding)/RCK (("regulation of $\underline{K}^+$ channel (activity)") proteins, which regulate the activity of K^+ transporters and channels by ligand binding (6;50-53). A well-studied protein containing an RCK domain is the K^+ channel MthK of *Methanobacterium thermoautotrophicum*. Its RCK domains form an octameric gating ring regulated by the binding of Ca^{2+} (50;54). Based on crystal structures of a truncated KtrA dimer from *Bacillus subtilis* with bound NADH and a truncated homogeneous TrkA dimer from *M. jannaschii* in complex with NAD^+, Roosild et al. (2002) proposed a dinucleotide-binding dependent conformational switch mechanism for KtrA, which regulates the K^+-transport activity of KtrB. Subsequently, others have shown that ATP binds with a much higher affinity to KtrA than do NAD^+ or NADH. Nevertheless, these studies supported the notion that conformational changes occur upon the binding of different nucleotides to KtrA (33;34). Crystal structures of KtrA displayed an octameric ring-like assembly comparable to that of MthK. Although different conformations with different bound nucleotides have been elucidated, the precise mechanism has not yet been identified due to potentially artificial nucleotid binding. However, Albright et al. (34) hypothesized an inactive conformation with bound NADH and an active conformation with ATP. The conformational switch in the octameric

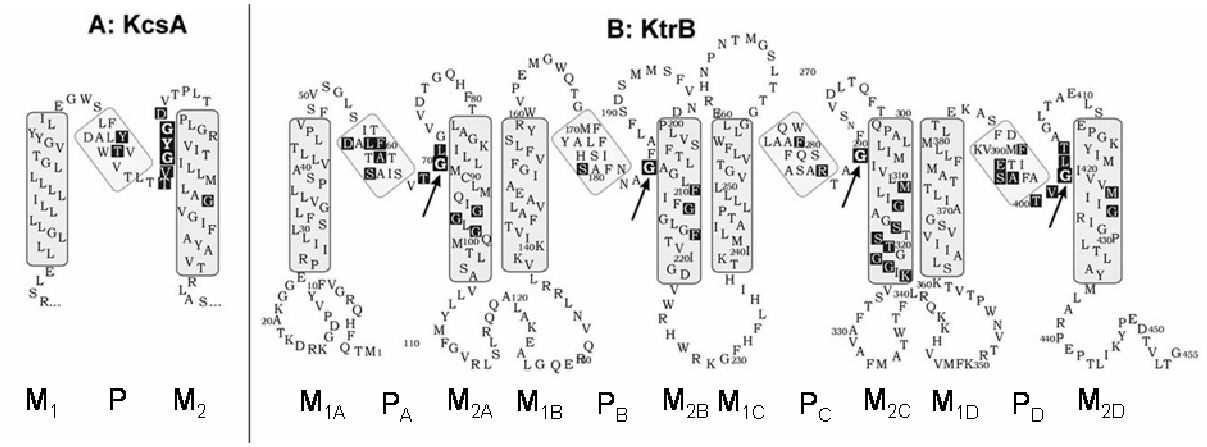

Figure 4**. Model of the secondary structure of the M_1PM_2 domain of KcsA (A) and the covalently linked KtrB tetramer from *Vibrio alginolyticus* (B).** Conserved residues in white on black, transmembrane helices in grey boxes, putative P-loop helices in light grey boxes, glycines forming the selectivity filter marked with arrows. Taken from Tholema et al, 2005 (29).

KtrA ring might cause an opening of KtrB by the movement of its cytoplasmic loops. In addition, Kröning et al. (33) demonstrated that ATP promotes the binding of KtrA to KtrB and that beside ATP a membrane potential is essential for transport activity of the KtrAB system.

The KtrB subunit

As mentioned above, the membrane-embedded, K^+-translocating subunit KtrB is a member of the superfamily of K^+ transporters, consisting of a fourfold MPM motif. A 2-D folding model of *Vibrio alginolyticus* KtrB (*Va*KtrB) is shown in figure 4 along with the 2-D model of KcsA. The simplified selectivity filter of *V. alginolyticus* comprising only one glycine residue per p-loop is highlighted by arrows. By use of site-directed mutagenesis it has been shown that these glycines are important for cation selectivity. An exchange of only one glycine residue for serine leads to Na^+ transport activity of the resulting KtrAB system (14;29), a situation, which is similar to that of the G/S exchange in p-loop A of plant HKT proteins. Recently, some additional conserved residues within the P-loop regions have been identified to be involved in K^+ transport activity. Mutagenesis of a conserved histidine residue in the α-helix of P_B of *Synechocystis* spec. KtrB PC6803 caused a decrease in V_{max} by a factor of 5-10 and an increase in K_m by a factor of 25 (55). This conserved histidine residue corresponds to residue H176 in *Va*KtrB. In figure 4, the structure of KtrB was modeled according to that of KcsA (24). However, M_{2C} and M_{2D} showed a striking amino acid sequence (13;23). In general, the topology of the stretches of residues appending motifs B to D was confirmed by PhoA-fusion experiments (56). However, PhoA fusions put behind residues within M_{2C2} suggested an abnormal flexibility of this region (56, see below). Region M_{2D} exhibits some specific signature sequences. Motif MxxGR in the middle of the membrane is highly conserved among all members of the superfamily and its arginine (*Va*KtrB position 427) only can be replaced by lysine without loss of function in *Synechocystis* KtrB (39). This residue may form a salt bridge with the glutamate in p-loop P_D (*Va*KtrB position 393). Finally, sub-family KtrB can easily be distinguished from the very similar sub-family TrkH by its signal sequence GRIG in the middle of M_{2D} in contrast to GRIE in TrkH (12).

The potassium channels KscA, Kir, and MthK with its covalently linked RCK domains were shown to form a single K^+ pore composed of four identical M_1PM_2 subunits. By contrast, both in the plasma membrane as well as in a detergent-solubilized, purified form KtrB forms dimers composed of a total of eight M_1PM_2 domains. By the use of crosslinkers with different lengths, M_{1B} and M_{2C} were identified to be located near the dimer twofold axis, thereby forming the dimer contact site. Also the C-terminal 10 amino acids were shown to be critical for both dimerization and transport activity, implicating that dimer formation is essential for the function of KtrB. Based upon results obtained from size exclusion chromatography combined with static light scattering measurements of a KtrAB complex, it has been concluded that one KtrB dimer binds to an octameric KtrA ring (34). Furthermore, the authors (57) concluded from crosslinking studies that the extracellular half of the KtrB monomer

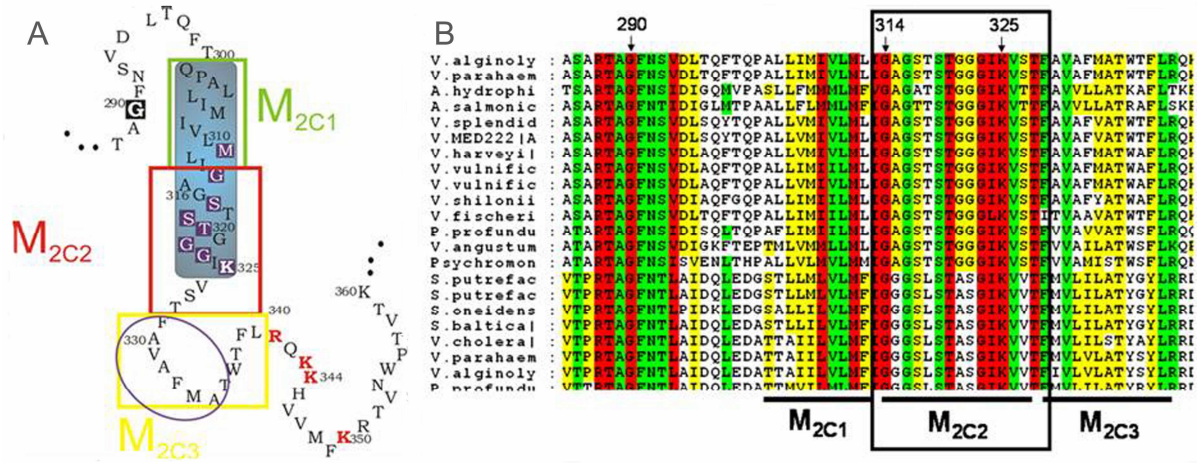

Figure 5. **Region M_{2C} of VaKtrB. A**: Schematic representation of how M_{2C} is supposed to fold across the membrane according to (29) (subdivision of M_{2C} into regions M_{2C1} to M_{2C3}); **B**, conserved residues in regions P_C and M_{2C2}. Increasing degree of conservation of single residues is indicated by the background color changing from white via yellow and green to red. The absolutely conserved *Va*KtrB residues G290 [selectivity-filter residue (23;29)], G314, and K325 (both M_{2C2} residues) are marked by arrows.

strongly resembles that of the KcsA tetramer, whereas the cytoplasmic halfs differ considerably. In order to demonstrate the activity of purified dimeric KtrB, the protein was reconstituted and the uptake of radioactive rubidium by potassium-loaded proteoliposomes was measured. The very slow uptake detected was interpreted as channel-like activity of KtrB solely driven by an electrochemical gradient. This result confirmed that reconstituted KtrB exhibits some transport activity.

Membrane region M_{2C} of KtrB

As already briefly mentioned, M_{2C} in KtrB exhibits a striking amino acid sequence in the middle of the putative membrane spanning part comprising many small and polar residues (A, G and S,T,K, respectively). This region is highly conserved among the KtrB family (see alignment, Fig. 5B) and, thus, should be of functional importance as discussed above. Durell and Guy (23) concluded that the structure of this region is hard to predict since many conformations are possible. However, they proposed two different conformational models for this segment. M_{2C} was divided into three subregions: M_{2C1}, M_{2C2} and M_{2C3} (see Fig. 5A). While M_{2C1} and M_{2C3} could be modeled as α-helices, the amino acid sequence of M_{2C2} points to random-coil and/or β-turn conformation. According to the first model, M_{2C1} and M_{2C3} span the membrane as α-helices with the C-terminus of M_{2C1} and the N-terminus of M_{2C3} in close proximity to each other while M_{2C2} is modeled as a loop that fills the cavity located just below the P-loops (Fig. 6, C and D). In the second conformation, M_{2C1} and M_{2C2} span the membrane with the latter in a coiled conformation. M_{2C3} lies on the inner surface of the membrane (Fig. 6, A and B). This is conceivable since M_{2C3} consists of seven apolar amino acids with an amphipathic character. In addition, this part is too short to form an additional membrane-spanning domain. However, in both conformations a lysine in M_{2C2} forms a putative salt bridge with an aspartate in M_{2B}. Durell and Guy (23) further hypothesized that an interaction with the regulatory KtrA subunit or the transport mechanism itself modulates a transition between the two models described. This transition might affect the opening and closing of the central ion pore. Finally it was discussed that even a protein deleted in M_{2C2} could be functional, thereby resulting in a constitutively active symporter or channel. Results of PhoA fusion studies supported the idea of a flexible nature of M_{2C2} (56;58). Accessibility studies by use of single cysteine mutants supported the second model and, thus, the amphipathic character of M_{2C3}. However, EPR data of spin-labeled residues collected so far did not confirm this notion, since all residues investigated were very immobile and most likely buried inside the protein. Only the exchanged residue T300C was located on the helix surface (56).

Aim of this thesis

The assumption that SKT proteins have evolved from simple KcsA-like potassium channels and that they consist of a fourfold

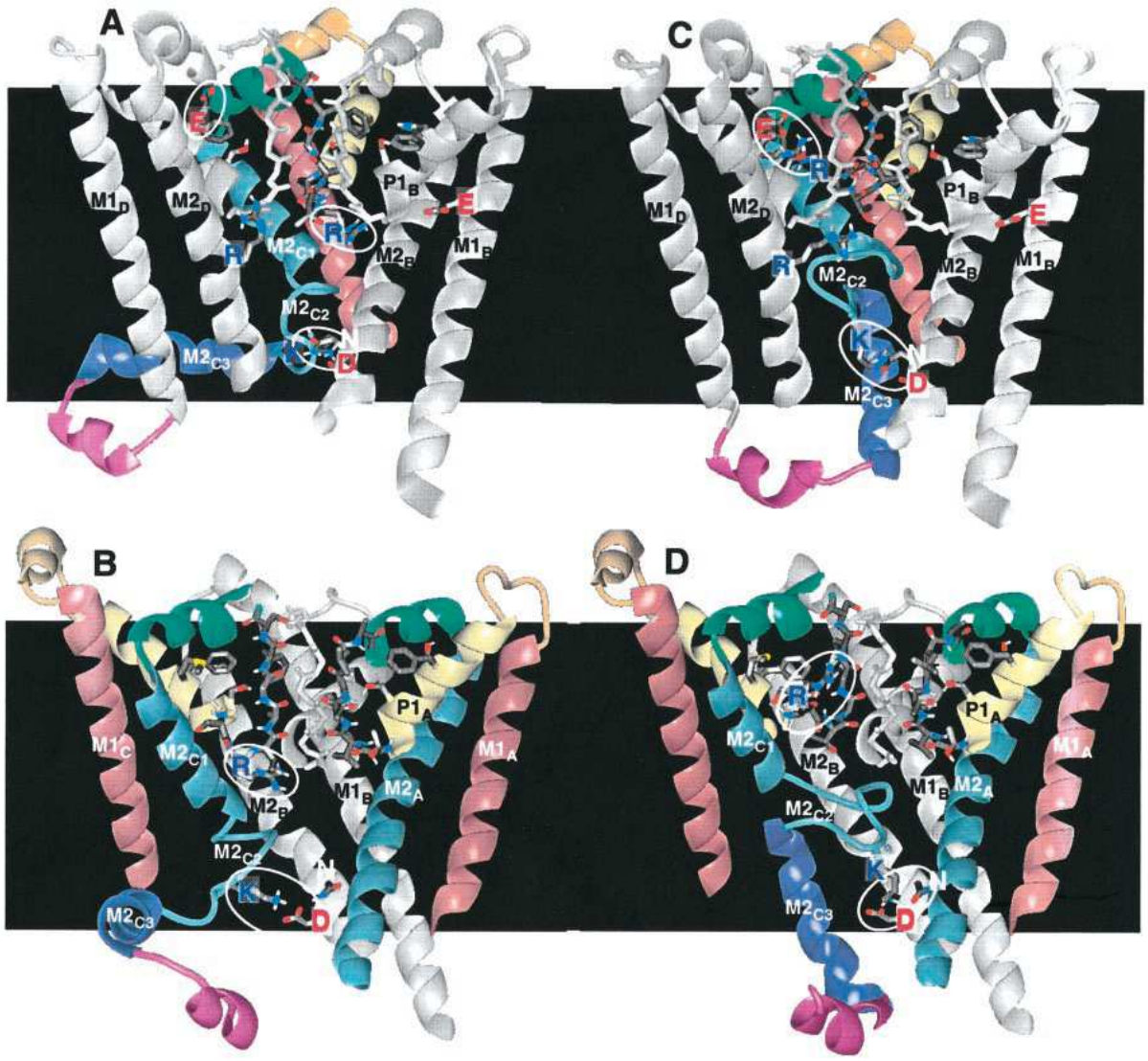

Figure 6. **Side views of KtrB models from KtrB of *Aquifex aeolicus* with different conformations of the P_C and M_{2C} segments.** In A and C, the MPM_C domain is marked in different colours while MPM_A and MPM_D are coloured white. In B and D, a different perspective is shown with MPM_C coloured evenly, MPM_A multi-coloured and MPM_B in white. A and B as well as C and D show the same models but in different perspectives. In A and B, M_{2C2} has a coiled conformation connecting M_{2C1} (spanning the membrane as α-helix) and M_{2C3} (lying as α-helix in the inner surface). In C and D, M_{2C1} and M_{2C3} span the membrane as α-helices while M_{2C2} forms a flexible loop that fills the cavity beyond the selectivity filter. In both models, a lysine in M_{2C2} forms a salt bridge with an aspartate in M_{2B}. This figure is taken from Durell and Guy, 1999 (23).

M_1PM_2 structure is mainly based on sequence alignments. Biochemical studies on some members of this superfamily confirmed this hypothesis in general (21;22). Investigations on the structure of *Va*KtrB by use of PhoA fusion studies also basically supported the M_1PM_2 structure for motifs B to D. However, because of its small and polar amino acids region M_{2C} was already hard to model in structural predictions. The subregion M_{2C2} appeared to be rather flexible and was supposed to form a gate inside the cavity of the protein (56). By use of accessibility studies, the proposed amphipathic character of M_{2C3} was shown, which led Vor der Brüggen (55) to the hypothesis that the second model of Durell and Guy (23), in which M_{2C3} lies in parallel to the membrane, is correct. However, a confirmed structural and functional model of this region was still missing at the beginning of this thesis. Hence, the aim of this thesis was to gain further insights into the role of M_{2C}.

In chapter II of this thesis preliminary tests on the functional overexpression, purification and reconstitution of *Va*KtrB-His_6 are presented. They serve as assays essential to the work

presented in chapters III and IV of this thesis. To this end existing protocols on the overexpression and purification of KtrB were checked and if necessary improved. Chapter II also contains light scattering experiments on *Va*KtrA, *Va*KtrB and *Va*KtrAB, similar to the ones published by Albright et al. (34). They had the aim to obtain further information on the subunit stoichiometry of the Ktr complex.

Chapter III concentrates on the functional role of M_{2C} and especially the M_{2C2} region. For this purpose plasmids encoding point mutations or partial to complete deletions in M_{2C2} were generated. The influence of these changes on the function of KtrB was analyzed among others by uptake studies of the cations K^+ and Na^+ into *E. coli* cells. The results indicate that region M_{2C2} possesses a flexible structure and forms a gate for K^+ transport through the KtrB protein.

Chapter IV focusses on the structural properties of M_{2C}. EPR analyses of spin-labeled, reconstituted single and double cysteine mutants were performed in order to gain information about the mobility and the polarity of single side chains and the distances between two labeled residues. The measurements were performed both, in the absence and in the presence of K^+ in order to monitor possible distance changes. Such changes would indicate structural rearrangements in the analyzed regions. Based on the EPR data, structural models of an open and a closed permeation pathway are presented. In order to demonstrate the activity of reconstituted, spin-labeled KtrB $^{86}Rb^+$ influx assays into proteoliposomes were performed. Finally, I checked with mutational analysis the presence of the putative salt bridge between K325 in M_{2C2} and D222 in M_{2B} of VaKtrB and conclude that this bridge does not exist.

REFERENCES

1. Stumpe, S., Schlösser, A., Schleyer, M., and Bakker, E. P. (1996) K^+ circulation across the prokaryotic cell membrane: K^+-uptake systems. In Konings, W. N., Kaback, H. R., and Lolkema, J.S., editors. *Handbook of Biological Physics: Transport Processes In Eukaryotic and Prokaryotic Organisms*, Elsevier Sience B.V., Amsterdam

2. Epstein W. (1986) *FEMS Microbiol.Rev.* **39,** 73-78

3. Dinnbier, U., Limpinsel, E., Schmid, R., and Bakker, E. P. (1988) *Arch.Microbiol.* **150,** 348-357

4. Booth, I. R. (1985) *Microbiol.Rev.* **49,** 359-378

5. Suelter, C. H. (1970) *Sience* **168,** 789-795

6. Kuo, M. M., Haynes, W. J., Loukin, S. H., Kung, C., and Saimi, Y. (2005) *FEMS Microbiol.Rev.* **29,** 961-985

7. McLaggan, D., Naprstek, J., Buurman, E. T., and Epstein, W. (1994) *J Biol.Chem.* **269,** 1911-1917

8. Csonka, L. N. and Epstein W. (1996) Osmoregulation. In Neidhardt, E. C., editor. *Escherichia coli and Salmonella typhimurium. Cellular and molecular biology*, ASM Press, Washington DC

9. Meury, J., Robin, A., and Monnier-Champeix, P. (1985) *Eur J Biochem.* **151,** 613-619

10. Bakker, E. P. (1993) Cell K^+ and K^+ transport systems in prokaryotes. In Bakker, E. P., editor. *Alkali cation transport systems in prokaryotes.*, CRC Press, Boca Raton, USA

11. Krulwich, T. A., Guffanti, A. A., and Seto-Young, D. (1990) *FEMS Microbiol.Rev.* **6,** 271-278

12. Durell, S. R., Bakker, E. P., and Guy, H. R. (2000) *Biophys.J.* **78,** 188-199

13. Durell, S. R., Hao, Y., Nakamura, T., Bakker, E. P., and Guy, H. R. (1999) *Biophys.J.* **77,** 775-788

14. Tholema, N., Bakker, E. P., Suzuki, A., and Nakamura, T. (1999) *FEBS Lett.* **450,** 217-220

15. Kawano, M., Abuki, R., Igarashi, K., and Kakinuma, Y. (2000) *J.Bacteriol.* **182,** 2507-2512

16. Bihler, H., Gaber, R. F., Slayman, C. L., and Bertl, A. (1999) *FEBS Lett.* **447,** 115-120

17. Haro, R. and Rodriguez-Navarro, A. (2002) *Biochim Biophys Acta.* **1564,** 114-122

18. Uozumi, N., Kim, E. J., Rubio, F., Yamaguchi, T., Muto, S., Tsuboi, A., Bakker, E. P., Nakamura, T., and Schroeder, J. I. (2000) *Plant Physiol* **122,** 1249-1259

19. Horie, T., Yoshida, K., Nakayama, H., Yamada, K., Oiki, S., and Shinmyo, A. (2001) *Plant J.* **27,** 129-138

20. Mosimann, M., Goshima, S., Wenzler, T., Lüscher, A., Uozumi, N., and Mäser, P. (2010) *Eukaryot Cell* published online ahead of print (26. February, 2010)

21. Kato, Y., Sakaguchi, M., Mori, Y., Saito, K., Nakamura, T., Bakker, E. P., Sato, Y., Goshima, S., and Uozumi, N. (2001) *Proc.Natl.Acad.Sci.U.S.A* **98,** 6488-6493

22. Buurman, E. T., Kim, K. T., and Epstein, W. (1995) *J.Biol.Chem.* **270,** 6678-6685

23. Durell, S. R. and Guy, H. R. (1999) *Biophys.J.* **77,** 789-807

24. Doyle, D. A., Morais, C. J., Pfuetzner, R. A., Kuo, A., Gulbis, J. M., Cohen, S. L., Chait, B. T., and MacKinnon, R. (1998) *Science* **280,** 69-77

25. Schrempf, H., Schmidt, O., Kummerlen, R., Hinnah, S., Muller, D., Betzler, M., Steinkamp, T., and Wagner, R. (1995) *EMBO J.* **14,** 5170-5178

26. Zhou, Y., Morais-Cabral, J. H., Kaufman, A., and MacKinnon, R. (2001) *Nature* **414,** 43-48

27. Cuello, L. G., Cortes, D. M., Jogini, V., Sompornpisut, P., and Perozo, E. (2010) *FEBS letters* **584,** 1126-1136

28. Liu, Y.-S., Sompornpisut, P., and Perozo, E. (2001) *Nat.Struct.Biol.* **8,** 883-887

29. Tholema, N., Vor der Brüggen, M., Mäser, P., Nakamura, T., Schroeder, J. I., Kobayashi, H., Uozumi, N., and Bakker, E. P. (2005) *J.Biol.Chem.* **280,** 41146-41154

30. van der Laan, M., Gassel, M., and Altendorf, K. (2002) *J.Bacteriol.* **184,** 5491-5494

31. Bertrand, J., Altendorf, K., and Bramkamp, M. (2004) *J.Bacteriol.* 1**86,** 5519-5522

32. Nakamura, T., Yamamuro, N., Stumpe, S., Unemoto, T., and Bakker, E. P. (1998) *Microbiology* **144**, 2281-2289

33. Kröning, N., Willenborg, M., Tholema, N., Hänelt, I., Schmid, R., and Bakker, E. P. (2007) *J.Biol.Chem.* **282,** 14018-14027

34. Albright, R. A., Ibar, J. L., Kim, C. U., Gruner, S. M., and Morais-Cabral, J. H. (2006) *Cell* **126,** 1147-1159

35. Parra-Lopez, C., Lin, R., Aspedon, A., and Groisman, E. A. (1994) *EMBO J* **13,** 3964-3972

36. Jiang, Y., Lee, A., Chen, J., Cadene, M., Chait, B. T., and MacKinnon, R. (2002) *Nature* **417,** 515-522

37. Schlösser, A., Meldorf, M., Stumpe, S., Bakker, E. P., and Epstein, W. (1995) *J Bacteriol.* **177,** 1908-1910

38. Strahl, H. and Greie, J. C. (2008) *Extremophiles* **12,** 741-752

39. Kato, N., Akai, M., Zulkifli, L., Matsuda, N., Kato, Y., Goshima, S., Hazama, A., Yamagami, M., Guy, H. R., and Uozumi, N. (2007) *Channels (Austin.)* **1,** 161-171

40. Thompson, F. L., Iida, T., and Swings, J. (2004) Biodiversity of Vibrios. *Microbiol.Mol.Biol.Rev.* **68,** 403-31

41. Uh, Y., Park, J. S., Hwang, G. Y., Jang, I. H., Yoon, K. J., Park, H. C., and Hwang, S. O. (2001) *Clin.Microbiol.Infect.* **7,** 104-106

42. Balebona, M. C., Andreu, M. J., Bordas, M. A., Zorrilla, I., Morinigo, M. A., and Borrego, J. J. (1998) *Appl.Environ.Microbiol.* **64,** 4269-4275

43. Nakamura, T., Matsuba, Y., Yamamuro, N., Booth, I. R., and Unemoto, T. (1994) *Biochim.Biophys Acta* **1219,** 701-705

44. Nakamura, T., Tokuda, H., and Unemoto, T. (1984) *Biochim.Biophys.Acta* **776,** 330-336

45. Nakamura, T., Kawasaki, S., and Unemoto, T. (1992) *J.Gen.Microbiol.* **138,** 1271-1276

46. Unemoto, T., Tokuda, H., and Hayashi, M. (1990) In Krulwich, T. A., editor. *Bacterial Energetics*, Academic Press, San Diego, CA

47. Tholema, N. (2002) KtrB, die K^+-translozierende Untereinheit des K^+-Aufnahmesystems KtrAB aus *Vibrio alginolyticus*: Analyse der Selektivitätsfilter-Glycinreste und der Topologie. Universität Osnabrück, Dissertation

48. Schlösser, A., Hamann, A., Bossemeyer, D., Schneider, E., and Bakker, E. P. (1993) *Mol.Microbiol.* **9,** 533-543

49. Wierenga, R. K., Terpstra, P., and Hol, W. G. (1986) *J Mol.Biol.* **187,** 101-107

50. Jiang, Y., Pico, A., Cadene, M., Chait, B. T., and MacKinnon, R. (2001) *Neuron* **29,** 593-601

51. Roosild, T. P., Castronovo, S., Miller, S., Li, C., Rasmussen, T., Bartlett, W., Gunasekera, B., Choe, S., and Booth, I. R. (2009) *Structure.* **17,** 893-903

52. Roosild, T. P., Miller, S., Booth, I. R., and Choe, S. (2002) *Cell* **109,** 781-791

53. Parfenova, L. V., Crane, B. M., and Rothberg, B. S. (2006) *J Biol.Chem.* **281,** 21131-21138

54. Zulkifli, L. and Uozumi, N. (2006) *J Bacteriol.* **188,** 7985-7987

55. Vor der Brüggen, M. (2007) Topologiestudien an der Domäne MPM_C der membanständigen Untereinheit B des K^+-Aufnahmesystems KtrAB aus *Vibrio alginolyticus*. Universität Osnabrück, Dissertation

56. Albright, R. A., Joh, K., and Morais-Cabral, J. H. (2007) *J.Biol.Chem.* **282,** 35046-35055

57. Löchte, S. (2008) Topology studies on the B-subunit from the K^{+}-uptake system KtrAB of *Vibrio alginolyticus*. Universität Osnabrück, Diploma thesis

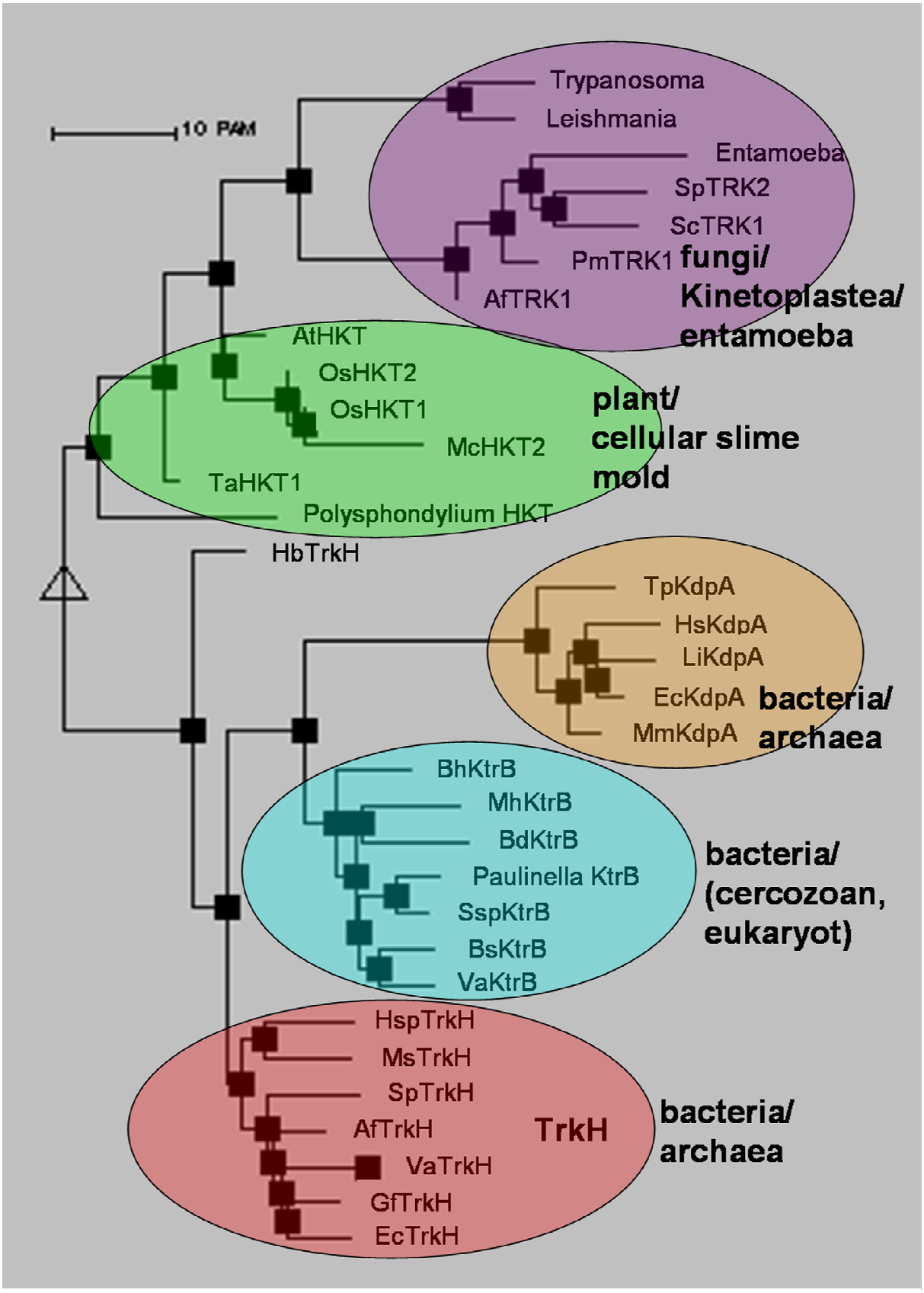

Appendix figure 1. **Phylogenetic tree of SKT proteins.** The five major branches are TrkH from bacteria and archaea, KtrB from bacteria (and cercozoan), KdpA from bacteria and archaea, HKT1,2 from plants and cellular slime molds as well as TRK1,2 from fungi, kinetoplastea, and entamoeba. The phylogenetic tree was designed by combining protein-protein BLAST and MultAlin. The scalebar corresponds to 10 percent accepted mutations.

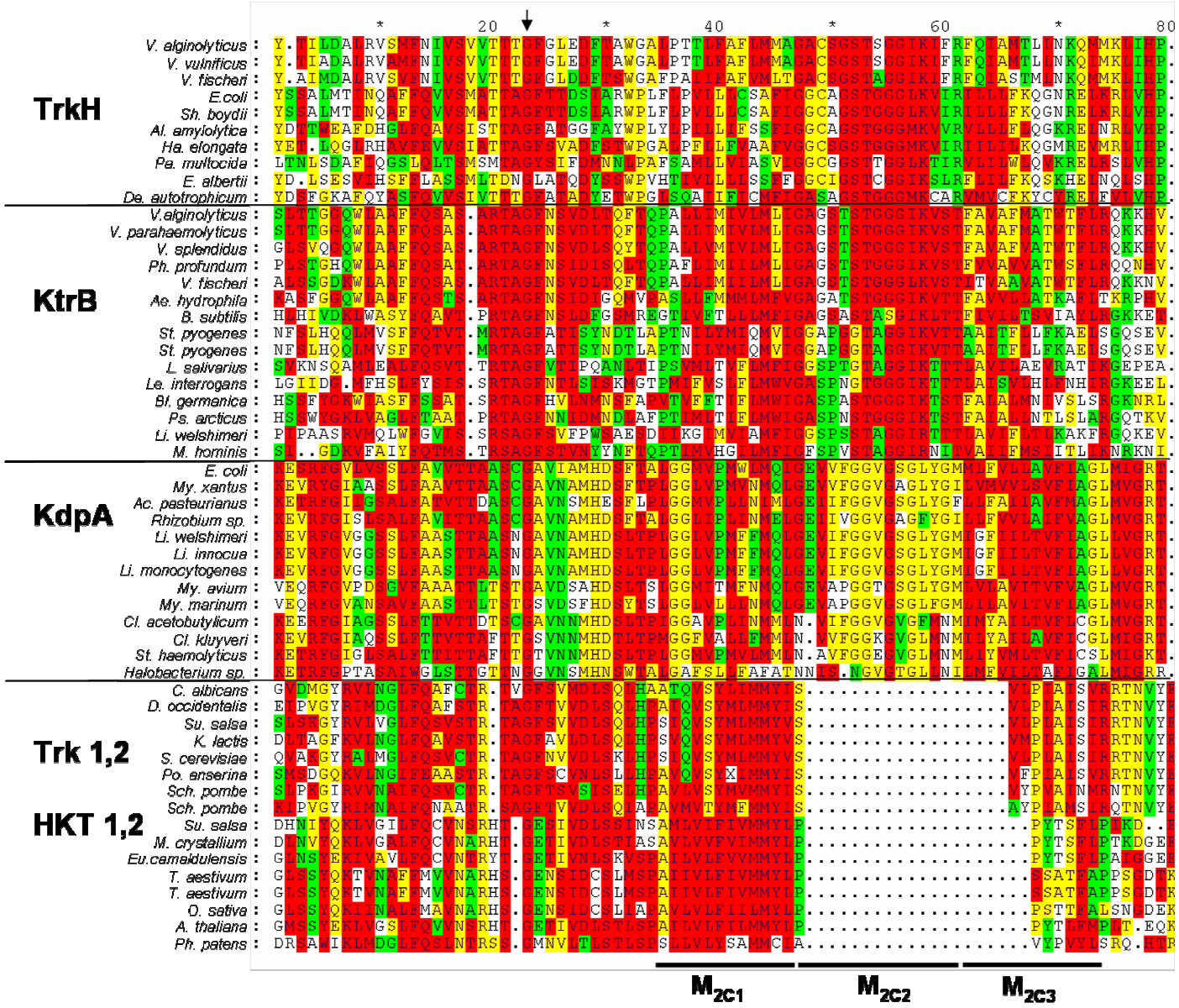

Appendix figure 2. **Alignment of P_C and M_{2C} of different SKT proteins.** Increasing degree of conservation of single residues is indicated by the background color changing from white via yellow and green to red. The absolutely conserved *Va*KtrB residue G290 [selectivity-filter residue (23;29)] is marked by the arrow.

Chapter II

II

FUNCTIONAL OVERPRODUCTION, PURIFICATION, AND RECONSTITUTION OF KtrB OF THE KtrAB TRANSPORT SYSTEM OF *VIBRIO ALGINOLYTICUS*

FUNCTIONAL OVERPRODUCTION, PURIFICATION, and RECONSTITUTION of KtrB of the KtrAB TRANSPORT SYSTEM of *VIBRIO ALGINOLYTICUS*

Inga Hänelt, Department of Microbiology, University of Osnabrück

Running title: Functional overproduction, purification and reconstitution of KtrB

In order to perform biochemical and biophysical approaches on membrane proteins their overproduction, solubilization, and purification as well as reconstitution in native form is a prerequisite. In this study, for subunit KtrB of the KtrAB complex from *Vibrio alginolyticus* a protocol has been developed to analyze the isolation of functional KtrB by showing its activity directly or indirectly during cell growth, after membrane vesicle preparation, and after reconstitution of purified protein into liposomes. In addition, static light scattering measurements are presented which confirm the presence of an octameric KtrA complex and a dimer of KtrB in solution, but raise doubt on the previously proposed 8 to 2 stoichiometry of KtrAB by rather proposing a 16 to 2 composition.

The first goal for structural and functional analysis of membrane proteins is its functional overexpression and purification (1). The correct folding of integral membrane proteins involves different steps like the targeting of synthesized polypeptide chains to the membrane as well as the insertion and assembly in the membrane (2;3). *Escherichia coli* is the most commonly used expression host (4). A variety of mutants and specialized plasmids are available to increase the amount of synthesized target protein. However, this overproduction often results in formation of aggregated material in inclusion bodies because the capacity of the cell to process the nascent membrane protein correctly is exceeded. In most cases, it is cumbersome to obtain refolded membrane proteins from these inclusion bodies. Hence, a functional overexpression of membrane proteins in the cytoplasmic membrane is most important (1). For the solubilization of membrane proteins the right choice of detergent is essential. First, the solubilized protein should remain actively folded; second, an efficient extraction from the membrane into the detergent micelles is necessary. Third, the detergent must be suitable concerning the temperature, the ionic strength, and the pH conditions of the desired purification procedure (5). In addition, for later reconstitutions of the solubilized protein into liposomes and thus the removal of detergent, the critical micelle concentration (CMC) must be taken into account (6). Certain methods for the removal of detergent like gel filtrations or dilutions can only be used at high CMCs, the use of biobeads is preferred at lower values (7).

The KtrAB system of *Vibrio alginolyticus* is a high affine, Na^+-dependent K^+ transporter. It consists of the membrane integral, K^+-translocating subunit KtrB and the cytoplasmic, regulatory subunit KtrA (8-13). KtrA, a member of the RCK/KTN-protein family, is supposed to regulate the K^+ transport by binding of ATP (14;15). In previous studies the protein complex as well as KtrB alone have been shown to be actively expressed in *E. coli* LB2003, a strain defect in its endogenous K^+ uptake systems Kup, Trk, and Kdp (16). However, KtrB alone looses Na^+-dependency, ion selectivity, and transport velocity; but its affinity for potassium is unchanged (8;9). Without any active K^+ uptake system LB2003 could not grow at K^+ concentrations below 10 mM. Under these conditions its cells die, since K^+ is the main cation in the cytoplasm of prokaryotes and is essential for processes like osmoregulation, pH homeostasis, and enzyme activation (17-21). The KtrB subunit consists of four MPM-motifs (transmembrane helix – pore loop – transmembrane helix), termed M_1PM_{2A} to $M_1PM_{2D,}$ and is believed to have evolved from simple KcsA-like K^+ channels by multiple gene duplication and gene fusion (22;23). KtrB belongs to the superfamily of potassium ion transporters (SKT). Other SKT proteins are TrkH and KdpA of prokaryotes, HKT1,2 of plants and protozoae, and TRK1,2 of fungi (22;23). Each p-loop of KtrB contains one conserved glycine residue which form the selectivity filter. It is simpler than the selectivity filter sequence TVGYG of KcsA, but highly conserved within the superfamily (8,9,24-26). From sequence alignments it has been predicted that the structure of KtrB is similar to KcsA; however, the C-terminal residues of M_{2C} and M_{2D} showed striking differences (23). Cross-linking studies confirmed that the periplasmic half of KtrB from *Bacillus subtilis* is quite similar to KcsA, while the cytoplasmic half differs. In addition, these studies revealed a dimer of KtrB within the cell membrane and in solubilized form (27) confirm-

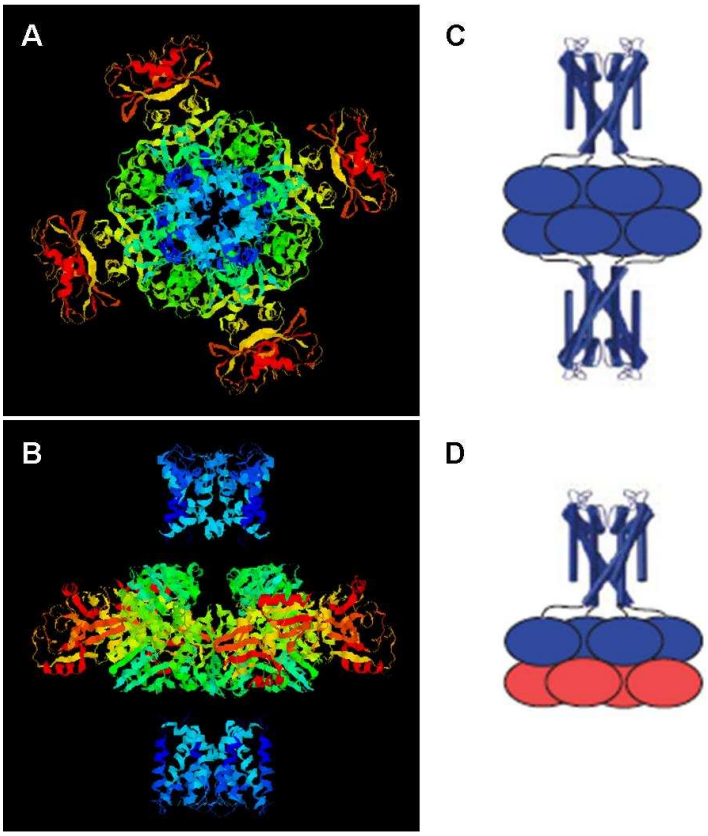

Figure 1. **The crystal structure MthK of *Methanobacterium thermoautotrophicum*. A** and **B** show the top and side view of the potassium channel MthK. The pore region is coloured in blue, the RCK domains are shown in multi colors. **C:** Cartoon on the analysed crystal structure with two channels arranged in a 'back-to-back' fashion. **D:** Cartoon of the proposed native MthK structure with the presence of the additional cytoplasmatic RCK domains (shown in red). Figures taken from (56).

ing light scattering (LS) data of solubilized KtrB of *B. subtilis* (15). Furthermore, an octamer of KtrA was determined by crystallization and light scattering data (15), while for the KtrAB complex a stoichiometry of 8:2 was proposed from light scattering measurements. In contrast, a different stoichiometry was shown for the well characterized, Ca^{2+}-gated K^+ channel MthK of *Methanobacterium thermoautotrophicum* (28), whose domains are similar to KtrA and KtrB. The MthK channel consists of four M_1PM_2 subunits with one covalently linked RCK domain each. The M_1PM_2 subunits form a pore similar to the KcsA channel. The four RCK domains together with four additional, cytoplasmic RCK domains are arranged as an octameric gating ring, which is regulated by the binding of Ca^{2+} (Fig. 1D). The composition of MthK was solved by combining biochemical approaches with a crystal structure showing MthK with the four cytoplasmic RCK domains deleted. Two channels were arranged in a 'back-to-back' fashion leading to the conclusion that the two channels shared their RCK domains (28) (Fig. 1A-C). In summary, for the MthK complex an arrangement of one pore with eight RCK domains was described.

In this study a protocol is presented which confirms protein activity and, therefore, natively folded protein during the overproduction and purification of KtrAB. In addition, a radioactive $^{86}Rb^+$ uptake assay for KtrB-containing proteoliposomes is established. By these procedures, KtrB activity can be examined during cell growth, vesicle preparation, and after reconstitution. Furthermore, light scattering measurements verified the dimerization of solubilized KtrB and the presence of octameric purified KtrA. However, the data point to a 16 to 2 or 8 to 1 stoichiometry of KtrA to KtrB in the KtrAB complex, which is in contrast to the previously proposed composition of 8 to 2 (15), but fits very well with the stoichiometry determined for MthK (28).

Experimental procedures

Strains, plasmids, growth conditions. The strains and plasmids used in this study are listed in table 1. Cells of *E. coli* LB2003 (16) containing plasmids pEL903 (8) or pIH301 were grown aerobically in medium K3 (8;31) with 0.2 % glycerol as carbon source. *ktrB* or *ktrAB* expression was induced in presence of 0.02% (w/v) L-arabinose. The cells were harvested either in the late exponential growth phase for protein purification or at an OD_{578} value of 0.8 for transport assays. For the overproduction of

Table 1. **Strains and plasmids used in this study**

strain/plasmid	features	reference/source
LB2003	F$^-$ *kup1* Δ*kdpFABC5* Δ*trkA rpsL metE thi rha gal*	(16)
BL21 (DE3)pLysS	F$^-$ *ompT hsdS*$_B$ (r^-_Bm^-_B) *gal dcm* (DE3)/pLysS; Cam^R	(32)
pEL903	pBAD18 containing *VaktrB* extended at its 3'-end with six His codons; Amp^R	(8)
pIH301	pBAD18 containing *VaktrAB*; *ktrA* carries a 5' extension starting with 10 His codons followed by a sequence for a factor Xa-digestion site; Amp^R	this study
pEL305	pET16b containing *VaKtrA*; Amp^R	(14)
pBAD18	cloning vector for *VaKtrB*; Amp^R; p_{BAD} promoter of the arabinose operon	(30)
pET16b	cloning vector; Amp^R	Novagen

His_{10}-KtrA, cells of strain BL21(DE3)pLysS/ pEL305 were grown as described by Kröning et al. (14).

Cell transport experiments. Depletion of the cells from alkali cations and net K^+- uptake by K^+-depleted LB2003 cells were carried out as described in (8). $^{86}Rb^+$-uptake was performed in the same manner; but the cell pellets cut off were lysed overnight in 0.5 mL 0.4 N NaOH. Radioactivity in the lysate was measured in a liquid scintillation counter after addition of 5 mL scintillation fluid.

Overproduction and purification of His_{10}-KtrAKtrB complexes, KtrB-His_6 and His_{10}-KtrA. Cells of strain LB2003 containing plasmid pIH301 or pEL903 were fermented in 30 L of K3 medium at 37 °C (31;33) in the presence of 0.2 % (v/v) glycerol and 0.02 (w/v) % L-arabinose to an OD_{578} value of 1.0-1.5, harvested by centrifugation, washed once with buffer S containing 600 mM NaCl, 10 % (w/v) glycerol, and 50 mM TrisCl, pH 8, and resuspended at 10 mg dry wt/mL of the buffer S in the presence of 1 mM EDTA and some DNAse. Cells were broken by sonication (8 x 30 sec, 30 sec break, 50% duty cycle, intensity 7) with a Branson 250 Sonifier II Cell Disruptor (Branson, Shelton, USA). Subsequently, the suspension was centrifuged for 15 min at 15.000 x g and its supernatant was centrifuged overnight at 100.000 x g. The pellet was suspended at 10 mg protein/mL of buffer S and its proteins were solubilized by incubation with 1 % (w/v) β-D-dodecylmaltoside (DDM) (Anatrace, Maumee, USA) in the presence of 1 % (v/v) protease-inhibitor cocktail P8849 (Sigma-Aldrich, Steinheim, Germany) for 1 h. at 4 °C, and centrifuged for 45 min at 200.000 x g in a 50.2 Ti Ultracentrifuge (Beckman, Frankfurt, Germany). The supernatant was incubated at a concentration of 150 mg of protein/mL of packed Ni^{2+}-NTA agarose (Qiagen, Hilden, Germany) in the presence of 10 mM imidazole in a 50 mL polypropylene column for 1 h. Subsequently, the agarose was washed with 50 volumes of buffer W, containing 200 mM NaCl, 20 mM TrisCl, pH 8, 5 mM β-mercaptoethanol, 10 % (w/v) glycerol, 0.04 % (w/v) β-D-dodecylmaltoside plus 50 mM imidazole. His-tagged protein was eluted with 3 volumes of buffer W containing 500 mM imidazole. The protein-containing samples were pooled and concentrated in a spin concentrator (Amicon Ultra-15, PLHK Ultracel-PL membrane, 100 kDa, Millipore, Billerica, USA) to 0.5 mL. The concentrates were further purified using size exclusion chromatography on a Superdex 200 10/300 column (flowrate 0.5 mL/min) in buffer W. For purification of His_{10}-KtrA, cells of strain BL21 (DE3)pLysS/pEL305 were treated as described above, but the supernatant of the high speed, overnight centrifugation containing the cytoplasm was used and was applied to the Ni^{2+}-NTA agarose.

For SDS-polyacrylamide gel electrophoresis (33), samples were diluted with an equal volume of twice concentrated sample buffer, containing 4 % (w/v) SDS, 12 % (v/v) glycerol, 50 mM TrisCl, pH 6,8, 2 % (w/v) β-mercaptoethanol, and 0.01 % (w/v) Serva blue G, and after separation stained with Coomassie brilliant blue.

Detection of proteins with antibodies. The amount of His-tagged KtrB in cells or cell

fractions used for purification or transport experiments was determined by Western blotting with a monoclonal mouse penta-His antibody (Qiagen, Hilden, Germany), followed by incubation with ImmunoPure antibody goat anti-mouse IgG labeled with alkaline phosphatase (Pierce, Rockford, USA) as secondary antibody. Immunodecoration was detected by the reaction of alkaline phosphatase with 5-bromo-4-chloro-3-indolyl phosphate and the precipitation of the product with 4-nitro blue tetrazolium chloride. For this purpose, an aliquot of the cell suspension containing 50 µg of cell protein was pelleted and taken up in 50 µL sample buffer. Samples of the low speed fraction, the cytoplasm, and the membrane were all diluted to a concentration of 1 mg/mL. The proteins in the samples were separated by SDS-polyacrylamide electrophoresis (33) and transferred to a nitrocellulose membrane (500 mA, 3 h), on which His-tagged KtrB was detected with the alkaline phosphatase reaction.

Preparation of right-side out vesicles. LB 2003 cells with and without KtrB were taken from the exponential growth phase and prepared as described by Kaback (34) except that Na^+ replaced K^+ throughout the whole procedure. Finally, the vesicles were dissolved in 50 mM NaP_i, pH 6.6 and 10 mM $MgSO_4$ (34;35). Vesicles were used within two hours after their preparation.

Vesicle transport experiments. The proline and rubidium ion transport assays by the Kaback vesicles were performed as described in (37). Briefly, both uptake assays were carried out under aerobic conditions in a reaction mixture of 200 µL for each sample. The suspensions contained 150 µg membrane protein, 50 mM NaP_i, pH 6.6, 10 mM $MgSO_4$, and 20 mM D-lactate. After 5 minutes of incubation at room temperature either 3.5 µM 1µCi/mL $_L$-[U-^{14}C]proline (Amersham) or 2 mM 1µCi/mL ^{86}RbCl (PerkinElmer) was added to each sample. Uptake was terminated by the addition of 2 mL ice cold 0.1 M lithium chloride, immediately filtered through 0.2 µm cellulose nitrate filters and washed twice with the same volume of LiCl. Radioactivity of each filter in 3 mL scintillation fluid was determined in a liquid scintillation counter.

Reconstitution into liposomes. For reconstitution of purified proteins, liposomes were prepared from acetone/ether-washed E. coli lipids (Avanti total lipid extract) and L-α-phosphatidylcholine from egg yolk (Sigma) in a ratio of 3:1 (w/w) (38). Unilamellar, small vesicles with relatively homogeneous size were prepared by dissolving the lipids in 50 mM KP_i, pH 7.0 to 20 mg/mL and sonicating the lipids until transparency under a stream of nitrogen with a Branson 250 Sonifier II Cell Disruptor (Branson, Shelton, USA), followed by three 'freezing in liquid nitrogen, slow thawing at room temperature' cycles, and final extrusion through a 400-nm polycarbonate filter (Avestin) (39). Subsequently, the liposomes were diluted with buffer W without DDM to 4 mg/ml and titrated with Triton X-100 (Sigma) just below 'detergent-saturation'. The turbidity of the suspension at 540 nm was used to monitor the physical state of the liposomes (40;41). The detergent-destabilized liposomes were mixed with purified protein in different ratios (w/w), and incubated for 30 min at room temperature under gentle agitation. To remove the detergent, polystyrene beads (Biobeads SM2, BioRad) were added at a wet wt of 40 mg/mL and the sample was incubated for another 15 min. Fresh Biobeads SM2 (40 mg/mL) were added to the sample four times and the incubations were continued at 4 °C for 15 min, 30 min, overnight, and 1 h, respecttively. The beads were removed and the mixture was diluted at least 2.5-fold with loading buffer containing 400 mM KCl, 10 mM Hepes, 5 mM N-methyl-D-glucamine (NMG), pH 7.6 to decrease the glycerol concentration below 4 %. After collecting the proteoliposomes by ultracentrifugation they were washed twice with loading buffer, finally dissolved to 20 mg/mL and three times frozen and thawed before further use.

$^{86}Rb^+$ uptake into proteoliposomes. The $^{86}Rb^+$ uptake into proteoliposomes was in principle performed as previously described (42;43). Briefly, the proteoliposomes preloaded with loading buffer were extruded through a 400 nm polycarbonate filter (Avestin) and diluted with the same buffer to 10 mg/mL. For each approach, the extraproteosomal buffer was exchanged against uptake buffer containing 400 mM sorbitol, 10 mM Hepes, and 5 mM NMG, pH 7.6 by spinning 80 µL through a preincubated spin desalting column (Zeba Spin Desalting Columns, 7 k MWCO, 0.5 mL, Pierce). Subsequently, 50 µL were diluted with 150 µL uptake buffer and for 5 minutes preincubated at room temperature. The uptake was started by the addition of 2.3 µCi/mL $^{86}Rb^+$ (PerkinElmer). Samples were taken at different time points by diluting 40 µL in 2 mL ice cold 0.1 M LiCl and filtration through a 200 nm cellulose nitrate filter (Millipore). The filter was

washed twice with 2 mL ice cold 0.1 M LiCl, added into a counting vial together with 3 mL scintillation fluid and its radioactivity was determined in a liquid scintillation counter. In parallel, the remaining, buffer-changed proteoliposomes were used to define the maximal uptake of $^{86}Rb^+$ (100%) after addition of 16 µM valinomycin. As negative control, uptake experiments were performed with equally treated protein free liposomes. To determine the total radioactivity, at the end of each approach 10 µL 2.3 µCi/mL $^{86}Rb^+$ were directly added to 3 mL scintillation fluid.

Size-exclusion chromatography coupled to light scattering, UV absorbance and refractive index measurements. SEC-LS/UV/RI measurements were performed with Dirk-Jan Slotboom at the Biochemistry Department of the University of Groningen using proteins, which were purified via affinity and size exclusion chromatography. Fractions of either KtrA, KtrB or KtrAB from the size exclusion chromatography were each pooled and concentrated to 200 µL as described above. SEC-LS/UV/RI of these preparations were performed on an Äkta purifier system using a Superdex 200 10/300 column (GE Helthcare), an additional light scattering detector (minidawn TREOS, Wyatt technologies), and a refractive index detector (Optilab Rex, Wyatt Technologies). The procedure in buffer W was performed as described in (44) in detail. As standard protein BSA was dissolved in buffer W and treated exactly in the same manner as the proteins analyzed. The data from the three detectors were entered into the Astra software package (Wyatt Technologies) and analyzed according to (44-46). In summary, the following three equations were used: To calculate the molecular mass of the proteins or the constant K with the help of BSA

$$M_p = K\frac{(LS)(UV)}{\varepsilon_p (RI)^2} \qquad [1],$$

with M_p as the molecular mass of the protein, K as instrument response factor, and ε_p as protein extinction coefficient was used. The latter was calculated directly from the amino acid sequence with the ProtParam tool on the ExPaSy server. For calculation of the detergent-lipid to protein ratio

$$\left(\frac{dn_c}{dc_p}\right) = k\frac{RI}{UV}\varepsilon \qquad [2]$$

and

$$\left(\frac{dn_c}{dc_p}\right) = 0.18 + \delta 0.134 \qquad [3]$$

were used, with the differential refractive index (dn_c/dc_p), which is defined as the ratio of the change in refractive index of the protein-detergent-lipid complex to the change of the protein concentration, k as an instrumental constant and

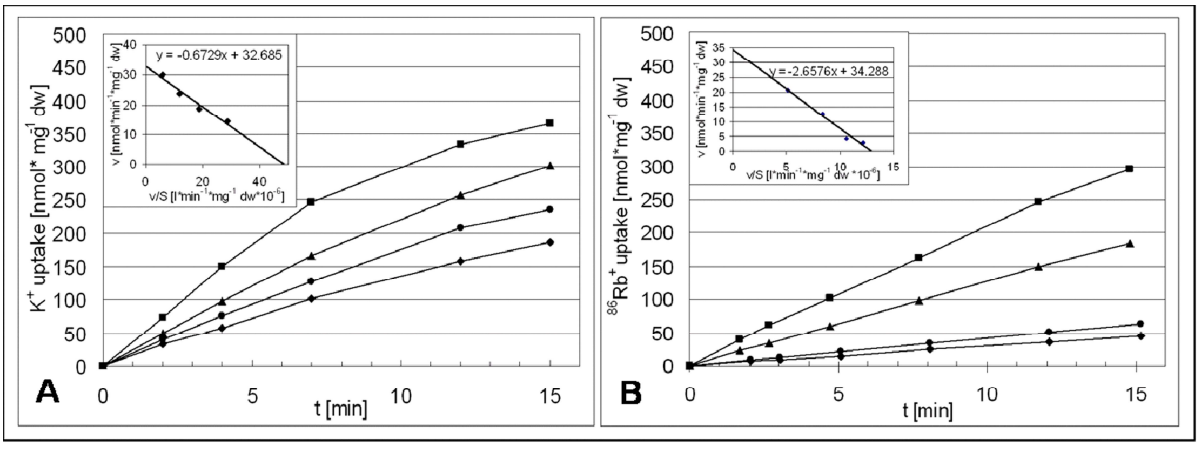

Figure 2. **K^+ and Rb^+ uptake by cells containing KtrB-His$_6$.** Plasmid-containing cells of strain LB2003 were grown and induced for *ktrB* expression with 0.02 % L-arabinose, according to *growth conditions*. For the K^+ and Rb^+ uptake experiments cells were suspended at 1 mg dry wt/ml of medium containing 200 mM NaHepes, pH 7.5, 0.2 % glycerol, and 0.02 % L-arabinose and shaken at room temperature. After 10 min KCl or ^{86}RbCl was added. For each data point a 1.0 mL sample was taken from the suspension and K^+ or $^{86}Rb^+$ content of the cells was determined. **A**: K^+ uptake, ◆---◆ 0.5 mM, ●---● 1 mM, ▲---▲ 2 mM,■---■ 5 mM KCl were added. From the Eadie-Hofstee plot (small graph) a V_{max} of 33 nmol.min^{-1}.mg^{-1} dw and a K_m of 0.67 mM were detected. **B**: $^{86}Rb^+$ uptake, ◆---◆ 0.25 mM, ●---● 0.4 mM, ▲---▲ 1.5 mM,■---■ 4 mM ^{86}RbCl were added. From the Eadie-Hofstee plot a V_{max} of 34 nmol.min^{-1}.mg^{-1} dw and a K_m of 2.66 mM were detected.

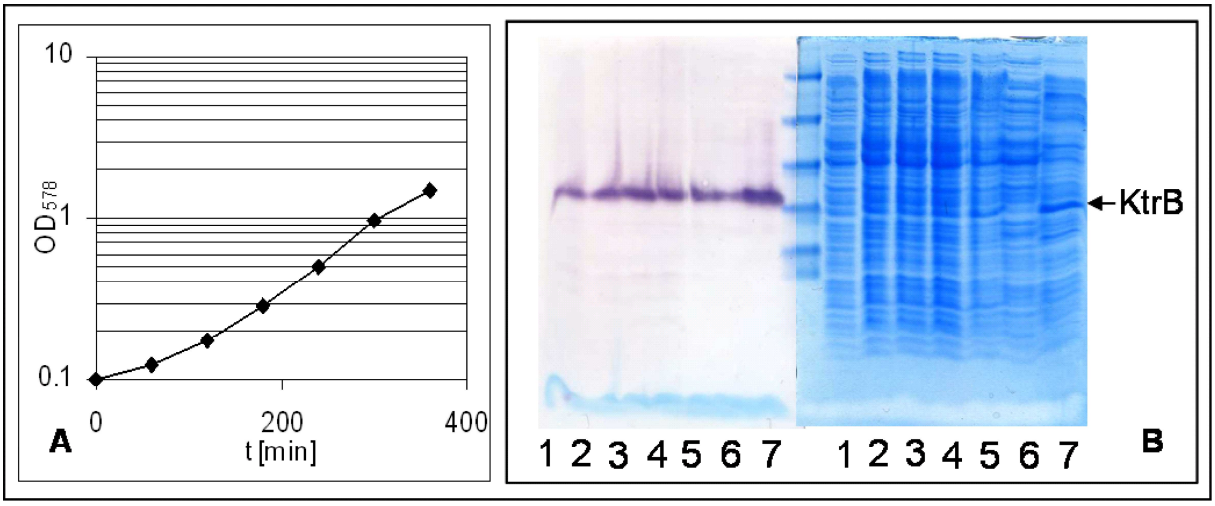

Figure 3. **Overproduction of KtrB-His$_6$ in LB2003/pEL903. A**: Growth curve of LB2003/pEL903 grown in K3 glycerol-containing minimal medium induced with 0.02% L-arabinose. **B**: KtrB production and fractionation during overproduction and cell disruption documented via Western blot analysis and Coomassie brilliant blue stained SDS-PAGE. 1: OD_{578} 0.24; 2: OD_{578} 0.5; 3: OD_{578} 1.0; 4: OD_{578} 1.45; 5: low speed pellet; 6: cytoplasm; 7: membrane fraction; each lane contains 15 µg of protein. In the Western blot analysis, KtrB-His$_6$ was detected by monoclonal mouse penta-His antibody.

δ as the weight ratio of bound lipids and detergents in the lipid-detergent-protein micelles. With the known molecular mass of 66.4 kDa for BSA and a constant dn_c/dn_p for soluble proteins of 0.18 the constant k was calculated.

Other methods. The protein concentration was determined according to Lowry et al. (47) or by measuring the absorbance A_{280} and by using the Lambert-Beer law: $A_{280} = \varepsilon/c$ to calculate the concentration with the protein specific molar extinction coefficient ε (48). A cell suspension with an OD_{578} value of 1.0 was taken to contain 0.3 mg dry wt/ml (49). Uptake of K^+ and Rb^+ by the cells was calculated as described in (8). Kinetics of cation uptake were determined by the Eadie-Hofstee method (50).

RESULTS and DISCUSSION

Active transport of K^+ and Rb^+ in E. coli LB2003 expressing KtrB-His$_6$. In the past, KtrB-His$_6$ was purified from *E. coli* Rosetta2^{TM} (DE3) pRARE2/pEL903 in order to perform biochemical and biophysical experiments. High amounts of protein were achieved (1 mg KtrB-His$_6$/5 l LB medium) by fermenting cells in a 5 l culture to an optical density up to 10, but due to the presence of all endogenous *E. coli* K^+ uptake systems, the activity of KtrB-His$_6$ could not be determined by transport or complementation assays. Therefore, to obtain direct evidence of actively folded His-tagged KtrB the protein was overproduced in strain LB2003, which lacks all endogenous K^+ uptake systems. By culturing these cells transformed with pEL903 in minimal medium with less than 10 mM potassium ions, growth can only be obtained in the presence of functional KtrB. Complementation studies of cells synthesizing His-tagged KtrB were comparable to those carrying WT-KtrB. Cell growth was observed even with K^+ concentration as low as 0.1 mM (data not shown). However, the kinetic analysis of the K^+ transport showed that His-tagged KtrB transported K^+ with a twenty-five-fold lower affinity than WT-KtrB [K_m values for K^+ uptake of about 0.6 and 0.02 respectively; Fig. 2A and (8)], whereas the V_{max} value did not change. In addition, the kinetics of $^{86}Rb^+$ uptake into LB2003/pEL903 were determined. Again, the uptake velocity was the same, but the affinity for Rb^+ was about fourfold lower than for K^+ [0.6 mM for K^+ and 2.7 mM for Rb^+, respectively, Fig. 2A and 2B]. The data obtained were in good agreement with KtrAB, for which a lower affinity for Rb^+ was described as well (51). However, K^+ could be replaced by Rb^+ quite efficiently, since transport activity of His-tagged KtrB was shown either by K^+ and Rb^+ uptakes.

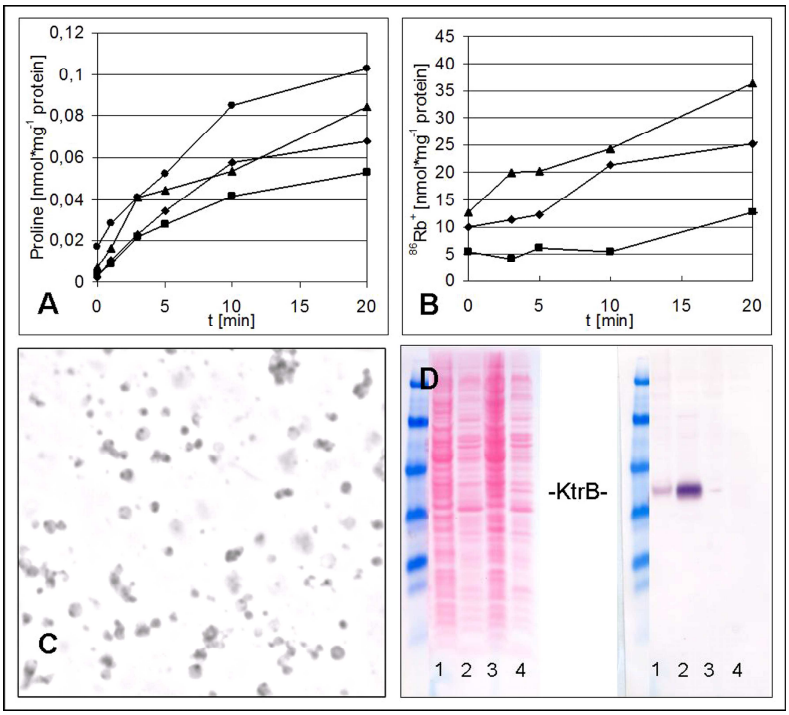

Figure 4. **Proline and rubidium ion uptake into right-side-out membrane vesicles.** The uptakes into Na-vesicles dissolved in 50 mM NaP_i, pH 6.6, 10 mM $MgSO_4$, and 20 mM D-lactate were started by either the addition of 3.5 µM 1µCi/mL $_L$-[U-^{14}C]proline (Amersham) or 2 mM 1µCi/mL ^{86}RbCl (PerkinElmer) and terminated by the addition of 2 mL ice cold 0.1 M lithium chloride, immediately filtered through 0.2 µm cellulose nitrate filters. **A:** Proline uptake by ◆ 165 µg, ▲ 81 µg or ●39 µg vesicle protein from LB2003/pEL903 containing KtrB-His_6 or ■ by vesicles from LB2003/pBAD18 without KtrB (150 µg).

Overproduction of KtrB-His_6 in LB2003 grown in the presence of low K^+ concentrations. In consequence of the positive complementation and the transport studies, cells were grown in glycerol-containing minimal medium with 3 mM KCl under permanent induction with 0.02% L-arabinose resulting in production of active KtrB-His_6 right from the start of the cultivation as indicated by the observed cell growth (Fig. 3A). The Western blot analysis of samples taken during cultivation showed that equal amounts of KtrB-His_6 per milligram total protein were present at any time supporting that more and more KtrB-His_6 was produced during cell growth. However, due to substrate limitation in the minimal medium the cells only grew to an optical density of 1.5 to 2. Thus a fermentation of the cells in 30 liters of glycerol-containing minimal medium was necessary to obtain sufficient amounts of recombinant protein. The harvested cells were disrupted by sonication and fractionated by low- and high-speed centrifugation resulting in a low-speed-fraction, the cytoplasm, and the membrane fraction. As demonstrated by Western blot analysis and SDS-PAGE approximately 70% of the His-tagged KtrB were found in the membrane fraction while around 30% were located in the low-speed-fraction (Fig. 3B, lanes 7 and 5, respectively), probably representing aggregated material in inclusion bodies and or aggregated cell fractions. Such a distribution of KtrB is comparable to that found for Rosetta2^{TM} (DE3) pRARE2/pEL903, however, now the system provides a guarantee of functional KtrB-His_6 in the membrane.

Right-side-out vesicles of KtrB-His_6-containing LB2003 showed Rb^+ uptake activity. In order to proof the activity of KtrB-His_6 in membrane vesicles independent of the cytoplasmic components, sodium-loaded, right-side-out vesicles were prepared from LB2003/pEL903 (Fig. 4D, lanes 1 and 2) and analyzed for uptake of $^{86}Rb^+$. Vesicles from LB2003/pBAD18 served as negative control (Fig. 4D, lanes 3 and 4). The well established lactate-activated [^{14}C]-proline transport was used as a control to verify the proper preparation of right-side-out vesicles. As shown in Fig. 4A both, vesicles with and without KtrB-His_6, revealed proline transport activity independent of the vesicle concentration. The uptake of $^{86}Rb^+$ into the vesicles also energized with lactate showed a distinct difference between vesicles containing KtrB-His_6 and control vesicles. Without KtrB only a residual $^{86}Rb^+$ uptake rate was observed, whereas the significant uptake dependent on KtrB was not much slower than the valinomycin-mediated uptake (Fig. 4B). In both approaches, the transport of proline as well as of rubidium ions, the uptake rates were about 50% slower than described in former publications (36;37). These observations could be explained by the type of cells used for the experiments: Strain LB2003 is an *E. coli* K12 derivative known to be difficult to handle in vesicle preparation (52) The picture taken from the membrane vesicle preparation (Fig. 4C) shows beside nicely shaped vesicles aggregates of vesicles and bulky components as has also been described by Kaback (34) for vesicles prepared

from K12 cells. Parts of these vesicles might be inactive, thus leading to an overestimation of active membrane vesicles resulting in a lower activity per mg of membrane protein. The preferred strain for vesicle preparation is *E. coli* ML308 and the data published for proline as well as rubidium ion transports were performed with right-side-out vesicles from this strain. Thus, the data support that the Rb^+ uptake was still very efficient, displaying the continued activity of KtrB-His_6 during membrane preparation.

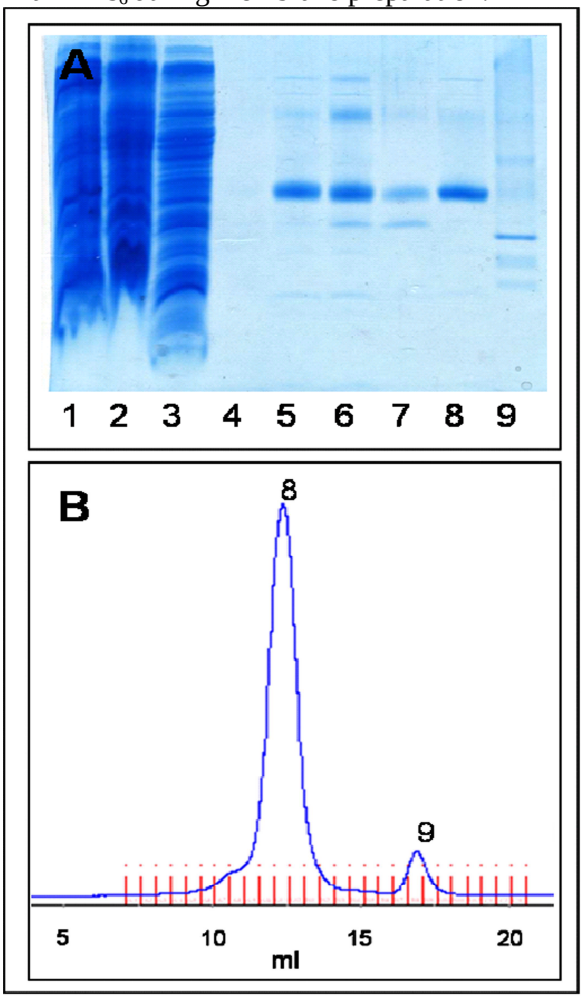

Figure 5. **Purification of KtrB-His_6 via Ni^{2+} affinity chromatography and gel filtation on a Superdex 200 column. A:** SDS-PAGE of the different solubilization and purification steps. 1: before solubilization; 2: supernatant after solubilization; 3: flow-through of the Ni-NTA matrix after 1 h of binding; 4: after washing with 50x buffer W with 50 mM imidazole; 5-7: elutions E_1-E_3 from Ni-NTA with buffer W with 500 mM imidazole; 8: pure KtrB-His_6 eluted at 12.5 ml in gel filtration in buffer W without imidazole; 9: degradation product of KtrB seperated via gel filtration at 17.5 ml. 10 µL of a sample were added per lane. **B**: Chromatogram of the UV_{280} absorbance of the gel filtration of KtrB-His_6 in buffer W on a Superdex 200 column. Numbers 8 and 9 correspond to A.

In addition, these measurements provide information about KtrB alone compared to the KtrAB system. Whereas the KtrAB complex requires ATP and a membrane potential for its activity (14), KtrB was shown here to transport rubidium ions in the absence of ATP. As a consequence, the data suggest that ATP is only involved in regulation of the KtrA oligomer, which thereby regulates the activity of the entire transport system as has been postulated by Kröning et al. (14) and Albright et al. (15). The role of the membrane potential on KtrB activity was not analyzed in the present study, since a membrane potential was still established over the membrane of the right-side-out vesicles.

Effective solubilization of KtrB obtained a monodispersed protein peak in gel filtration. In the next step DDM was used to solubilize all membrane proteins to finally purify KtrB-His_6. It has been reported that high concentrations of detergent decrease the enzyme activity (53), therefore, the DDM concentration was decreased from 1.5% to 1% (w/v). In addition, the protein concentration was lowered from 20 mg/mL to 10 mg/mL. Under these conditions at least 90% of the membrane-bound protein was solubilized (Fig. 5A, lanes 1 and 2.). In the subsequent affinity chromatography via Ni^{2+}-NTA agarose, KtrB-His_6 was purified to considerable purity, but with a degradation product still present (Fig. 5A, lanes 5-7). For removal of this contamination gel filtration on a Superdex 200 column was performed. Beside a monodispersed peak at 12 to 12.5 ml (Fig. 5B, no. 8) a small peak at 17.5 ml (Fig. 5B, no. 9) was visible. While the first peak contained the pure His-tagged KtrB protein, the second peak comprised the degradation product. With this purification protocol 5 mg KtrB-His_6 were purified from a 30 L cell culture. Thus, similar amounts per g cells were obtained compared to the previously described protocol, but KtrB is present in high purity and in an active conformation.

Slow $^{86}Rb^+$ uptake into KtrB-His_6-containing proteoliposomes revealed a channel-like activity. For several K^+ channels uptake was determined based on a countertransport assay (42;43). For that purpose, trace amounts of radioactively-labeled rubidium ions were added to proteoliposomes preloaded with high K^+ concentrations (400 mM KCl) followed by a rapid exchange of external K^+ by sorbitol. For active channels this procedure resulted in an efflux of K^+, thereby creating an internally negative membrane potential, which in turn drives the uptake of $^{86}Rb^+$ into the proteoliposomes. The

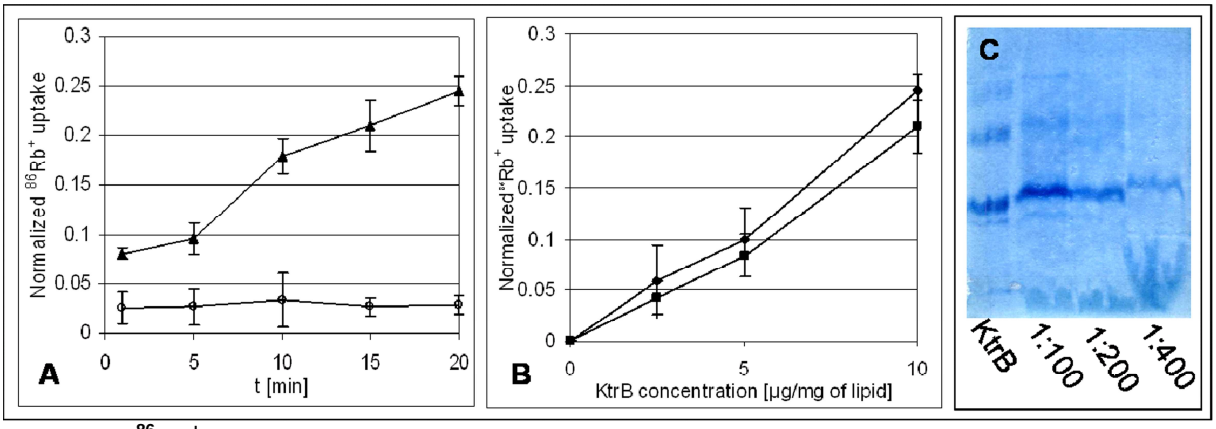

Figure 6. **$^{86}Rb^+$ uptake into KtrB-His$_6$-containing proteoliposomes.** **A**: Time dependence of normalized rubidium uptake of ▲ proteoliposomes with 10 µg of KtrB per mg of lipids and ◇ empty liposomes treated equally as the proteoliposomes. **B**: Plot of normalized rubidium uptake at ■ 15 and ◆ 20 minutes as a function of the amount of protein present in proteoliposome preparation. Error bars correspond to standard deviation calculated from two independent measurements, uptakes normalized against the uptake with the addition of 16 µM valinomycin. **C**: SDS PAGE of KtrB before and after the reconstitution. Theoretically equal amounts of KtrB before the reconstitution and after a 1:100 reconstitution. 1:200 corresponds to 50% and 1:400 to 25% of the 1:100 reconstitution. In addition to the sample buffer 2.5 mM SDS was added to the lipid containing samples to improve the seperation.

influx of rubidium ions after the addition of valinomycin served as a control, and was counted as the maximal uptake rate. In this study Rb^+ uptake experiments according to this protocol were performed applying proteoliposomes created by a different protocol and by stopping the uptake by dilution of the samples 1:50 in ice cold 0.1 M LiCl and subsequent filtration of the proteoliposomes through cellulose nitrate filters. The new method of reconstitution worked well for KtrB-His$_6$ as shown in Fig. 5C and the filter assay, a well established method in the laboratory of Bert Poolman (Groningen University), is very quick resulting in exact time points. Fig. 6A shows the uptake of $^{86}Rb^+$ via KtrB into the liposomes. Within 20 minutes 25 % rubidium ions compared to the valinomycin control were taken up, whereas no significant uptake was observed for liposomes without protein. Fig. 6B demonstrates that the uptake of rubidium ions was proportional to the protein concentration. At a ratio of 10 µg KtrB per mg of lipids no saturation was observed demonstrating the high quality of the reconstitution method. Parallel to this study Albright et al. (27) published data from an equally performed experiment, however, in their hands, saturation was reached already at a concentration of 5 µg/mg lipid. Furthermore, the uptake observed was by a factor of 2.5 slower, although the same protein to lipid ratio was used. In conclusion, the results clearly demonstrate that the purification and reconstitution protocol allowed the reconstitution of highly active KtrB protein.

The low Rb^+ uptake rates indicate that reconstituted KtrB alone shows channel-like activity as has been also discussed by Albright et al. (27). For a channel-like activity no further energy is needed and the uptake is driven just by the presence of an electrochemical gradient as observed in these measurements. However, the slow uptake compared to the fast flow of K^+/Rb^+ through the potassium channel KcsA (saturation within 3 minutes, (42)) revealed that not only the complete KtrAB system, but also the K^+-translocating subunit KtrB alone must consist of specific differences resulting in a transporter instead of a channel. A specific transporter architecture might cause sterical hindrance for the free diffusion of K^+/Rb^+. An additional, so far non identified gate, proposed to be present in every transporter (54;55), could be the reason. Such two gates instead of only one normally enable an occluded state of the transported substrate, which is indispensable for transport activity against a corresponding gradient. If channeling is needed instead of transporting, as in this assay, this additional gate might hinder the activity. Nevertheless, the data revealed at least the functionality of the solubilized and reconstituted KtrB protein allowing further structural and functional analyses.

KtrA forms an octamer in solution, KtrB a dimer, but the purified KtrAB complex has rather a 16 to 2 than an 8 to 2 stoichiometry. In order to gain an understanding on the stoichiometry of both, the single subunits and the KtrAB complex, size-exclusion chromato-

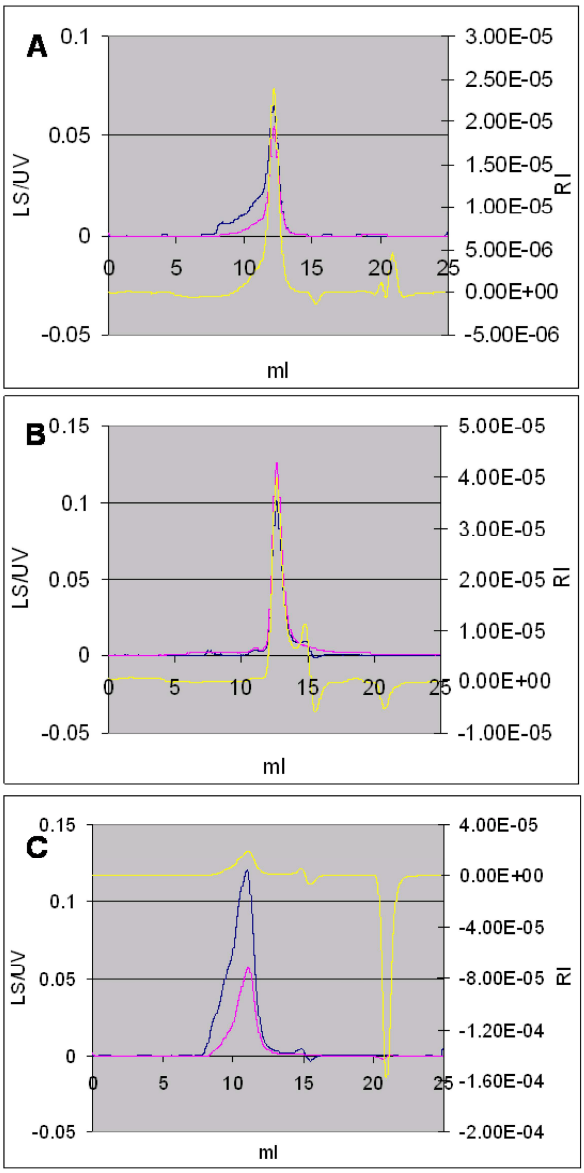

Figure 7. **Size exclusion chromatography combined with light scattering, UV, and refractive index measurements on His_{10}-KtrA, KtrB-His_6, and His_{10}-KtrAB.** Measurements were performed on a Superdex 200 column with proteins purified via Ni^{2+}-NTA affinity chromatography and size exclusion chromatography in buffer W without imidazole. The three signals were detected in a row by three independent detectors during gel filtration. **A**: Chromatograms of His_{10}-KtrA. **B**: Chromatograms of KtrB-His_6. **C**: Chromatograms of His_{10}-KtrAB. In blue: light scattering, in pink: UV_{280} absorbance, in yellow: refractive index.

graphy coupled to light scattering, UV absorbance, and refractive index measurements (SEC-LS/UV/RI) was performed with the purified proteins. For that purpose, KtrB and the KtrAB complex were purified according to the protocol presented in this study. In addition, KtrA was purified from the cytoplasm where it is present at least in part. KtrA has been shown to be synthesized actively in *E. coli* before (14), thus it was not necessary to change this protocol. The affinity chromatography and gel filtration procedure was performed identically with all three preparations. In addition, BSA as a well characterized protein was used on SEC-LS/UV/RI to calculate the buffer-dependent constants K in equation [1] and k in equation [2], which were necessary to estimate the molecular mass and the detergent-lipid to protein ratio of the target proteins from equations 1 to 3 by using the values for (UV), (LS) and (RI) detected in the SEC. From these measurements, an oligomeric state of 7.99 for KtrA was calculated (Fig. 7A) with a molecular mass of 210.5 kDa (by Debye fitting method with ASTRA software, Wyatt Technology Corporation). The calculated oligomeric state of KtrB was 2.26 with a molecular mass of 112.1 kDa (Fig. 7B). Thus, these data confirmed the oligomeric states determined by Albright et al. (15) before. As expected, no detergent was attached to KtrA, a soluble protein peripherally attached to the membrane-bound KtrB. The aberration of 0.26 for KtrB resulted from the slight overlap of the protein peak with the peak of the detergent-lipid micelles. This peak occurred from lipid molecules, which remained associated with KtrB during the purification procedure and leaked off into the buffer of the injected samples. Therefore, mixed lipid-detergent micelles were formed at the expense of pure detergent micelles as demonstrated by the following negative peak (Fig. 7B, yellow RI and blue LS chromatogram). This disturbed the accuracy of the calculation. For KtrB a lipid-detergent to protein ratio of 1.01 (w/w) was calculated corresponding to an associated detergent micelle of 122.3 kDa. The complex of KtrB with detergent and lipid molecules thus had a total molecular mass of 234.4 kDa, which is very similar to 238 kDa calculated in (15). For the calculation of the KtrAB complex, different stoichiometries with different total molar extinction coefficients have been taken into account to find the best fit between the theoretical molecular masses and the calculated molecular masses based on the (UV), (RI) and (LS) values together with the corresponding extinction coefficient (Tab. 2). Since all RCK domains of different systems described so far formed dimers or a multiple of this, only these where followed in the calculation of KtrA. KtrB was assumed to exist as monomer or dimer only.

theor. stoichiometry	Extinction coefficient	M_W (pred)	M_W (calc) at 11.35ml
8x KtrA+ 2x KtrB	0.57011034	309.94	573.737606
8x KtrA+ 1x KtrB	0.46977055	260.276	608.549837
8x KtrA+ 0x KtrB	0.322	210.612	887.822336
4x KtrA+ 2x KtrB	0.69773351	204.634	409.724897
4x KtrA+ 1x KtrB	0.57011034	154.97	501.444669
4x KtrA+ 0x KtrB	0.322	105.306	887.822336
10x KtrA+ 2x KtrB	0.53409746	362.593	535.255855
12x KtrA+ 2x KtrB	0.50721741	415.246	563.621807
16x KtrA+ 2x KtrB	0.46977055	520.552	608.549837

Table 2. **Summary of calculated and predicted molecular masses for different stoichiometries of KtrAB.** The extinction coefficients were calculated from the amino acid sequence of KtrA and KtrB with ProtParam, the predicted molecular masses were calculated from the molecular masses of the subunits and the calculated molecular weights were calculated with equation [1]. The best match is shown in red.

From these calculations 16-fold KtrA with 2-fold KtrB resulted as the best match (calculated 608.5 kDa/predicted 520.5 kDa), but with a large deviation of 88 kDa (as highlighted in Table 2). This deviation resulted from the non-Gaussian distribution of each curve. The injected protein solution was probably not completely homogeneous, thereby preventing a correct calculation. Nevertheless, this calculation differed strongly from the predictions of Albright et al. (15), proposing an 8 to 2 composition.

The octameric structure of KtrA was also shown by crystal structures (15). With different adenin-containing compounds a square or a rectangle conformation was crystallized with either a 4-fold or a 2-fold symmetry. A similar gating ring was also found for MthK-RCK with an up-and-down architecture (28) However, only the 4-fold symmetry was found for MthK (28). Albright et al. (15) discussed conclusively a conformational change induced by the binding of different compounds resulting in an opening and closing of the ring. In compliance with each other, we also found a dimeric conformation of KtrB in solution, which was confirmed by Albright et al. (27) with crosslinking studies in the membrane-bound KtrB as well as in solution. In additional light scattering measurements of KtrAB complexes Albright et al (15) found an 8 to 2 stoichiometry, which led them to the conclusion that the octameric KtrA ring binds to a dimer of KtrB. Since the KtrB monomer is proposed to be very asymmetric at the cytoplasmic half of the membrane (15;23) they argued that only a dimer would fit with the observed 2- or 4-fold symmetry of the octameric KtrA ring and showed that its diameter is big enough to insert a KtrB dimer (Fig. 8B). They further hypothesized that the changes found in the octameric ring might move some cytoplasmic loops of the KtrB

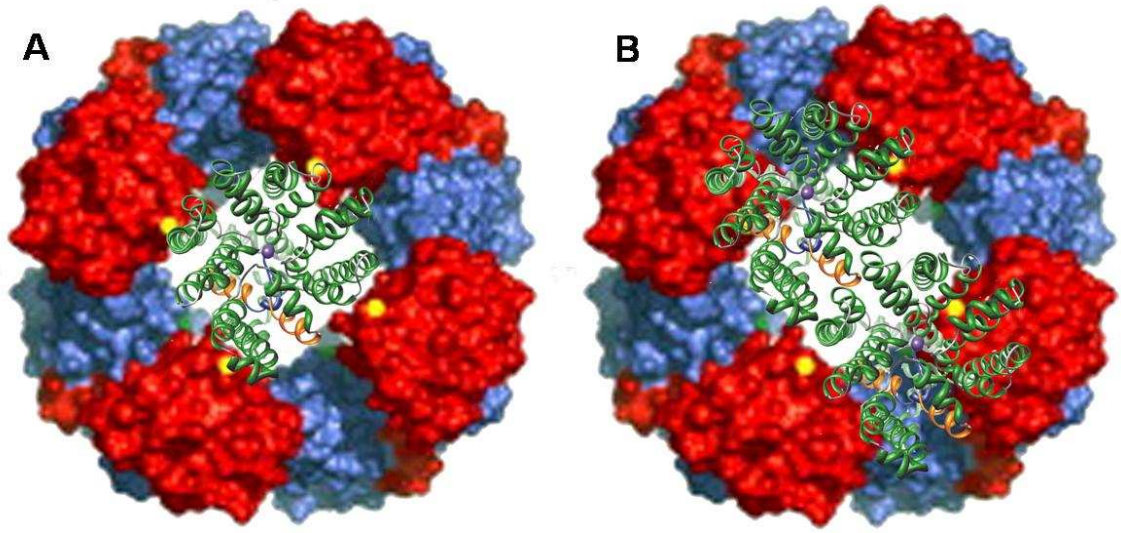

Figure 8. **Modeling the interaction of the octameric KtrA ring with KtrB.** The octameric ring of KtrA (shown in blue and red) illustrates the crystal structure (15), the hypothetical structure of KtrB shown in green is taken from (23). **A:** Monomeric KtrB centered on top of the octameric KtrA ring as shown for MthK (28). **B:** Dimer of KtrB on top of the octameric ring as proposed by Albright et al. (27).

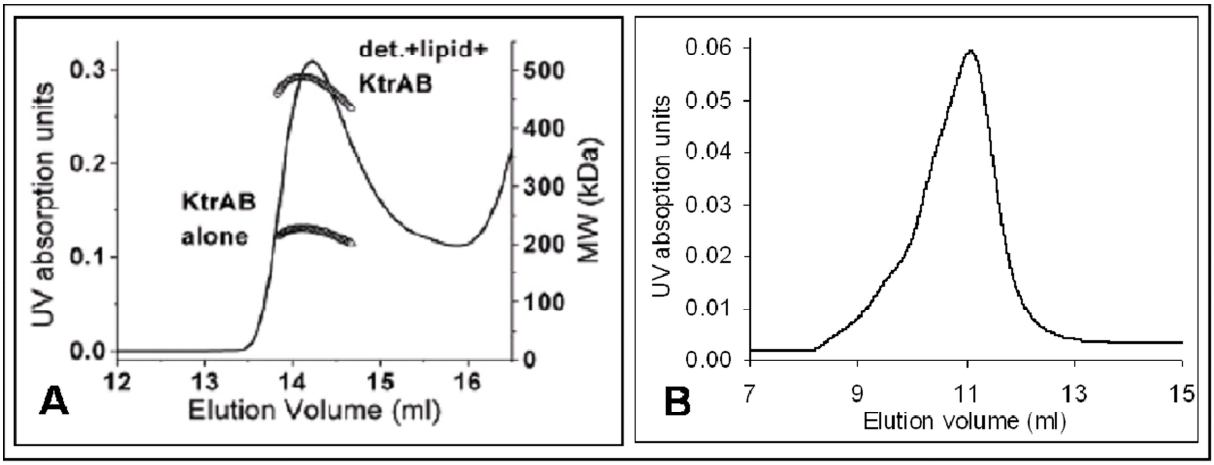

Figure 9. **UV_{280} chromatograms of KtrAB formed by mixing purified KtrA and KtrB or by purifying the KtrAB complex.** Comparison of UV_{280} chromatograms published by Albright et al. (15) **(A)** and detected in the measurements presented in this study **(B)**.

dimer, which open and close the pore. This assumption is well argued, but striking evidence is missing so far. The K^+ channel MthK, as the most prominent example, has been shown to consist of a tetrameric channel subunit with four covalently linked RCK domains and four independent RCK domains, in total forming an octameric ring (28). This in principal reveals a 1 to 8 stoichiometry. According to this, the 16:2 stoichiometry calculated from measurement obtained in this study could represent two KtrAB complexes with a 8:1 stoichiometry stacked together back- to-back similar to the observed crystal structure of MthK (28). Such a conformation/ aggregation might stabilize the protein in solution. A modeling of one KtrB on top of the octameric KtrA ring (Fig. 8A) thus demonstrates another possible arrangement of the subunits to each other. Since KtrB was predicted to contain large cytoplasmic loops (23), one can argue that these would enable the fit of the monomer on the 2-fold as well as on the 4-fold symmetric octameric KtrA ring observed in (15). In this context it is worthwhile mentioning that the KtrAB complex analyzed by Albright et al. (15) was formed in vitro and that functional assays for the complexes are completely missing. In contrast, the KtrAB complex in this study was purified from the LB2003 strain grown in minimal medium with only 3 mM potassium chloride thus allowing an immediate control of the synthesis of a functional KtrAB complex. Another interesting point are the chromatograms of the SEC-LS/UV/RI measurements. Although the deviation between the calculated and the predicted molecular mass presented by Albright et al. (15) was very small (1 kDa) compared to the aberration from the calculation in this studiy (88 kDa), their chromatogram as well showed no Gaussion distribution of the peak (compare Fig. 9A and B) leading to the conclusion that their calculations might be improper as well. In both measurements more than one conformation appeared to be present. Thus, further investigations with the isolated KtrAB complex are necessary to improve the purification with a subsequent repeat of the light scattering measurements. In addition, a functional assay to analyze the transport activity of differently purified and/or formed KtrAB complexes would be important to assess the relevance of the found stoichiometry.

CONCLUSION

The two main problems discussed in this study affect each other, but vice versa solving one problem would help to solve the other one. With a functional transport assay, the differences affected by different purification and also reconstitution methods could be visualized. Once a protocol is established for KtrB alone, it should be easily transferred to the complex as well. This of cause would also allow to further investigate the influence of different adenine-containing compounds or cations on the transport activity as well. Vice versa a proper purification resulting in a functionally folded protein is most important to end up with a functional assay for a reconstituted transporter. With the procedure and methods presented here, this was shown at least for subunit KtrB. Although only a channel-like activity was observed for KtrB with the proteoliposomal uptake assay it can be assumed that this displays an active protein analyzed with an improvable method.

REFERENCES

1. Geertsma, E. R., Groeneveld, M., Slotboom, D. J., and Poolman, B. (2008) *Proc.Natl.Acad.Sci.U.S.A* **105,** 5722-5727

2. Dalbey, R. E. and Chen, M. (2004) *Biochim.Biophys.Acta* **1694,** 37-53

3. Drew, D., Froderberg, L., Baars, L., and De Gier, J. W. (2003) *Biochim.Biophys.Acta* **1610,** 3-10

4. Raman, P., Cherezov, V., and Caffrey, M. (2006) *Cell Mol.Life Sci.* **63,** 36-51

5. Wang, D. N., Safferling, M., Lemieux, M. J., Griffith, H., Chen, Y., and Li, X. D. (2003) *Biochim.Biophys.Acta* **1610,** 23-36

6. de Lima, S. H. and Ciancaglini, P. (2000) *Biochem.Educ.* **28,** 178-182

7. Rigaud, J. L., Levy, D., Mosser, G., and Lambert, O. (1998) *Eur Biophys J* 305-319

8. Tholema, N, Vor der Brüggen, M., Mäser, P, Nakamura, T., Schroeder, J. I., Kobayashi, H., Uozumi, N., and Bakker, E. P. (2005) *J.Biol.Chem.* **280,** 41146-41154

9. Tholema, N., Bakker, E. P., Suzuki, A., and Nakamura, T. (1999) *FEBS Lett.* **450,** 217-220

10. Nakamura, T., Yuda, R., Unemoto, T., and Bakker, E. P. (1998) *J.Bacteriol.* **180,** 3491-3494

11. Kawano, M., Abuki, R., Igarashi, K., and Kakinuma, Y. (2000) *J.Bacteriol.* **182,** 2507-2512

12. Matsuda, N., Kobayashi, H., Katoh, H., Ogawa, T., Futatsugi, L., Nakamura, T., Bakker, E. P., and Uozumi, N. (2004) *J.Biol.Chem.* **279,** 54952-54962

13. Holtmann, G., Bakker, E. P., Uozumi, N., and Bremer, E. (2003) *J.Bacteriol.* **185,** 1289-1298

14. Kröning, N., Willenborg, M., Tholema, N., Hänelt, I., Schmid, R., and Bakker, E. P. (2007) *J.Biol.Chem.* **282,** 14018-14027

15. Albright, R. A., Ibar, J. L., Kim, C. U., Gruner, S. M., and Morais-Cabral, J. H. (2006) *Cell* **126,** 1147-1159

16. Stumpe, S. and Bakker, E. P. (1997) *Arch.Microbiol.* **167,** 126-136

17. Stumpe, S., Schlösser, A., Schleyer, M., and Bakker, E. P. (1996) K^+ circulation across the prokaryotic cell membrane: K^+-uptake systems. In Konings, W. N., Kaback, H. R., and MacKinnon, R., editors. *Handbook of Biological Physics: Transport Processes In Eukaryotic and Prokaryotic Organisms*, Elsevier Sience B.V., Amsterdam

18. Nissen, P., Hansen, J., Ban, N., Moore, P. B., and Steitz, T. A. (2000) *Science* **289,** 920-930

19. Booth, I. R. (1985) *Microbiol.Rev.* **49,** 359-378

20. Epstein W. (1986) *FEMS Microbiol.Rev.* **39,** 73-78

21. Dinnbier, U., Limpinsel, E., Schmid, R., and Bakker, E. P. (1988) *Arch.Microbiol.* **150,** 348-357

22. Durell, S. R., Hao, Y., Nakamura, T., Bakker, E. P., and Guy, H. R. (1999) *Biophys.J.* **77,** 775-788

23. Durell, S. R. and Guy, H. R. (1999) *Biophys.J.* **77,** 789-807

24. Bertrand, J., Altendorf, K., and Bramkamp, M. (2004) *J.Bacteriol.* **186,** 5519-5522

25. van der Laan, M., Gassel, M., and Altendorf, K. (2002) *J.Bacteriol.* **184,** 5491-5494

26. Mäser, P., Hosoo, Y., Goshima, S., Horie, T., Eckelman, B., Yamada, K., Yoshida, K., Bakker, E. P., Shinmyo, A., Oiki, S., Schroeder, J. I., and Uozumi, N. (2002) *Proc.Natl.Acad.Sci.U.S.A* **99,** 6428-6433

27. Albright, R. A., Joh, K., and Morais-Cabral, J. H. (2007) *J.Biol.Chem.* **282,** 35046-35055

28. Jiang, Y., Lee, A., Chen, J., Cadene, M., Chait, B. T., and MacKinnon, R. (2002) *Nature* **417,** 515-522

29. Novy, R., Drott, D., Yaeger, K., and Mierendorf, R. (2001) *inNovations* 1-3

30. Guzman, L. M., Belin, D., Carson, M. J., and Beckwith, J. (1995) *J Bacteriol.* **177,** 4121-4130

31. Epstein, W. and Kim, B. S. (1971) *J Bacteriol.* **108,** 639-644

32. Studier, F. W. (1991) *J Mol.Biol.* **219,** 37-44

33. Schägger, H. and von Jagow, G. (1987) *Anal.Biochem.* **166,** 368-379

34. Kaback, H. R. (1971) *Methods Enzymol.* 99-120

35. Altendorf, K., Harold, F. M., and Simoni, R. D. (1974) *J Biol.Chem.* **249,** 4587-4593

36. Hirata, H., Altendorf, K., and Harold, F. M. (1973) *Proc.Natl.Acad.Sci.U.S.A* **70,** 1804-1808

37. Altendorf, K., Hirata, H., and Harold, F. M. (1975) *J Biol.Chem.* **250,** 1405-1412

38. Driessen, A. J. and Konings, W. N. (1993) *Methods Enzymol.* **221,** 394-408

39. Mayer, L. D., Hope, M. J., and Cullis, P. R. (1986) *Biochim.Biophys.Acta* **858,** 161-168

40. Knol, J., Sjollema, K., and Poolman, B. (1998) *Biochemistry* **37,** 16410-16415

41. Knol, J., Veenhoff, L., Liang, W. J., Henderson, P. J., Leblanc, G., and Poolman, B. (1996) *J.Biol.Chem.* **271,** 15358-15366

42. Heginbotham, L., Kolmakova-Partensky, L., and Miller, C. (1998) *J Gen.Physiol* **111,** 741-749

43. Nimigean, C. M. (2006) *Nat.Protoc.* **1,** 1207-1212

44. Slotboom, D. J., Duurkens, R. H., Olieman, K., and Erkens, G. B. (2008) *Methods* **46,** 73-82

45. Wen, J., Arakawa, T., and Philo, J. S. (1996) *Anal.Biochem.* **240,** 155-166

46. Wei, Y., Li, H., and Fu, D. (2004) *J Biol.Chem.* **279,** 39251-39259

47. Lowry, O. H., Rosebrough, N. J., Farr, A. L., and Randall, R. J. (1951) *J Biol.Chem.* **193,** 265-275

48. Pace, C. N., Vajdos, F., Fee, L., Grimsley, G., and Gray, T. (1995) *Protein Sci.* **4,** 2411-2423

49. Bakker, E. P. and Mangerich, W. E. (1981) *J.Bacteriol.* **147,** 820-826

50. Fersht, A. (1985) *Enzyme structure and mechanism*, W. H. Freeman and company, New York

51. Tholema, N.(2002) KtrB, die K^+-translozierende Untereinheit des K^+-Aufnahmesystems KtrAB aus *Vibrio alginolyticus*: Analyse der Selektivitätsfilter-Glycinreste und der Topologie**.** Universität Osnabrück, Dissertation

52. Kaback, H. R. (1972) *Biochim.Biophys Acta* **265,** 367-416

53. Tandon, S. and Horowitz, P. M. (1987) *J Biol.Chem.* **262,** 4486-4491

54. Gadsby, D. C. (2009) *Nat.Rev.Mol.Cell Biol.* **10,** 344-352

55. Gadsby, D. C. (2004) *Nature* **427,** 795-797

FOOTNOTES

The SEC-LS/UV/RI measurements presented in this chapter were performed at the Department of Biochemistry, University of Groningen, The Netherlands in collaboration with Dr. Dirk-Jan Slotboom.

Chapter III

III

GAIN OF FUNCTION MUTATIONS IN MEMBRANE REGION M_{2C2} OF KtrB OPEN A GATE CONTROLLING K^+ TRANSPORT BY THE KtrAB SYSTEM FROM *VIBRIO ALGINOLYTICUS*

Published in 2010 in J. Biol. Chem **285**, 10318-10327

GAIN OF FUNCTION MUTATIONS IN MEMBRANE REGION M_{2C2} OF KtrB OPEN A GATE CONTROLLING K^+ TRANSPORT BY THE KtrAB SYSTEM FROM *VIBRIO ALGINOLYTICUS**

Inga Hänelt, Sara Löchte[#], Lea Sundermann, Katharina Elbers, Marc Vor der Brüggen, and Evert P. Bakker

Department of Microbiology,University of Osnabrück

Running title: Gain of function mutations open a K^+-transport gate in KtrB

KtrB, the K^+-translocating subunit of the Na^+-dependent bacterial K^+ uptake system KtrAB consists of four M_1PM_2 domains, in which M_1 and M_2 are transmembrane helices and P indicates a p-loop that folds back from the external medium into the cell membrane. Transmembrane stretch M_{2C} is with its forty residues unusually long. It consists of three parts, the hydrophobic helices M_{2C1} and M_{2C3}, which are connected by a non-helical M_{2C2} region, containing conserved glycine, alanine, serine, threonine and lysine residues. Several point mutations in M_{2C2} led to a huge gain of function of K^+ uptake by KtrB from the bacterium *Vibrio alginolyticus*. This effect was exclusively due to an increase in V_{max} for K^+ transport. Na^+ translocation by KtrB was not affected. Partial to complete deletions of M_{2C2} also led to enhanced V_{max} values for K^+ uptake via KtrB. However, several deletion variants also exhibited higher K_m values for K^+ uptake, and at least one deletion variant, $KtrB_{\Delta 326-328}$ transported Na^+ also faster. The presence of KtrA did not suppress any of these effects. For the deletion variants, this was due to a diminished binding of KtrA to KtrB. PhoA studies indicated that M_{2C2} forms a flexible structure within the membrane allowing M_{2C3} to be directed either to the cytoplasm or (artificially) to the periplasm. These data are interpreted to mean i) that region M_{2C2} forms a flexible gate controlling K^+ translocation at the cytoplasmic side of KtrB, and ii) that M_{2C2} is required for the interaction between KtrA and KtrB.

This chapter has been published as Hänelt et al. in J. Biol. Chem 285, 10318-10327, 2010

FOOTNOTES

* We thank Eva Limpinsel for expert technical assistance. This work was supported by SFB431, Teilprojekt P6 from the Deutsche Forschungsgemeinschaft.

Present address, Abteilung Biophysik, University of Osnabrück, D-49076 Osnabrück, Germany

The PhoA-fusion studies presented in this chapter derived from the PhD thesis of Dr. Marc Vor der Brüggen (2007) and from the diploma thesis of Sara Löchte (2008). Sara Löchte in addition performed the GFP-fusion studies, Marc Vor der Brüggen the LacZ fusions. Plasmids pEL903-100, $pKtrB_{S317\rightarrow C}$, $pKtrB_{T318\rightarrow C}$, $pKtrB_{T320\rightarrow C}$, and $pKtrB_{S327\rightarrow C}$ were produced by Marc Vor der Brüggen in his thesis. Plasmids encoding amino acid exchanges of KtrB residues 314, 316, 321, 322, and 324 were produced by Lea Sundermann during her diploma thesis (2008, under my supervision). She also performed first growth and K^+ uptake experiments with the corresponding derivates, which were subsequently reproduced and extended. Katharina Elbers produced plasmids $pKtrAB_{G316\rightarrow S}$, $pKtrAB_{T318\rightarrow C}$, $pKtrAB_{K325\rightarrow Q}$, $pKtrAB_{\Delta 314-328}$, $pKtrAB_{\Delta 318-329}$, and $pKtrAB_{\Delta 326-328}$ (bachelor thesis, 2009, under my supervision) and performed the corresponding K^+ uptakes assays as well as first co-purification assays of these complexes. Eva Limpinsel and Evert P. Bakker performed the assays regarding the KtrB deletion variants.

Chapter IV

IV

MEMBRANE REGION M_{2C2} IN SUBUNIT KtrB OF THE K^+-UPTAKE SYSTEM KtrAB FROM *VIBRIO ALGINOLYTICUS* FORMS A FLEXIBLE GATE CONTROLLING K^+ FLUX; AN ELECTRON PARAMAGNETIC RESONANCE STUDY

MEMBRANE REGION M_{2C2} IN SUBUNIT KtrB OF THE K^+-UPTAKE SYSTEM KtrAB FROM *VIBRIO ALGINOLYTICUS* FORMS A FLEXIBLE GATE CONTROLLING K^+ FLUX; AN ELECTRON PARAMAGNETIC RESONANCE STUDY*

Inga Hänelt[1,#,¶], Dorith Wunnicke[2,#], Meike Müller-Trimbusch[2,§], Marc Vor der Brüggen[1], Inga Kraus[1], Evert P. Bakker[1], and Heinz-Jürgen Steinhoff[2]

[1]Department of Microbiology, University of Osnabrück

[2]Department of Physics, University of Osnabrück

Running title: Membrane region M_{2C2} forms a flexible gate

The K^+-translocating subunit from the K^+ transporter KtrAB contains a fourfold M_1PM_2 motif, reminiscent of the M_1PM_2 motif of K^+ channels. M_1 and M_2 stand for transmembrane stretches and P for a pore-forming loop. Transmembrane stretch M_{2C} is unusual long. In its middle part, termed M_{2C2}, it contains several small and polar amino acids. Region M_{2C2} is flanked by the two α-helices M_{2C1} and M_{2C3} and may form a flexible gate controlling K^+ translocation at the cytoplasmic side of the membrane. In this study we confirm this notion by using continuous wave and pulsed EPR measurements of single and double spin-labeled cysteine variants of KtrB. Most residues in M_{2C2} were shown to be quite immobile pointing to a compact structure. However, the high polarity of some residues indicated the surrounding of an aqueous cavity. Upon the addition of K^+ ions M_{2C2} residue T318R1 moved both with respect to M_{2B} residue D222R1 and to M_{2C3} residue V331R1, but not with respect to M_{2C1}-residue M311R1. Other residues within M_{2B}, M_{2C1}, and M_{2C3} did not move with respect to each other upon the addition of K^+ ions. Two new models for the structure of the M_{2C2} gate inside the KtrB protein were developed by rotamer library analysis using an existing KtrB model. The structure of the open conformation is based on the distances determined between double spin-labeled residues in the presence of K^+ ions and that of the closed conformation on these measurements in the absence of K^+. Since a flexible M_{2C2} gate is missing in potassium channels, it is interpretted to be a transporter-specific structure.

Proteins of the superfamily of potassium transporters (termed SKT proteins) occur in all organisms except animals and are involved in the uptake of K^+ and in some cases Na^+ by the cells (1-3). They are of high importance since the monovalent cations Na^+ and K^+ play a major role in pH-homeostasis and osmoregulation of the cells (4-7). SKT proteins contain a fourfold repeated M_1PM_2 domain, in which M_1 and M_2 stand for transmembrane stretches and P for a p-loop that folds back from the external medium to the middle of the membrane. They are believed to have evolved from simple KcsA-like potassium channels by multiple gene duplications and gene fusions (1;8-10). The four domains $M_{1A}P_AM_{2A}$ to $M_{1D}P_DM_{2D}$ are covalently linked via cytoplasmic loops to one subunit, which differs from the homo-tetrameric KcsA channel composing of four identical M_1PM_2 subunits. The four p-loops are supposed to form together the narrowest part of the K^+-permeation pathway and function as a K^+-selectivity filter (1-3;11). In most SKT proteins one conserved glycine residue within each p-loop is part of this filter (3;12-15). Its composition is less complex than in potassium channels, where the filter is formed by the well-conserved sequence TVGYG from each subunit (16). Sequence alignment studies have shown that major parts of the four M_1PM_2 domains of the different SKT proteins are similar to that of KcsA (11). However, especially their transmembrane stretches M_{2C} and M_{2D} are different. These deviations in SKT proteins are thought to distinguish a cation transporter from a cation channel by either hindering the free diffusion of ions down their electrochemical gradient or by enabling the active transport of ions against this gradient. Positively charged residues in M_{2D} of different SKT proteins have been shown to be essential for cation-transport activity (17). Kato et al. proposed that one or more salt bridges are formed between these residues and negatively charged residues in the pore region, which might reduce electrostatic repulsion during cation permeation and stabilize the transporter structure. Less is known about the function of the deviating region M_{2C}. With about thirty residues it is unusually long and in the middle it contains a cluster of the small and polar residues like alanine, glycine, serine and threonine. This feature is conserved among the prokaryotic SKT protein families

KtrB, TrkH and KdpA (1;2;11). Only these three families require for activity at least one additional subunit, which lead to the hypothesis that an interaction of the additional subunit with the M_{2C} region might control the transporter activity (11).

KtrAB is a sodium dependent bacterial K^+-uptake system with KtrB as the potassium translocating subunit and KtrA as the regulatory subunit (3;12;18-21). KtrA is located on the cytoplasmic site of the membrane and is a member of the KTN/RCK- protein family (4;22). It is proposed to regulate K^+ transport by binding of ATP (23;24). It confers velocity, K^+ selectivity and Na^+ dependency to the transporter (3). The SKT protein KtrB alone transports K^+ slowly and independent of sodium ions. In addition, it transports Na^+ with a relatively low affinity (3). The structure of KtrB has been modeled according to the crystal structure of KcsA (11). Most parts were comparable to KcsA but especially the C-termini of M_{2C} and M_{2D} deviated. Crosslinking studies support the notion that the external half of KtrB is similar to that of KcsA, but also show that its cytoplasmic half is different (25). A problem in the modeling of KtrB was the structure of transmembrane stretch M_{2C}. Durell and Guy (11) devided this region into three parts: M_{2C1} to M_{2C3}. While M_{2C1} and M_{2C3} are likely to form α-helices, M_{2C2} with its above mentioned residues alanine, glycine, serine, and threonine may form a random coil or β-turn structure. The authors (11) proposed two possible models: In the first M_{2C1} and M_{2C3} span the membrane as α-helices and M_{2C2} forms a flexible linker inside the cavity just below the selectivity filter. In model 2, M_{2C1} and M_{2C2} span the membrane with the latter in a coiled conformation while according to its partial amphipathic character M_{2C3} lies on the inner surface of the membrane. In both models a salt bridge is proposed to be present between a highly conserved lysine residue in M_{2C2} (residue K325 in *Va*KtrB) and a not universally conserved aspartate residue at the C-terminus of M_{2B} (residue D222 in *Va*KtrB).

In a recent mutation study we showed the functional importance of the M_{2C2} region from *Va*KtrB for the transport mechanism (26). Point and deletion mutations led to an increased K^+ transport velocity while the affinity was mostly unaffected. The presents of KtrA did not suppress this gain of function effect. Deletions in M_{2C2} diminished the binding of KtrA to KtrB, supporting the suggestion that this region is important for the interaction of the translocating subunit KtrB with the regulatory subunit KtrA. PhoA-fusion studies showed that M_{2C2} posses a flexible structure (26). Together, these results led us to propose that region M_{2C2} forms a flexible gate controlling K^+ translocation at the cytoplasmic side of KtrB. In the present study we present evidence in support of this notion. We investigated K^+ dependent dynamic and structural properties of the M_{2C} region of *Va*KtrB by electron paramagnetic resonance (EPR), using the technique of site-directed spin labeling of single and double cysteine *Va*KtrB variants. The data allowed us to test and reject the two Durell and Guy models (11). We propose two new models, one for the open state of KtrB in the presence of K^+ ions, and one for its closed state in the absence of K^+. Both from EPR measurements and from K^+-transport studies with *Va*KtrB variants in which residues D222 and K325 were replaced, we conclude that these two residues do not form a salt bridge

.

Experimental Procedures

Strains, plasmids, and growth conditions. The strain and plasmids used in this study are listed in the supplemental table. Plasmids containing point mutations in codons of *VaktrB* were generated from plasmid pEL903-100 by PCR using the quick change mutagenesis kit from Stratagene, La Jolla, USA. Cells of *E. coli* LB2003 (27) containing plasmids pEL903-100 or its derivates were grown aerobically in medium K3 or K30 (3;28) with 0.2 % glycerol as a carbon source. The expression of *ktrB* was induced by the presence of 0.02% L-arabinose. The cells were harvested either in the late exponential growth phase (for protein purification) or at an OD_{578} of 0.8 (for transport assays).

Overproduction, purification and spin labeling of KtrB-His$_6$ variants. Cells of strain LB2003 containing plasmid pEL903 or one of its derivates were fermented in 30 L of K3 or K30 (29) medium at 37 °C in the presence of 0.2 % glycerol (v/v) and 0.02 % L-arabinose (w/v) up to an OD_{578} of 1.0-1.5. The cells were broken and the protein was solubilized with β-D-dodecylmaltoside (DDM) as previously described (26). The supernatant was incubated at a concentration of 150 mg of protein/mL of packed Ni^{2+}-NTA agarose (Qiagen, Hilden, Germany) in the presence of 10 mM imidazole in a 50 mL polypropylene column for 1 h. Subsequently, the agarose was washed with 30 volumes of buffer W, containing 200 mM NaCl, 20 mM TrisCl, pH

8, 5 mM β-mercaptoethanol, 10 % glycerol (w/v), 0.04 % DDM (w/v) plus 50 mM imidazole. To remove the β-mercaptoethanol the agarose was washed with 15 volumes of degassed buffer W without β-mercaptoethanol plus 50 mM imidazole. The spin label (1-oxyl-2,2,5,5-tetramethlpyrroline-3-methyl)-methanethiosulfonate (TRC, Toronto, Canada), dissolved at a concentration of 1 mM in the same buffer, was added to the Ni-NTA bed in order to react overnight at 4 °C with the cysteine residues. Subsequently, free spin label was washed out with 30 volumes of buffer W without β-mercaptoethanol plus 50 mM imidazole. His-tagged, spin-labeled protein was eluted with 3 volumes of buffer W without β-mercaptoethanol containing 500 mM imidazole. The protein containing samples were pooled and concentrated in a spin concentrator (Amicon Ultra-15, PLHK Ultracel-PL membrane, 100 kDa, Millipore, Billerica, USA) to 0.5 mL. The concentrates were further purified using size exclusion chromatography on a Superdex 200 10/300 column (flowrate 0.5 mL/min) in buffer W without β-mercaptoethanol. Small samples of the different fractions were diluted with an equal volume of twice concentrated sample buffer, containing 4 % SDS (w/v), 12 % glycerol (v/v), 50 mM TrisCl (pH 6,8), 2 % β-mercaptoethanol (v/v), and 0.01 % Serva blue G (w/v). The proteins in these samples were separated by SDS-polyacrylamide gel electrophoresis (29) and stained with Coomassie brilliant blue.

Reconstitution into liposomes. For the reconstitution of purified, spin-labeled proteins, liposomes were prepared from acetone/ether washed *E. coli* lipids (Avanti total lipid extract) and egg yolk L-α-phosphatidylcholine (Sigma) in a ratio of 3:1 (w/w) (30). Unilamellar, small vesicles with relatively homogenous size were prepared by suspending lipids at 20 mg/mL of 50 mM potassium-phosphate buffer, pH 7.0 and sonicating the suspension under a stream of nitrogen until transparency with a Branson 250 Sonifier II Cell Disruptor (Branson, Shelton, USA). The liposomes were then subjected to three cycles of freezing in liquid nitrogen, slow thawing at room temperature, and extrusion through a 400-nm polycarbonate filter (Avestin) (31). Subsequently, the liposomes were diluted with buffer W without DDM to 4 mg/ml and titrated with Triton X100 (Sigma) to a value just below 'detergent-saturation' point, as monitored by the turbidity of the suspension at 540 nm (32;33). The detergent-destabilized liposomes were mixed with purified, spin-labeled protein in a 1 to 30 ratio (w/w), and incubated for 30 min at room temperature under gentle agitation. In order to remove the detergent, polystyrene beads (Biobeads SM2) were added at a wet weight of 40 mg/mL and the sample was incubated for 15 min at room temparature. Fresh Biobeads SM2 (40 mg/mL) were added four times with incubations at 4 °C of 15 min, 30 min, overnight and 1 h, respectively. The beads were removed and the mixture was diluted at least 2.5-fold with the appropriate buffer in order to decrease the glycerol concentration below 4 %. After collecting the proteoliposomes by ultracentrifugation they were washed twice with the same buffer. Finally, the proteoliposomes were dissolved to 20 mg/mL and three times frozen and thawed before further use. For EPR measurements of single labled mutants buffer W without β-mercaptoethanol, glycerol and DDM was used. In order to determine distances between two spin labeled residues by EPR, the proteoliposomes were dissolved in buffer containing 200 mM triethanolamine Hepes, pH 7.5. After the EPR spectrum was taken 0.1 mM KCl was added to the samples directly before the second EPR measurement.

EPR measurements. Room temperature continuous wave (cw) EPR spectra at X-band were recorded using a Magnettech Miniscope MS200 X-band (~ 9.4 GHz) spectrometer equipped with a rectangular TE102 resonator. A sample volume of 10 µL was loaded into glass capillaries with a 0.9 mm inner diameter. The microwave power was set to 10 mW and the B-field modulation amplitude adjusted to 0.15 mT in order to avoid saturation and to obtain high signal-to-noise ratio EPR spectra.

For interspin distance determination in the range of 1-2 nm low temperature cw EPR spectra at X-band (~ 9.4 GHz) and 160 °K were recorded using a homemade EPR spectrometer equipped with a Super High Sensitivity Probehead (Bruker). Temperature stabilization was achieved by a continuous flow helium cryostat (ESR 900, Oxford Instruments) in combination with a temperature controller (ITC 503S, Oxford Instruments). The microwave power was adjusted to 0.2 milliwatt and the B-field modulation amplitude to 0.25 mT, while the magnetic field was measured by a B-NM 12 B-field meter (Bruker). Sample volumes of 30-40 µL were loaded into EPR quartz capillaries for cw EPR measurements and frozen in liquid nitrogen before insertion into the resonator.

Pulse EPR experiments (DEER) were performed at X-band (~ 9.4 GHz) and 50 °K on a Bruker Elexsys 580 spectrometer for interspin distance determination in the range of 2-6 nm. The spectrometer was equipped with a 3-mm split ring resonator (ER 4118X-MS3, Bruker) and a continuous flow helium cryostat (ESR900, Oxford Instruments) controlled by a temperature controller (ITC 503S, Oxford Instruments). All measurements were performed using the four-pulse DEER sequence:

$$\pi/2(\upsilon_{obs}) - \tau_1 - \pi\,(\upsilon_{obs}) - t' - \pi\,(\upsilon_{pump}) - (\tau_1 + \tau_2 - t') - \pi\,(\upsilon_{obs}) - \tau_2 - echo \quad (34)$$

A two-step phase cycling (+ ‹x›, - ‹x›) was performed on $\pi/2(\upsilon_{obs})$, while for all pulses at the observer frequency the ‹x› channels were applied. The dipolar evolution time is given by $t = t' - \tau_1$, whereas time t' is varied, and τ_1 and τ_2 are kept constant. Data were analyzed only for $t > 0$ with DeerAnalysis 2006 (35; 36). The resonator was overcoupled to Q ~ 100; the pump frequency υ_{pump} was set to the center of the resonator dip which coincided with the maximum of the nitroxide EPR spectrum. The observer frequency υ_{obs} was set to the low field local maximum of the absorption spectrum which resulted in a 65 MHz Offset. All experiments were realized with observer pulse lengths of 16 ns for $\pi/2$ and 32 ns for π pulses and a pump pulse length of 12 ns. Deuterium modulation was averaged by adding traces at eight different τ_1 values, starting at $\tau_{1,0}$ = 200 ns and incrementing by $\Delta\tau_1$ = 8 ns. For all DEER measurements 30-40 µl of the sample solution was filled into EPR quartz capillaries and frozen in liquid nitrogen before insertion into the resonator.

Fitting of Experimental cw EPR Spectra. Fitting of experimental cw EPR spectra detected at low temperature reveals the average interspin distance in the range of 1-2 nm using the program DipFit (37). For this purpose, the simulated dipolar broadened EPR spectra were fitted to the experimental one, and best-fit parameters for the interspin distance and distance distribution considering a Gaussian distribution of interspin distances were determined. During the fitting procedure, the *g* tensor values, the A_{xx} and A_{yy} values of the hyperfine tensor and the Lorentzian and Gaussian line width parameters were fixed. In detail, A_{xx} and A_{yy} were set to 0.52 and 0.45 mT, respectively, and the g tensor values to g_{xx} =2.0085, g_{yy} =2.0063, g_{zz}=2.0023. The A_{zz} value of the hyperfine tensor was variable. The EPR spectra were convoluted with a field-independent line shape function composed of a superposition of 28% Lorentzian and 72% Gaussian of 0.50 and 0.41 mT widths, respectively. The fraction of the singly spin-labeled component is in the range of 30-50 %.

Analysis of Experimental DEER spectra. The analysis of the experimental DEER spectra yields information about interspin distances and distance distributions in the range of 2-6 nm. Separation of the intermolecular background contribution from the intramolecular contribution elucidates interspin distances within one nanoscopic object. The experimental echo decay was background-corrected using a homogeneous three-dimensional spin distribution followed by normalization of the function. Interspin distances and distance distributions were derived by fitting the background-corrected dipolar evolution function using Tikhonov regularization as implemented in DEERAnalysis2006 (35;36).

Rotamer Library Analysis. Interspin distances and distance distributions were simulated using a pre-calculated rotamer library based on spin labeled residues as described before (38). The rotamer library comprehends 98 rotamers of MTSSL bound to cysteine which replace the individual native residues of interest. The energy and there from the population for each of the rotamers were calculated in consideration of a Lennard-Jones potential at 175 °K which is equivalent to the glass transition temperature for a water-glycerol mixture. The glass transition temperature most likely reflects the ensemble of spin label conformations obtained at 50 °K. Finally, the populations for the respective rotamer were then used as weights in the simulation of the interspin distance and distance distribution.

$^{86}Rb^+$ uptake into proteoliposomes. The uptake of $^{86}Rb^+$ by proteoliposomes was determined in principle as described in (39;40). Briefly, proteoliposomes preloaded with loading buffer (400 mM KCl, 10 mM Hepes and 5 mM N-methyl-D-glucamine, pH 7.6) were extruded through a 400 nm polycarbonate filter (Avestin) and diluted with the same buffer to 10 mg/mL. Subsequently, the extraproteosomal buffer was exchanged against uptake buffer containing 400 mM sorbitol, 10 mM Hepes and 5 mM N-methyl-D-glucamine, pH 7.6 by spinning 80 µL of the proteoliposomes through a spin desalting column preincubated with uptake buffer (Zeba Spin Desalting Columns, 7 k MWCO, 0.5 ml, Pierce). Directly afterwards 50 µL of the suspension were diluted with 150 µL uptake buffer and 5 minutes preincubated at room temperature. Uptake was started by the addition of 2.3 µCi/mL of $^{86}Rb^+$ (PerkinElmer). Samples were taken at different time points by diluting 40 µL of the suspension with 2 mL of an ice-cold 0.1 M LiCl solution and immediate filtering through a 200 nm cellulose nitrate filter (Millipore). The filter was washed twice with 2 mL ice cold 0.1 M LiCl and put into 3 mL of liquid-scintillation fluid in a 5 mL counting vial. Radioactivity was determined in a liquid scintillation counter. In parallel, the proteoliposomes remaining after the external buffer exchange step were used to determine the maximally possible $^{86}Rb^+$ uptake (100 % value). To this end 16 µM valinomycin was added to the suspension and $^{86}Rb^+$ uptake was determined as described above. In addition, uptake experiments were performed with equally treated liposomes without KtrB protein as a negative control.

Other methods. Protein concentrations were determined according to (41) or by measuring the absorbance A_{280} and by using the KtrB specific molar-extinction coefficient ε calculated from its amino acid composition. A cell suspension with an OD_{578} value of 1.0 was taken to contain 0.3 mg dry wt/mL (42). Depletion of the cells from K^+, and net K^+- uptake by K^+-depleted LB2003 cells were carried out as described in (3). Kinetics of K^+ uptake was determined by the Eadie-Hofstee method (43).

RESULTS

Sample preparation and purification of KtrB-His$_6$ variants to perform EPR measurements. From our previous studies we concluded that region M_{2C2} with its small and polar amino acids

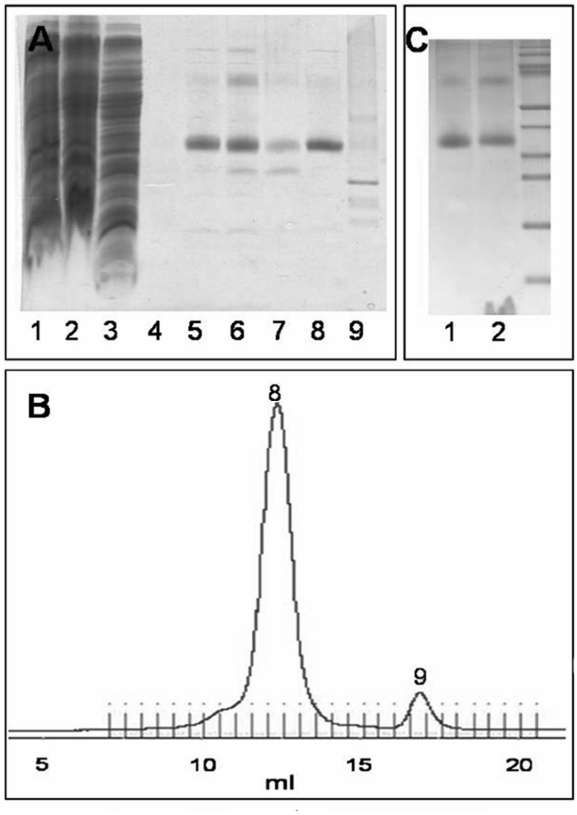

Figure 1. **Purification and reconstitution of spin-labeled KtrB$_{T318R1}$-His$_6$. A:** SDS PAGE during solubilization and purification. Lane 1: membrane fraction; lane 2: supernatant after solubilization of the membrane fraction; lane 3: flow-through of the Ni-NTA column after 1 h of binding the solubilisate to it; lane 4: flow through after spin label binding to the protein on the column and extensive washing with buffer W with 50 mM imidazole without β-mercapto-ethanol; lanes 5-7: elution-fractions E_1-E_3 of the spin-labeled protein from the Ni-NTA column with buffer W with 500 mM imidazole without β-mercaptoethanol; lane 8: spin-labeled KtrB-His$_6$ eluted at 12.5 ml via gel filtration in buffer W without imidazole and β-mercaptoethanol; 9: degradation product of KtrB separated via gel filtration at 17.5 ml. 10 µL of a sample were added per lane. **B**: Chromatogram giving A_{280} against the volume of the gel filtration of the spin-labeled KtrB-His$_6$ variant in buffer W without β-mercaptoethanol on a Superdex 200 column. Numbers 8 and 9 correspond to the fractions analyzed in lanes 8 and 9 of panel A, respectively. **C:** SDS PAGE of the reconstitution of spin-labeled KtrB variants. Lane 1: 5 µg of solubilized protein; lane 2: the theoretically equivalent amount of KtrB after reconstitution in liposomes from *E. coli* phospholipids and egg PC.

is involved in the K^+ transport process by forming a gate inside the pore region of KtrB

controlling the passage of K^+ through the protein. In order to obtain more information about the structure of the M_{2C2} region we inserted single cysteine residues into cys-less *Va*KtrB-His_6. These variants were overproduced in an active form in *E. coli* LB2003, by growing the cells at low K^+ concentrations (26). Subsequently, cw EPR measurements on purified, spin labeled and reconstituted KtrB variants were conducted. The activity of the unlabeled variants was analyzed in whole cell transport experiments by measuring net K^+ uptake by K^+-depleted LB2003 cells. Most of these variants were analyzed in the previous study, where several were found to be either inactive or their overproduction was strongly inhibited ((i.e. $KtrB_{G314C}$, $KtrB_{G316C}$, $KtrB_{G321C}$, $KtrB_{G322C}$, $KtrB_{G323C}$, and $KtrB_{K325C}$ (26)). Other variants like $KtrB_{A315C}$, $KtrB_{I324C}$ and $KtrB_{V326C}$ aggregated during overproduction or purification (data not shown). Thus, only few amino acid residues mutated to cysteines remained for the analysis of region M_{2C2} (i.e. S317C, T318C, T320C, K325C, and S327C). In addition, we examined the following variants with single cysteine exchanges: D222C (forms presumably a salt bridge with residue K325), C90 (the natural single residue in *Va*KtrB), T300C (presumably at the N-terminus of M_{2C}), M211C (an M_{2C1} residue), V331C, F339C, L340C (all M_{2C3} residues), and R343C (presumably at the C-terminus of M_{2C}). Finally, we constructed double cysteine variants in order to measure distances between the two labeled residues (i.e. D222C/T318C, D222C/S327C, M311C/T318C, T318C/V331C, and T327C/V331C). The K^+-uptake activity of most of these variants was examined in *E. coli* LB2003 as described in (3). It exhibited equal affinities and similar to increased V_{max} values compared to His-tagged KtrB or its cys-less KtrB derivative ((26) and data not shown).

The SDS PAGE of Fig. 1A documents exemplarily the solubilisation and purification of $KtrB_{T318C}$. Proteins were solubilized effectively from the cytoplasmic membrane with 1 % (w/v) of the detergent DDM (Fig. 1A, lanes 1 and 2). From the Ni-NTA affinity chromatography with its washing and labeling steps (Fig. 1A, lane 4) resulted a relative pure $KtrB_{T318R1}$-His_6 preparation (Fig. 1A, lanes 5- 7), whereas R1 indicates the bound spin label. The protein was further purified by gel filtration on a Superdex 200 10/300 column. This achieved the separation of the KtrB-variant protein from its degradation products (Fig. 1A, lanes 8 and 9, and Fig. 1B, numbers 8 and 9, respectively). Subsequently, spin labeled $KtrB_{T318R1}$-His_6 was reconstituted in a 1:30 ratio into liposomes with an efficiency of circa 80 % (Fig. 1C). The proteoliposomes were washed and dissolved in the desired buffer.

Spin labels do not affect the uptake activity of KtrB variants. The influx of $^{86}Rb^+$ into K^+-loaded proteoliposomes was measured exemplarily for some mutants in an assay similar to that described in (39;40) in order to show that spin-labeled, reconstituted KtrB-His_6 variants were active in this system. Reconstituted KtrB-His_6 served as positive control. The relatively slow $^{86}Rb^+$ uptake observed for this construct was in accordance with the findings of Albright et al. (25). Within 20 minutes 25 % of the maximum uptake was achieved (Fig. 2B). Figure 2A shows time courses of normalized $^{86}Rb^+$ uptakes into some KtrB variants containing proteoliposomes. While the control liposomes were almost inactive (Fig. 2A, diamonds), $KtrB_{S327R1V331R1}$ containing proteoliposomes were similar to the WT-KtrB (Fig. 2A, triangles and circles, respectively). The activity of $KtrB_{T318R1}$ was a factor of 1.5 lower than that of wildtype (Fig. 2A, quadrates), but was still much higher than the activity of liposomes. As shown in figure 2B influx through $KtrB_{S327R1}$ and $KtrB_{M311R1T318R1}$ was also comparable to that of the WT-KtrB, whereas uptake through $KtrB_{T318R1V331R1}$ was reduced by 50 %. We conclude that the spin-labeled variants are active and that the presence of the label neither inhibits nor activates $^{86}Rb^+$ uptake via KtrB in proteoliposomes.

Analysis of side chain mobility and polarity in membrane region M_{2C}. In order to obtain information about the orientation of single labeled cysteine residues inside the protein, room temperature EPR spectra were taken from the reconstituted samples. The inverse central line width [ΔH_{PP}^{-1}] is an indicator for the structural environment of the spin label. The higher this value, the higher is the mobility as well as the reorientational freedom of the spin label and the lower are the secondary and tertiary interactions. A comparison of the different spectra is presented in figure 3. Almost all of the spectra are dominated by an immobile component. For residues C90R1 and L340R1 the mobile component prevails. Only residues T300C and R343C show distinct mobile spectra. The ΔH_{PP}^{-1} values plotted according to (44; 45) show (Fig. 3) that the whole M_{2C} region was imbedded inside a compact structure. The found two

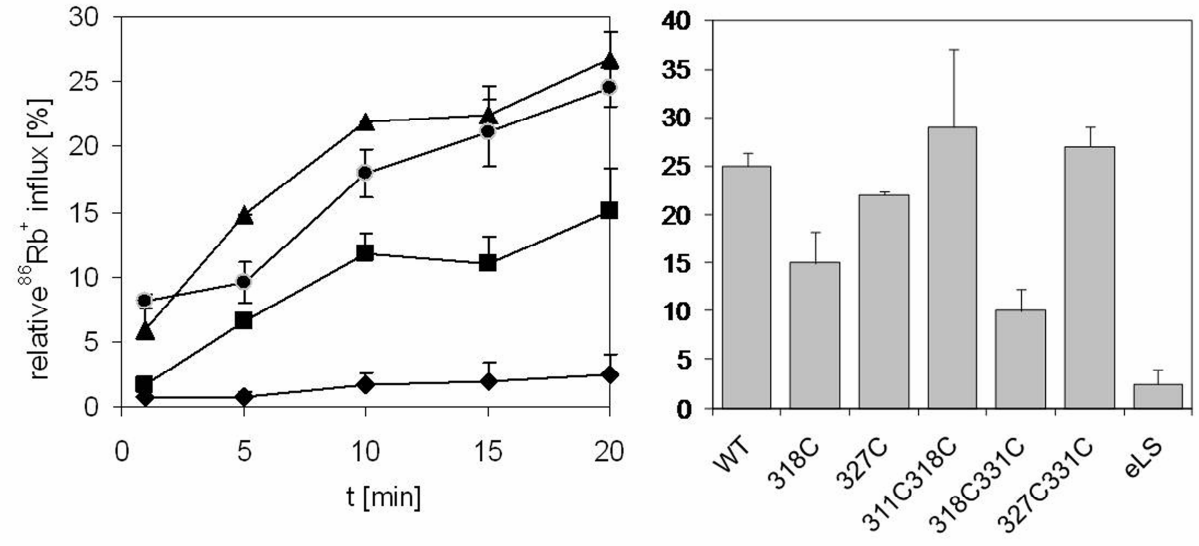

Figure 2. **$^{86}Rb^+$ uptake by proteoliposomes containing spin-labeled KtrB-His$_6$ variants. Left**: Time dependence of normalized rubidium uptake of • WT-KtrB containing protoeoliposomes, ▲ $KtrB_{S327R1V331R1}$ containing proteoliposomes, ■ $KtrB_{T318R1}$ containing proteoliposomes, and ◆ control liposomes without protein prepared according to the same procedure as proteoliposomes. **Right**: Normalized rubidium uptake after 20 minutes by proteoliposomes containing spin-labeled KtrB variants. Error bars correspond to standard deviations calculated from two independent measurements, uptakes normalized against the uptake measured after the addition of 16 µM valinomycin to the same proteoliposome preparation; eLS, control liposomes.

components in almost all spectra, however, point to flexibility of the region, since a heterogeneous distribution of the labeled residues must have been present. Only residues T300R1 and R343R1 came off the membrane, confirming that they are N- and C-terminal to the M_{2C}-transmembrane stretch, respectively.

Subsequently, those preparations with sufficient spin-labeled KtrB were frozen and measured at 160 °K to obtain the powder spectra of the corresponding samples. Hyperfine splitting A_{ZZ} values calculated from low temperature (160 °K) cw X-band EPR spectra of singly spin-labeled residues gave information about the polarity of these residues. The higher the A_{ZZ} value, the more polar is the surrounding of the spin label. As determined for transmembrane helix F of bacteriorhodopsin, an A_{zz} value of 3.7 mT corresponds to a high polarity outside the membrane and a value of 3.35 mT argues for a low

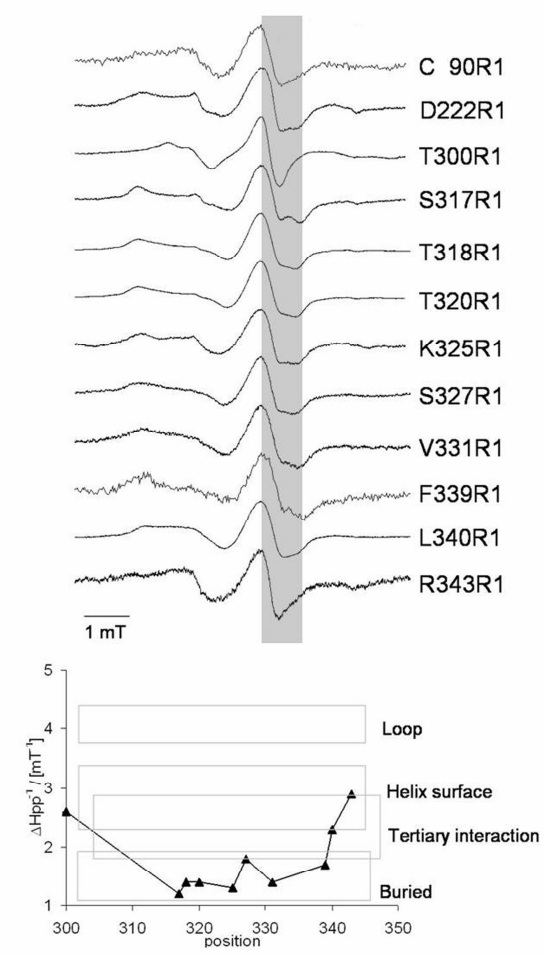

Figure 3. **Room temperature cw EPR spectra of single labeled, reconstituted KtrB variants. Top:** Observed spectra of the labeled variants. The ΔH_{pp} area is highlighted in grey. **Bottom:** ΔH_{PP}^{-1} values plotted against the position according to Mchaourab et al. (44) and Hubbel et al. (45) demonstrating the mobility and the orientation of the spin labeled residues.

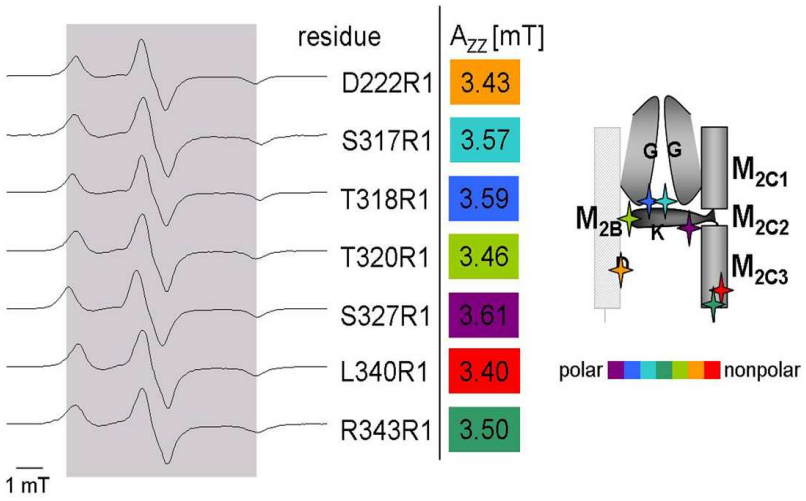

Figure 4. **Low temperature (160 °K) cw EPR spectra of singly labeled, reconstituted KtrB variants. Left:** Experimental obtained spectra of the labeled residues. The $2A_{ZZ}$ area is highlighted in grey. **Right:** Schematic illustration of how the residues could be orientated in the protein. The calculated A_{ZZ} values are plotted into a recently proposed cartoon of helices M_{2B} and M_{2C} (26). The colored stars indicate the polarity of the residues in a range from purple for polar to red for nonpolar.

polarity and a positioning in the middle of a lipid bilayer (46).

The spectra detected for the spin-labeled KtrB variants are shown in figure 4. The calculated A_{ZZ} values vary from 3.4 mT for residue L340R1 to 3.61 mT for residue V327R1. In the proposed 2- and 3-D model of *Va*KtrB (see below, figure 7, models 3 and 4) residue V327 is located in the middle of the membrane, while L340 is close to the cytoplasmic surface. Since region M_{2C} is proposed to be part of the permeation pathway, its polarity profile does not follow the profile of α-helix F of bacteriorhodopsin. The cavity of the protein should be filled with water allowing higher polarities of residues orientated to the central pore. From the detected A_{ZZ} values we conclude, that residues S317R1, T318R1 and V327R1 are oriented to the cavity and are accessible for water molecules, while residues D222R1, T320R1 and L340R1 are relative nonpolar and buried either within the protein or within the membrane phospholipids. Residue K343R1 displays an intermediate value with 3.5 mT and appears to stick just out of the membrane. A schematic illustration of how the residues could be located within the protein is shown in the right-hand part of figure 3. Exemplary measurements of singly labeled variants in the absence of both, K^+ and Na^+ by using triethanolamine Hepes, pH 7.5 did not show remarkably changes in their mobilities and their polarities, respectively (data not shown).

Table 1. **Experimental and calculated interspin distances.** Experimental interspin distances in the absence and in the presence of potassium are derived using DEERAnalysis2006 (36) and DipFit (37). Calculated interspin distances of different KtrB models using the rotamer library approach (38). Model 3 and 4 are based on model 1 (see figure 7) taking into account the distances of Columns 1 and 2, respectively.

	experimental interspin distance r (nm)		calculated interspin distance r (nm)			
	- K^+	+ K^+	model 1	model 2	model 3	model 4
D222R1/ T318R1	1.8 ± 0.1[a]	1.4 ± 0.1	2.1 2.4	1.9	1.8	1.5
D222R1/ S327R1	>1.8	>1.8	1.5	0.9 1.25	1.7	1.5 2.0
M311R1/ T318R1	3.5 ± 0.2	3.5 ± 0.2	2.3	2.0	2.9 3.7	3.0
T318R1/ V331R1	1.5 ± 0.1	1.7 ± 0.1	2.4 2.9	2.9	3.2	1.7
S327R1/ V331R1	1.1 ± 0.1	1.1 ± 0.1	0.8	1.8	1.0	0.6 1.0

[a] The fraction of the singly spin-labeled component is in the range of 30-50 %.

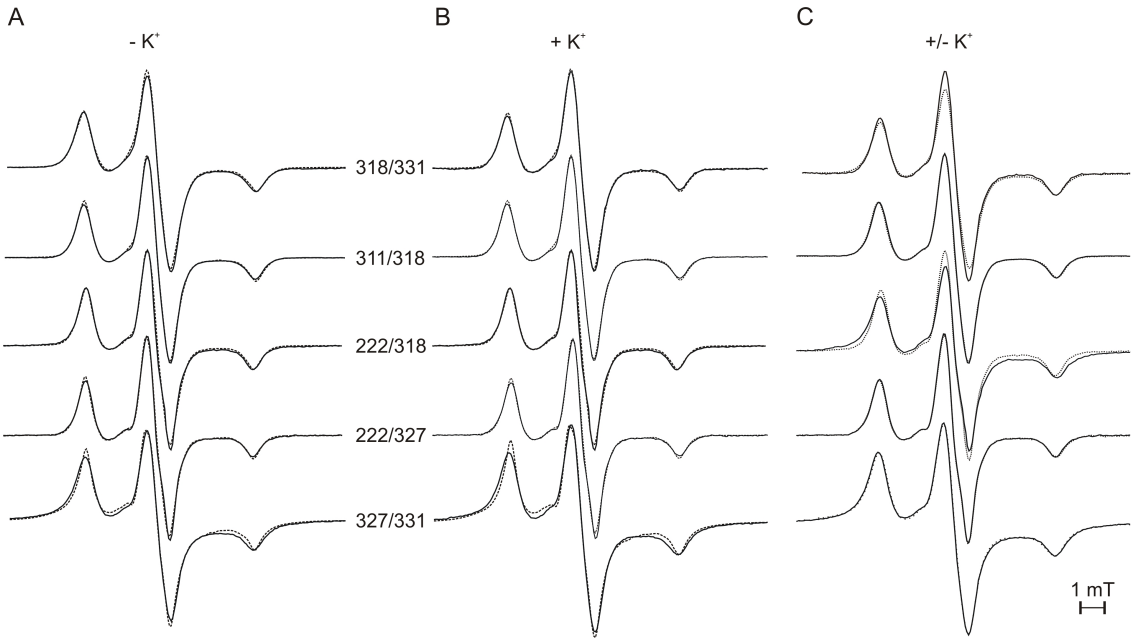

Figure 5. **Low temperature (160 °K) cw EPR spectra measured at X-band (~ 9.4 GHz) in the absence and in the presence of K^+. A-B:** Experimentally obtained spectra are represented by solid black lines and simulated EPR spectra by dashed black lines. **C**: Comparison of the observed EPR spectra in the absence (solid black lines) and in the presence of K^+ (dotted black lines), respectively. All plots are spin normalized.

Distances between spin-labeled double cysteine variants reveal K^+-dependent motions of M_{2C2}-residue T318R1. In order to reveal the structure and the movement of the subregion M_{2C2} upon the addition of potassium, interspin distances within double labeled variant molecules were obtained by using cw and pulse EPR spectroscopy at 160 °K and 50 °K, respectively. For this purpose low temperature experiments were taken in the absence and in the presence of K^+ ions, as depicted in figures 5 and 6. Mean distances of the experimental determined EPR spectra are given in table 1. For double mutant D222R1/T318R1 the interspin distance decreased from 1.8 nm (± 0.1 nm) to 1.4 nm (± 0.1 nm) upon K^+ addition. The data for T318R1/V331R1 revealed a mean distance at 1.5 nm (± 0.1 nm), which shifted to 1.7 nm (± 0.1

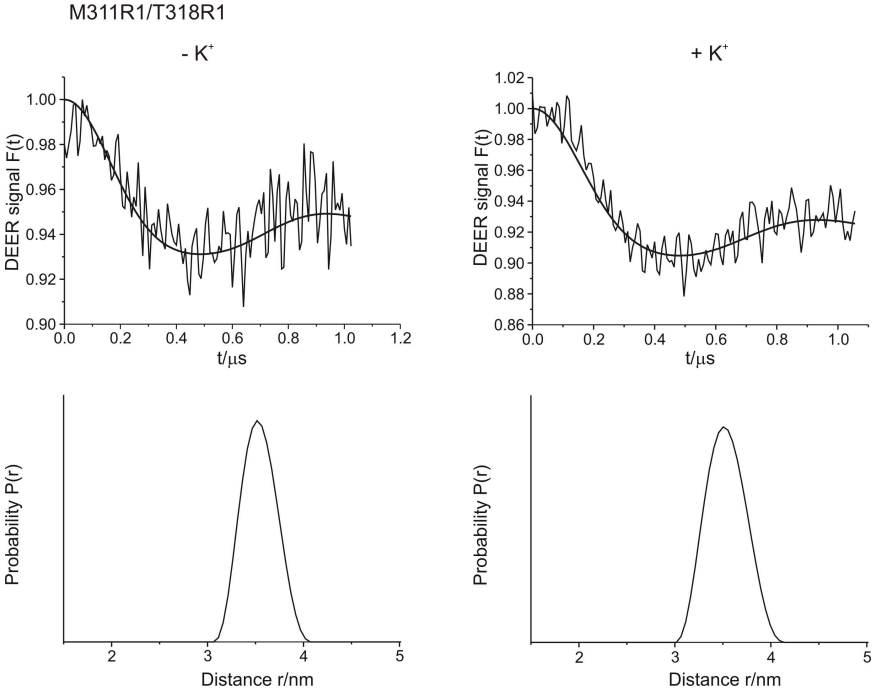

Figure 6. **DEER analysis of the double mutant M311R1/T318R1 in the absence (left) and in the presence of K^+ (right).** Above: background corrected dipolar evolution data F(t). Bottom: distance distributions P(r) obtained by Tikhonov regularization (DeerAnalysis2006) (36). Distance distributions are normalized by amplitude.

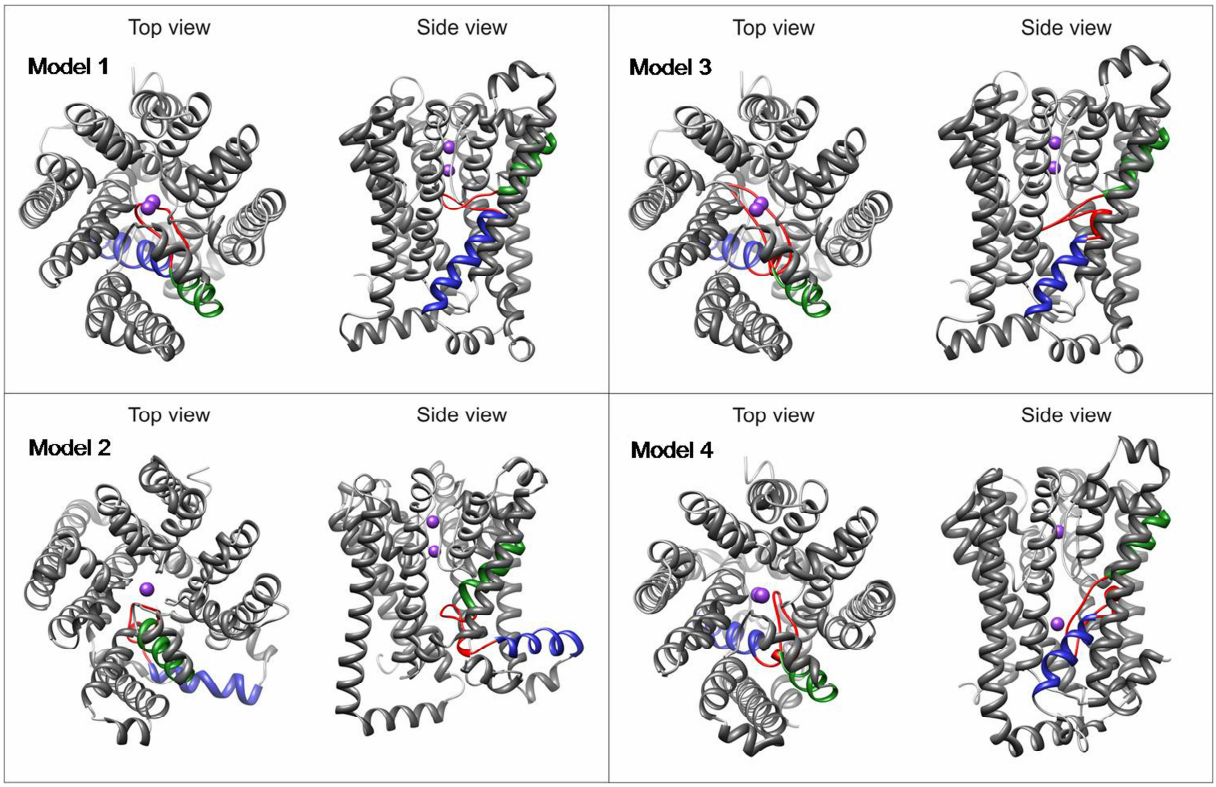

Figure 7. **Schematic representation of different KtrB models.** Models 1 and 2 are taken from (11). In model 1 M_{2C1} and M_{2C3} span the membrane together and M_{2C2} forms a loop inside the membrane. In model 2 M_{2C1} and M_{2C2} span the membrane and M_{2C3} lies as an α-helix on the cytoplasmic surface of the membrane. Models 3 (closed structure) and 4 (open structure) were generated by the rotamer library approach (38). They are based on model 1 taking into account the measured distances between double spin-labeled residues in the presence and absence of K^+ ions, respectively (table 1). Regions M_{2C1} is highlighted in green and M_{2C3} in blue, the linker region M_{2C2} in red and the potassium ions in purple. The top view is taken from the periplasm. In the side views top and bottom represent the periplasm and cytoplasm, respectively.

nm) upon K^+ activation. The interspin distance between D222R1 and S327R1 in absence and presence of K^+ lay above 1.8 nm which is equivalent to the upper limit of cw EPR spectroscopy. Due to the poor signal-to-noise ratio a pulse EPR experiment could not be realized and therefore potential changes in the interspin distance could not be resolved. In contrast, using pulse EPR spectroscopy the experimental derived interspin distances for double mutant M311R1/T318R1 exhibited distance distributions with one well defined peak centered at 3.5 nm (± 0.2 nm) both in the presence and the absence of K^+. The distance distributions were identical for S327R1/V331R1 in presence and absence of K^+, exhibiting a mean distance of 1.1 nm (± 0.1 nm). We conclude that the addition of K^+ causes a movement of M_{2C2} residue T318R1 with respect to both membrane stretch M_{2B} residue D222R1 and M_{2C3} residue V331R1, but not to the unexpectedly remote M_{2C1} residue M311R1. Under this condition, no movement was detected between residues S327R1 and V331R1.

Rotamer Library Analysis for different KtrB Models. In order to compare the distance distributions obtained by cw and pulse EPR spectroscopy with structural models for KtrB, we performed a rotamer library analysis for positions D222, M311, T318, S327 and V331 based on the two structure models from Durell and Guy (11). Figure 8 shows distance distributions derived from the rotamer library analysis. The mean interspin distances expected on the basis of these two models are compared with the experimental values in table 1. It is evident that both models are not supported by the experimental data. For model 1 the interspin distances between the chosen positions differ about 0.3-1.2 nm from the data of table 1. For model 2 the distance between D222R1 and T318R1 is correct with respect to the data without the addition of K^+, but the other distances are off by 0.6-1.5 nm. In view of these

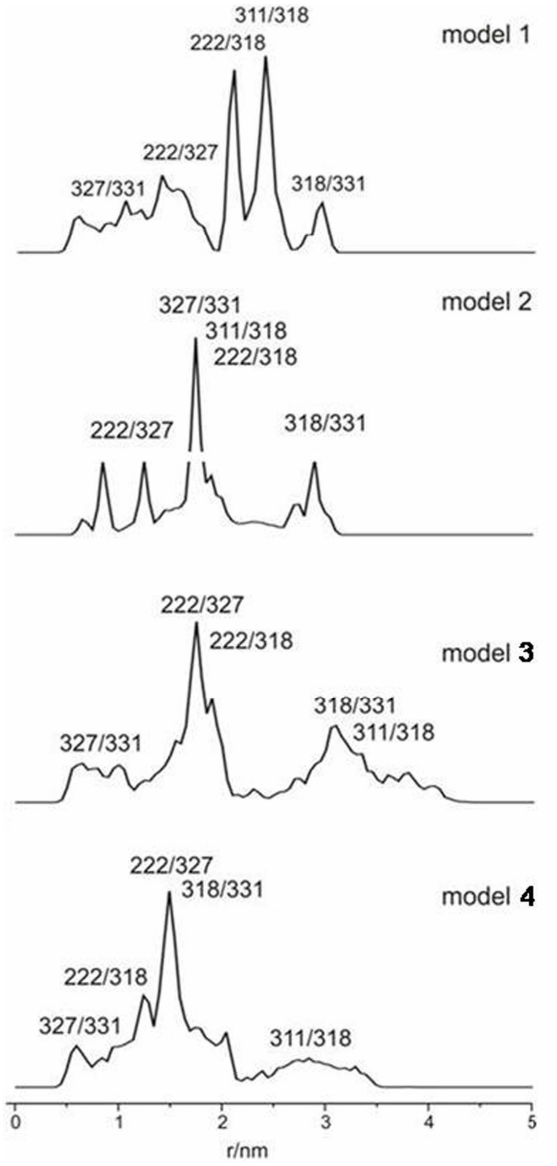

Figure 8. **Simulated interspin distance distributions of different KtrB models using the rotamer library approach (38).** Residue numbers indicate the spin label pair which contributes to the calculated distance distribution. See table 1 for the measured distances. Models 1 to 4 are described in the text and the legend to figure 7.

discrepencies we developed two additional models for the structure of KtrB by rotamer library analysis taking into account both the polarity data of single residues (figure 2) and the interspin distance data (table 1). As in model 1 we assumed that region M_{2C2} forms a flexible loop inside the membrane. In addition, we fixed the complete molecular structure except for that of M_{2C2}. Model 3 gives the closed state of KtrB in the absence of K^+ ions. In it M_{2C2} spans and thereby blocks the cavity, and points towards helices M_{1B} and M_{2B}. However, in this model the interspin distance between position T318 and V331 deviates by 1.7 nm (± 0.1 nm) from the experimental value (table 1, columns 1 and 5, respectively). Without a displacement of helix M_{2B} it is not possible to bring the residue T318 closer to residue V331. For the other double-labeled variants there is reasonable agreement between the calculated distances in model 3 and the experimental data within the limits of 0.1-0.6 nm. Model 4 represents the structure with an open M_{2C2} gate and is based on the distance measurements in the presence of K^+ ions. In this model, the region M_{2C2} is oriented alongside the cavity. The calculated distances in this model for the double-labeled variants reproduce the obtained experimental data within 0.1 to 0.5 nm (table 1, columns 2 and 6, respectively).We conclude that during the transport cycle of KtrB K^+ causes a downward movement of the linker region M_{2C2} alongside the cavity, thereby opening its gate.

No salt bridge is formed between residues D222 and K325. Durell and Guy (11) proposed for both structural models of KtrB the formation of a salt bridge between a lysine residue in M_{2C3} and an aspartate residue at the N-terminus of M_{2B}, corresponding to the *Va*KtrB residues K325 and D222, respectively. The large distance of more than 1.8 nm both in the presence and absence of K^+ between D222R1 and the two residues C-terminal to K325 located V327R1 (table 1) suggest, that a salt bridge between residues K325 and D222 is unlikely to exist. In order to test the salt-bridge hypothesis *Va*KtrB residues D222 and K325 were changed to neutral, equally charged, and pairwise to reversely charged amino acids and net K^+ uptake via the new KtrB variants into LB2003 cells was determined. A neutral amino acid at one of the two positions would avoid the formation of the putative salt bridge and could result in an increased transport activity. In contrast, an exchange of the charged amino acids against each other or the replacement of one amino acid for an equally charged amino acid should enable the formation of the salt bridge and would not effect KtrB activity. As shown in figure 9, V_{max} values of the single amino acid variants $KtrB_{D222C}$, $KtrB_{D222K}$, $KtrB_{K325C}$, $KtrB_{K325D}$, $KtrB_{K325H}$, and $KtrB_{K325Q}$ were increased. Also the double mutant $KtrB_{D222C,K325C}$ and the exchange mutant $KtrB_{D222K,K325D}$ transported K^+ significantly faster than did WT-KtrB. However, variants $KtrB_{K325R}$ and especially $KtrB_{D222N}$ showed transport activi-

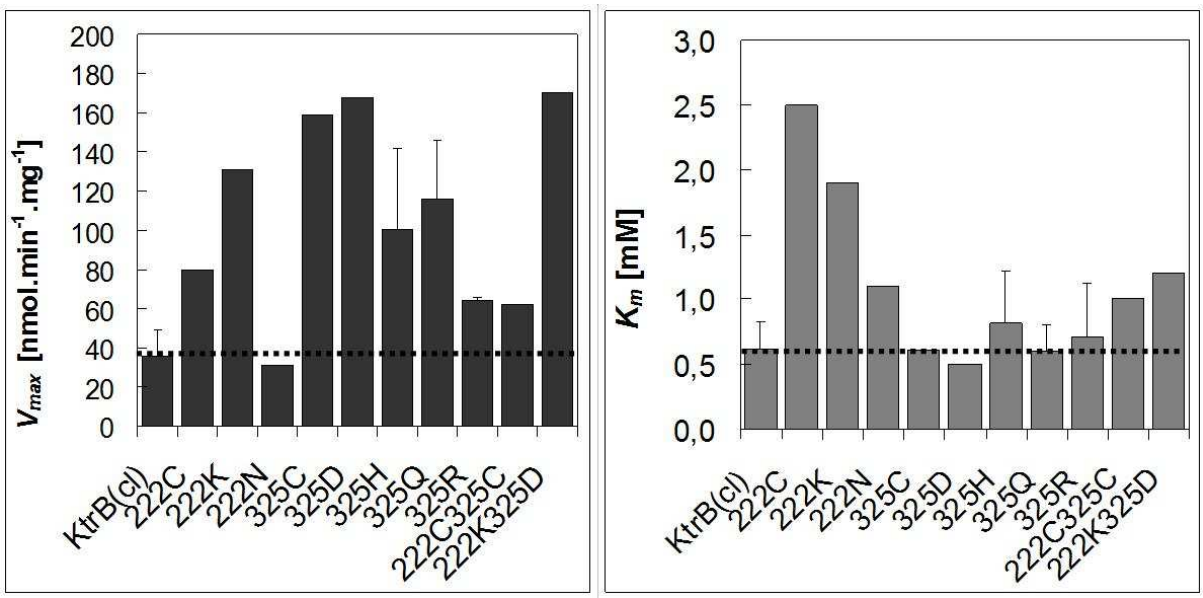

Figure 9. **Kinetic parameters of K^+ uptake by cells containing KtrB variants with single or double amino acid changes in the putative salt-bridge residues D222 and K325.** Plasmid-containing cells of strain LB2003 were grown and induced for *ktrB* expression with 0.02 % L-arabinose as described in the experimental procedures. For the K^+-uptake experiment K^+-depleted cells were suspended at 1 mg dry wt/mL of medium containing 200 mM NaHepes, pH 7.5, 0.2 % glycerol, and 0.02 % L-arabinose. The suspension was shaken at room temperature. After 10 min KCl was added at following concentrations: 0.5 mM; 1 mM; 2 mM; and 5 mM. For each data point a 1.0 mL sample was taken from the suspension and its cell K^+ content was determined by flame photometry. V_{max} and K_m were determined by the Eadie-Hofstee-method.

ties comparible to that of the wildtype. In addition, for variants $KtrB_{D222C}$ and $KtrB_{D222K}$ the affinity for potassium was decreased. Since at the one hand the uptake velocity of the exchange variant $KtrB_{D222K,K325D}$ was increased and at the other hand the mutation from the negatively charged aspartate to the neutral asparagine at position 222 had no effect, the presence of the salt bridge between *Va*KtrB residues D222 and K325 can be excluded.

DISCUSSION

In a recent publication we have shown that subregion M_{2C2} of the potassium-translocating subunit KtrB is of flexible nature (26). Point and deletion mutations in this region caused a gain of function due to a tenfold increase of V_{max} for K^+ transport. These findings led us to the hypothesis that M_{2C2} might form a gate controlling K^+ translocation at the cytoplasmic side of KtrB. However, we could not distinguish between the two models proposed by Durell and Guy (11) in the past (Fig. 7, models 1 and 2, respectively), although we preferred the first model. In order to gain more information about the structure and the dynamics of the M_{2C2} region, we performed EPR measurements in the presence and the absence of K^+ ions. Depending on the presence or absence of this ion, M_{2C2} residue T318R1 moved with respect to residues in both M_{2B} and M_{2C3}, but not with respect to residue in helix M_{2C1}, confirming that region M_{2C2} is flexible and that it may move during the K^+-transport cycle. From the interspin distances obtained from several double cysteine mutants combined with the rotamer library analysis we could exclude both models proposed by Durell and Guy (11). The distances measured varied too much from the distances predicted from the analysis (table 1, columns 3 and 4). In addition, the proposed salt bridge (11) was foreclosed by both, EPR data and transport studies with mutations in the involved amino acids. This was not amazing, because in contrast to the lysine residue (K325 in *Va*KtrB) its putative salt bridge partner (D222 in *Va*KtrB) is not conserved as a negative residue in all KtrB proteins. However, the analysis of the mobility and especially the polarity of single labeled residues as well as the above mentioned K^+-dependent movement of residue T318R1 argue in favor of the presence of a flexible linker inside the cavity of the protein as proposed in the Durell and Guy model 1 (11). The M_{2C2} region of KtrB appeared to be encircled by a compact structure since the spin mobility was limited. But

due to the high polarity calculated for some residues we also assumed that parts of M_{2C2} should by accessible for water. These data suggested that this linker lies in the cavity of the potassium permeation pathway as depicted in the right-hand side of figure 4. Hence, starting from model 1 we calculated structures for the open and a closed conformation of KtrB by rotamer library analysis (figure 7, models 3 and 4, respectively). While the open conformation in the presence of K^+ (model 4) displays good agreement with the experimental data (table 1), the distance of 1.5 nm between T318R1 and V331R1 observed in the absence of K^+ was not reflected by model 3. In order to obtain a better fit helix M_{2B} must be displaced to bring the two residues closer together. Since the two Durell and Guy structures were modeled on the basis of the KcsA-channel tetramer (9;11), we can not exclude a different arrangement of parts of KtrB. With cross-linking studies Albright et al. (25) have shown that the cytoplasmic half of KtrB differs from that of KcsA in the channel structure. They proposed several arrangements of the inner helices, leading to an expansion of the cytoplasmic part of the K^+-permeation pathway in KtrB. In addition, we can not exclude other rearrangments in KtrB during the transport cycle. In KcsA especially the bundle of M_2 helices moves considerably during the transition from the closed to the open state of the channel (47;48), and it may be that such changes also occur in KtrB during the K^+-transport cycle. Further site-directed spin labeling EPR experiments on other parts of the proposed K^+-permeation pathway will unravel additional structural features of KtrB in dependence of K^+ ions, thereby helping us to improve the existing KtrB models.

This study confirms that M_{2C2} may form a gate for K^+ permeation at the cytoplasmic side of KtrB (26). This feature distinguishes KtrB from a K^+ channel and is supposed to be transporter-specific. Deletion of M_{2C2} increases both, the V_{max} and the K_m values for K^+ transport via KtrB, but does not render KtrB into a K^+ channel. We interpret this to mean that either the deletion of the M_{2C2} region did not remove the complete gate or that KtrB contains a second gate, presumably at the periplasmic side of the membrane (26), as it is proposed for all transporters (49).

A M_{2C2} sequence as in KtrB with its small and polar amino acids is only present in SKT proteins which require at least one additional subunit for activity. Thus, Durell and Guy (1;2) proposed M_{2C2} to be of functional importance for the interaction of the subunits. We have recently shown that parts of M_{2C2} are indeed involved in the binding of KtrB to the regulatory subunit KtrA (26). This raised the question whether KtrA effects the structure and function of this region. However, transport assays combining gain of function mutants of KtrB with KtrA did not show any influence of KtrA on the activity (26). In order to further adress this question, EPR measurements as presented here should be performed in the presence of KtrA. The distances between the residues might change by that indicating a rearrangement of the structure. In face of the fact that KtrA did not suppress the effects of the mutants, we propose that KtrA does not close the M_{2C2}-gate but might constitutively open it when bound. This would explain the increased transport velocity of KtrAB compared to KtrB alone described previously (26). The transport activity for potassium should then be regulated by the KtrA subunit. EPR data on KtrAB thus might represent the open conformation of model 4 both, in the presence and the absence of potassium.

REFERENCES

1. Durell, S. R., Hao, Y., Nakamura, T., Bakker, E. P., and Guy, H. R. (1999) *Biophysical Journal* **77,** 775-789

2. Durell, S. R., Bakker, E. P., and Guy, H. R. (2000) *Biophys.J.* **78,** 188-199

3. Tholema, N., Vor der Brüggen, M., Mäser, P., Nakamura, T., Schroeder, J. I., Kobayashi, H., Uozumi, N., and Bakker, E. P. (2005) *J.Biol.Chem.* **280,** 41146-41154

4. Stumpe, S., Schlösser, A., Schleyer, M., and Bakker, E. P. (1996) K^+ circulation across the prokaryotic cell membrane: K^+-uptake systems. In Konings, W. N., Kaback, H. R., and

Lolkema, J. S., editors. *Handbook of Biological Physics, Volume 2: Transport processes in in eukaryotic and prokaryotic organelles*, Elsevier Science B.V., Amsterdam, Vol. 2, 473-500

5. Booth, I. R. (1985) *Microbiol.Rev.* **49,** 359-378

6. Epstein, W. (1986) *FEMS Microbiol.Rev.* **39,** 73-78

7. Dinnbier, U., Limpinsel, E., Schmid, R., and Bakker, E. P. (1988) *Arch.Microbiol.* **150,** 348-357

8. Schrempf, H., Schmidt, O., Kümmerlen, R., Hinnah, S., Müller, D., Betzler, M., Steinkamp, T., and Wagner, R. (1995) *Embo J.* **14,** 5170-5178

9. Doyle, D. A., Cabral, J. M., Pfuetzner, R. A., Kuo, A., Gulbis, J. M., Cohen, S. L., Chait, B. T., and MacKinnon, R. (1998) *Science* **280,** 69-77

10. Kuo, A., Gulbis, J. M., Antcliff, J. F., Rahmann, T., Lowe, E. D., Zimmer, J., Cuthberson, J., Ashcroft, F. M., Ezaki, T., and Doyle, D. A. (2003) *Science* **300,** 1922-1926

11. Durell, S. R. and Guy, H. R. (1999) *Biophys.J.* **77,** 789-807

12. Tholema, N., Bakker, E. P., Suzuki, A., and Nakamura, T. (1999) *FEBS Lett.* **450,** 217-220

13. Mäser, P., Hosoo, Y., Goshima, S., Horie, T., Eckelman, B., Yamada, K., Yoshida, K., Bakker, E. P., Shinmyo, A., Oiki, S., Schroeder, J. I., and Uozumi, N. (2002) *Proc.Natl.Acad.Sci.U.S.A.* **99,** 6428-6433

14. van der Laan, M., Gassel M, and Altendorf K (2002) *J.Bacteriol.* **184,** 5491-5494

15. Bertrand, J., Altendorf, K., and Bramkamp, M. (2004) *J.Bacteriol.* **186,** 5519-5522

16. Zhou, Y., Morais-Cabral, J. H., Kaufmann, A., and MacKinnon, R. (2001) *Nature* **414,** 43-48

17. Kato, N., Akai, M., Zulkifli, L., Matsuda, N., Kato, Y., Goshima, S., Hazama, A., Yamagami, M., Guy, H. R., and Uozumi, N. (2007) *Channels (Austin.)* 1, 161-171

18. Nakamura, T., Yuda, R., Unemoto, T., and Bakker, E. P. (1998) *J.Bacteriol.* **180,** 3491-3494

19. Kawano, M., Abuki, R., Igarashi, K., and Kakinuma, Y. (2000) *J.Bacteriol.* **182,** 2507-2512

20. Matsuda, N., Kobayashi, H., Katoh, H., Ogawa, T., Futatsugi, L., Nakamura, T., Bakker, E. P., and Uozumi, N. (2004) *J.Biol.Chem.* **279,** 54952-54962

21. Holtmann, G., Bakker, E. P., Uozumi, N., and Bremer, E. (2003) *J.Bacteriol.* **185,** 1289-1298

22. Roosild, T. P., Miller, S., Booth, I. R., and Choe, S. (2002) *Cell* **109,** 781-791

23. Albright, R. A., Vazquez Ibar, J.-L., Kim, C. U., Gruner, S., and Morais-Cabral, J. H. (2006) *Cell* **126,** 1147-1159

24. Kröning, N., Willenborg, M., Tholema, N., Hänelt, I., Schmid, R., and Bakker, E. P. (2007) *J.Biol.Chem.* **282,** 14018-14027

25. Albright, R. A., Joh, K., and Morais-Cabral, J. H. (2007) *J.Biol.Chem.* **282,** 35046-35055

26. Hänelt, I., Löchte, S., Sundermann, L., Elbers, K., Vor der Brüggen, M., and Bakker, E. P. (2010) *J.Biol.Chem.* **285,** 10318-10327

27. Stumpe, S. and Bakker, E. P. (1997) *Arch.Microbiol.* **167,** 126-136

28. Epstein, W. and Kim, B. S. (1971) *J Bacteriol.* **108,** 639-644

29. Schägger, H. and von Jagow, G. (1987) *Anal.Biochem.* **166,** 368-379

30. Driessen, A. J. and Konings, W. N. (1993) *Methods Enzymol.* **221,** 394-408

31. Mayer, L. D., Hope, M. J., and Cullis, P. R. (1986) *Biochim.Biophys.Acta* **858,** 161-168

32. Knol, J., Sjollema, K., and Poolman, B. (1998) *Biochemistry* **37,** 16410-16415

33. Knol, J., Veenhoff, L., Liang, W. J., Henderson, P. J., Leblanc, G., and Poolman, B. (1996) *J.Biol.Chem.* **271,** 15358-15366

34. Pannier, M., Veit, S., Godt, G., Spiess, H. W. (2000) *J Magn Res* **142,** 331-340

35. Jeschke, G., Bender, A., Paulsen, H., Zimmermann, H., Godt, A. (2004) *J Magn Res* **169,** 1-12

36. Jeschke, G., Chechik, V., Ionita, P., Godt, A., Zimmermann, H., Banham, J., Timmel, C. R., Hilger, D., Jung, H. (2006) *Appl Magn Reson* **30,** 473-498

37. Steinhoff, H. J., Radzwill, N., Thevis, W., Lenz, V., Brandenburg, D., Antson, A., Dodson, G., Wollmer, A. (1997) *Biophys J* **73,** 3287–3298

38. Jeschke, G., Polyhach, Y. (2007) *Phys Chem Chem Phys* **9,** 1895 –1910

39. Heginbotham, L., Kolmakova-Partensky, L., and Miller, C. (1998) *J Gen.Physiol* **111,** 741-749

40. Nimigean, C. M. (2006) *Nat.Protoc.* **1,** 1207-1212

41. Lowry, O. H., Rosebrough, N. J., Farr, A. L., and Randall, R. J. (1951) *J Biol.Chem.* **193,** 265-275

42. Bakker, E. P. and Mangerich, W. E. (1981) *J.Bacteriol.* **147,** 820-826

43. Fersht, A. (1985) *Enzyme structure and mechanism*, second edition Ed., W.H. Freeman and Company, New York, p. 475

44. Mchaourab, H. S., Lietzow, M.A., Hideg, K., Hubbell, W. L. (1996) *Biochemistry* **35,** 7692-7704

45. Hubbell, W.L., Mchaourab, H. S., Altenbach, C., Lietzow, M. A. (1996) *Structure* **4,** 779-783

46. Savitsky, A., Kühn, M., Duché, D., Möbius, K., and Steinhoff, H. J. (2004) *J. Phys. Chem. B.* **108,** 9541-9548

47. Cortes, D. M., Cuello, L. G., and Perozo, E. (2001) *J. Gen. Physiol.* **117,** 165-180

48. Uysal, S., Vásquez, V., Tereshko, V., Esaki, K., Fellouse, F. A., Sidhu, S. S., Perozo, E, Kossiakoff, A. (2009) *Proc.Natl.Acad.Sci.U.S.A.***106,** 6644-6649

49. Gadsby, D. C. (2009) *Nature Rev.Mol.Cell Biol.* **10,** 344-352

FOOTNOTES

*We thank H. Robert Guy for making the atomic coordinates of models 1 and 2 of figure 7 available to us, Gea Schuurman-Wolters and Bert Poolman for introducing I.H. to the techniques of reconstitution of KtrB into proteoliposomes and Eva Limpinsel for expert technical assistance. This work was supported by SFB431 (projects P6 and P18) from the Deutsche Forschungsgemeinschaft.

[#]Both authors contribute equally to this work.

[¶]Current address: Department of Biochemistry, University of Groningen, The Netherlands

[$]Current address: Department of Biophysical Chemistry , University of Groningen, The Netherlands

Parts of this study derived from the PhD thesis of Dr. Marc Vor der Brüggen (2007). In detail, he produced plasmids pKtrB$_{T300C}$, pKtrB$_{S317C}$, pKtrB$_{T318C}$, pKtrB$_{S327C}$, pKtrB$_{V331C}$, pKtrB$_{F339C}$, pKtrB$_{L340C}$, and pKtrB$_{R343C}$. The RT cw EPR spectra of residues C90R1, T300R1, F339R1, L340R1, and R343R1 and the LT cw EPR of R343R1 were detected by Marc Vor der Brüggen and Meike Döbber (group of Prof. H.-J. Steinhoff). The EPR spectra of residue S327R1 were taken from the master thesis of Inga Kraus (2009, under my supervision). Dorith Wunnicke of the Department of Physics, group of Heinz-Jürgen Steinhoff, performed all other EPR measurements of samples prepared by me and did first data analyses and the rotamer library analysis. Together, Dorith and I developed the two new KtrB models.

Supplemental Table 1. **Strains and plasmids used in this study**

strain/plasmid	features	reference/source
LB2003	F^- *kup1* Δ*kdpFABC5* Δ*trkA rpsL metE thi rha gal*	(1)
pEL903	pBAD18 containing *VaktrB* extended at its 3'-end with six His codons; Amp^R	(2)
pEL903-100	pEL903 encoding cys-less KtrB ($KtrB_{C90\rightarrow S}$); Amp^R	(3)
$pKtrB_{D222C}$	pEL903-100 encoding the change D→C in *ktrB* codon 222	this study
$pKtrB_{D222K}$	pEL903-100 encoding the change D→K in *ktrB* codon 222	this study
$pKtrB_{D222N}$	pEL903-100 encoding the change D→N in *ktrB* codon 222	this study
$pKtrB_{T300C}$	pEL903-100 encoding the change T→C in *ktrB* codon 300	this study
$pKtrB_{G314C}$	pEL903-100 encoding the change G→C in *ktrB* codon 314	(3)
$pKtrB_{A315C}$	pEL903-100 encoding the change A→C in *ktrB* codon 315	(3)
$pKtrB_{G316C}$	pEL903-100 encoding the change G→C in *ktrB* codon 316	(3)
$pKtrB_{S317C}$	pEL903-100 encoding the change S→C in *ktrB* codon 317	(3)
$pKtrB_{T318C}$	pEL903-100 encoding the change T→C in *ktrB* codon 318	(3)
$pKtrB_{G321C}$	pEL903-100 encoding the change G→C in *ktrB* codon 321	(3)
$pKtrB_{G322C}$	pEL903-100 encoding the change G→C in *ktrB* codon 322	(3)
$pKtrB_{G323C}$	pEL903-100 encoding the change G→C in *ktrB* codon 323	(3)
$pKtrB_{I324C}$	pEL903-100 encoding the change I→C in *ktrB* codon 324	(3)
$pKtrB_{K325C}$	pEL903-100 encoding the change K→C in *ktrB* codon 325	(3)
$pKtrB_{K325D}$	pEL903-100 encoding the change K→D in *ktrB* codon 325	(3)
$pKtrB_{K325H}$	pEL903-100 encoding the change K→H in *ktrB* codon 325	(3)
$pKtrB_{K325Q}$	pEL903-100 encoding the change K→H in *ktrB* codon 325	(3)
$pKtrB_{K325R}$	pEL903-100 encoding the change K→R in *ktrB* codon 325	(3)
$pKtrB_{V326C}$	pEL903-100 encoding the change V→C in *ktrB* codon 326	(3)
$pKtrB_{S327C}$	pEL903-100 encoding the change S→C in *ktrB* codon 327	(3)
$pKtrB_{V331C}$	pEL903-100 encoding the change V→C in *ktrB* codon 331	this study
$pKtrB_{F339C}$	pEL903-100 encoding the change F→C in *ktrB* codon 339	this study
$pKtrB_{L340C}$	pEL903-100 encoding the change L→C in *ktrB* codon 340	this study
$pKtrB_{R343C}$	pEL903-100 encoding the change R→C in *ktrB* codon 343	this study
$pKtrB_{D222CT318C}$	pEL903-100 encoding the changes D→C in *ktrB* codon 222 and T→C in ktrB codon 318	this study
$pKtrB_{D222CS327C}$	pEL903-100 encoding the changes D→C in *ktrB* codon 222 and S→C in ktrB codon 327	this study
$pKtrB_{D222KK325D}$	pEL903-100 encoding the changes D→K in *ktrB* codon 222 and K→D in ktrB codon 325	this study
$pKtrB_{M311CT318C}$	pEL903-100 encoding the changes M→C in *ktrB* codon 311 and T→C in ktrB codon 318	this study
$pKtrB_{T318CV331C}$	pEL903-100 encoding the changes T→C in *ktrB* codon 318 and V→C in ktrB codon 331	this study
$pKtrB_{S327CV331C}$	pEL903-100 encoding the changes S→C in *ktrB* codon 327 and V→C in ktrB codon 331	this study

REFERENCES

1. Stumpe, S. and Bakker, E. P. (1997) *Arch.Microbiol.* **167,** 126-136

2. Tholema, N., Vor der Brüggen, M., Mäser, P., Nakamura, T., Schroeder, J. I., Kobayashi, H., Uozumi, N., and Bakker, E. P. (2005) *J.Biol.Chem.* **280,** 41146-41154

3. Hänelt, I., Löchte, S., Sundermann, L., Elbers, K., Vor der Brüggen, M., and Bakker, E. P. (2010) *J.Biol.Chem.* **285,** 10318-10327

Chapter V

V

OUTLOOK

OUTLOOK

In the past investigations on the K^+ translocating subunit KtrB of the Na^+-dependent K^+ transport system Ktr from *Vibrio alginolyticus* mainly concentrated on its function. By mutagenesis studies on the putative selectivity filter sequences of KtrB one conserved glycine residue per p-loop was identified forming a simpler selectivity filter than the K^+ channel KcsA. It was shown that the B subunit in the absence of KtrA transports K^+ independent of Na^+ but with a lower velocity. In addition, it transports sodium ions but with a lower affinity than that for potassium ions (1).

The structural information about the B subunit mainly derived from sequence alignments of the KtrB with the KcsA sequence. While most parts were predicted to be similar to the KcsA M_1PM_2-motifs especially the sequences of the cytoplasmic halves of M_{2C} and M_{2D} differed (2;3). These structural differences were predicted to compose some transporter-specific features. Positively charged amino acids in M_{2D} recently were shown to be essential for transporter activity (4). Less is known about the structure and function of M_{2C}. While the first (M_{2C1}) and the third (M_{2C3}) part of this helix can be modeled as α-helices, M_{2C2} with its small and polar amino acids rather forms a random coil or β-turn structure. According to these structural predictions, two models of KtrB were proposed. In the first model, M_{2C1} and M_{2C3} span the membrane as α-helices, while M_{2C2} forms a loop that fills the cavity just beneath the selectivity filter. In the second model, M_{2C1} and M_{2C2} span the membrane with M_{2C2} adopting a coiled conformation. According to its amphipathic character M_{2C3} lies on the inner surface of the membrane (2).

The studies presented in this thesis mainly concentrated on this M_{2C} region. Point mutations and partial to complete deletions in M_{2C2} led to a gain of function. The uptake velocity for K^+ was significantly increased while the affinity was decreased for only some deletion variants. The Na^+ uptake was increased for at least deletion variant $KtrB_{\Delta 326\text{-}328}$. In addition, intensive PhoA fusion studies have shown the flexible nature of M_{2C2}. These data were interpreted in a way that M_{2C2} forms a flexible gate controlling K^+ translocation at the cytoplasmic side of KtrB (5). By cw and DEER EPR measurements on spin-labeled residues, the structural properties of M_{2C} were further analyzed. The data confirmed that M_{2C2} forms a flexible loop positioned in the cavity of the protein. From EPR measurements in the presence and absence of K^+ two structural models were developed, one in an open and the other one in a closed conformation. The already existing models of KtrB have been excluded by these modelings (2). In the open conformation, M_{2C2} is oriented alongside the cavity, while it blocks the cavity in the closed conformation. A downward movement of the linker region M_{2C2} in the presence of K^+ was proposed, thus enabling its passage through the KtrB protein. Since such a flexible gate is missing in the KcsA potassium channel, this sorting mechanism is interpreted as a transporter-specific feature. In general, transporters are proposed to contain two gates to enable an occluded state of the transported substrate (here K^+) (6). M_{2C2} may form the gate of KtrB at its cytoplasmic side.

However, X-ray crystallography on KtrB is indispensable to get more detailed information about its structure. Crystal structures in the presence and absence of K^+ would be a great benefit to propose a gating mechanism. Additional EPR measurements on distinct residues chosen from such structures would help to further characterize the gating mechanism. In addition, electrophysiology measurements on reconstituted wild-type protein and KtrB variants as produced in the present studies would yield further insides into the functional properties of KtrB. M_{2C2} could represent a backflow barrier inside KtrB, which hinders the flow of potassium along its gradient from the cytoplasm to the external side. From the models presented in this thesis one could conclude that the linker cannot open to the external side because of sterical hindrance with the structure of the selectivity filter. KtrB might be an inwardly rectifying transporter due to this linker region. If this is the case, the movement of this region to open the permeation pathway could be explained by simple electrostatic repulsion between potassium ions coming from the outside and the highly conserved, positively charged lysine residue in M_{2C2}. Such repulsion could be promoted by the closing of a so far unknown gate at the extracellular side of KtrB. This hypothesis would also explain why the deletion of M_{2C2} led to an increase in V_{max}. The opening of M_{2C2} was omitted, which increased the uptake velocity. The mobility analysis of EPR data of singly labeled residues indicated a very high fitting accuracy of M_{2C2} inside the protein structure with only little space for variations. Very small and conservative exchan-

ges, which also resulted in a gain of function, might have displayed a half-open conformation, since the perfect fit of the closed conformation was avoided by the mutations. In order to further investigate this hypothesis the electrophysiological properties of wildtype protein and the variants should be analyzed to gain detailed information on ion selectivity and conductance. However, electrophysiology studies performed so far failed. The current of KtrB could be too low to be detected by black-lipid bilayer measurements. A newly developed method of solid supported membrane consisting of an alkanethiol monolayer (Thiol) with a lipid monolayer (PC) on top (SSM), which were shown to be more sensible for other transport systems like PutP (personal communication K. Fendler and (7)), could be worth trying.

In addition, the deletion studies on M_{2C2} of KtrB in presence of KtrA have shown that some deletions diminished the binding of KtrA to KtrB. However, bound KtrA did not affect the gain of function of KtrB variants (5). In future studies one should analyze the importance of KtrA for both, the structure of the M_{2C2} region and the function of the KtrAB transport system. As discussed in this thesis, KtrA might open the M_{2C2} gate enabling the faster flow of K^+ through the pore. With respect to the structure of the M_{2C2} region similar EPR measurements as presented in this thesis should be performed in presence of KtrA. The orientation of M_{2C2} in the presence and absence of K^+ should be analyzed. A constitutive opened gate could be present. Under this condition, the cytoplasmic half of the system might be controlled by structural changes in KtrA and no longer by the M_{2C2} region. However, opening and closing of the transporter could also be a more dynamic process in a cell. KtrA bound to M_{2C2} of KtrB could open the gate, while the separation of KtrA from KtrB could close the M_{2C2} gate again. Both, conformational changes in KtrA or the binding of KtrA to KtrB should be regulated by an intracellular signal/ ligand. In order to further investigate the regulation of KtrA and/or the KtrAB system a specific K^+ transport assay should be developed. The rubidium influx assay presented in this thesis is based on channeling not on transporting. To my knowledge no assay is present so far to study K^+ transporter activity in vitro. Such an assay would for example enable a fast screening for the influence of different nucleotides like ATP, NAD^+ and NADH on transporter activity and might cast some light on the regulation of KtrA and the KtrAB system. From that knowledge further EPR measurements could follow to analyze structural changes in the presence or the absence of regulating nucleotides. However, X-ray crystallography on KtrAB would be the best alternative to gain detailed structural information of the complex. Such a result will also settle the question, whether the KtrAB complex possesses an 8:2 (8) or a 16:2 stoichiometry (my preliminary data).

As discussed in detail in the general introduction, a M_{2C2}-like structure might also be present in KdpA and TrkH since a similar amino acid sequence is conserved among these transporter subunits (9). The cytoplasmic gate, which is also involved in the binding of an additional regulatory subunit (here KtrA), might be a general feature of these transporters. In order to verify this hypothesis, similar assays as presented and discussed in this thesis should be performed with KdpA and TrkH.

REFERENCES

1. Tholema, N., Vor der Brüggen, M., Mäser, P., Nakamura, T., Schroeder, J. I., Kobayashi, H., Uozumi, N., and Bakker, E. P. (2005) *J.Biol.Chem.* **280,** 41146-41154

2. Durell, S. R. and Guy, H. R. (1999) *Biophys.J.* **77,** 789-807

3. Durell, S. R., Hao, Y., Nakamura, T., Bakker, E. P., and Guy, H. R. (1999) *Biophysical Journal* **77,** 775-789

4. Kato, N., Akai, M., Zulkifli, L., Matsuda, N., Kato, Y., Goshima, S., Hazama, A., Yamagami, M., Guy, H. R., and Uozumi, N. (2007) *Channels (Austin.)* **1**, 161-171

5. Hänelt, I., Löchte, S., Sundermann, L., Elbers, K., Vor der Brüggen, M., and Bakker, E. P. (2010) *J.Biol.Chem.* **285,** 10318-10327

6. Gadsby, D. C. (2009) *Nature Rev.Mol.Cell Biol.* **10,** 344-352

7. Schulz, P., Garcia-Celma, J.J., and Fendler, K. (2008) *Methods* **46,** 97-103

8. Albright, R. A., Vazquez Ibar, J.-L., Kim, C. U., Gruner, S., and Morais-Cabral, J. H. (2006) *Cell* **126,** 1147-1159

9. Durell, S. R., Bakker, E. P., and Guy, H. R. (2000) *Biophys.J.* **78,** 188-199

Zeit, Danke zu sagen!

Zu allererst möchte ich mich herzlich bei meinem Doktorvater Prof. Dr. Evert P. Bakker bedanken. Sie haben an mich geglaubt und mir die Möglichkeit gegeben, an diesem spannenden Projekt zu arbeiten. Sie haben mir die Freiheit gelassen, meine eigenen Ideen zu verwirklichen und standen mir doch stets mit Rat und Tat zu Seite. Besonders dankbar bin ich Ihnen auch, weil Sie mir sowohl den Aufenthalt an der Universität Groningen als auch den Besuch diverser Konferenzen ermöglicht haben. Diese haben nicht nur meinen wissenschaftlichen Horizont erheblich erweitert.

Herrn Prof. Dr. Karlheinz Altendorf danke ich für die Übernahme des Co-Referats. Besonders aber bedanke ich mich für die Möglichkeit in Ihrer Arbeitsgruppe promoviert haben zu dürfen und bis zum heutigen Tag auch bei Ihnen stets ein offenes Ohr gefunden zu haben.

Herrn Prof. Dr. H.-J. Steinhoff schulde ich meinen Dank dafür, dass sämtliche ESR-Messungen in seiner Arbeitsgruppe Makromolekülstruktur durchgeführt werden durften.

Liebe Dorith, herzlichsten Dank für Dein unermüdliches Messen, Deine Geduld und Deinen besonders zum Schluss sehr großen Einsatz, um die Fertigstellung dieser Arbeit zu ermöglich. Meike, auch Dir ein herzliches Dankeschön fürs Legen der noch holprigen, aber doch wichtigen Grundsteine.

Prof. Dr. Bert Poolman, Prof. Dr. Dirk-Jan Slotboom, Gea Schuurman-Wolters und allen anderen Mitgliedern der Arbeitsgruppe Enzymology der Universität Groningen danke ich für die schöne und sehr lehrreiche Zeit in ihrer Abteilung. Das Erlernte war mir eine wichtige Basis für die gesamte Promotion.

Mein nicht mehr vorhandenes Labor 118 - allen voran Eva Limpinsel, aber natürlich auch Marc, Nadine, Corinna, Sara, Lea, Inga, Katharina und all die anderen - ich danke Euch für die fruchtbare Zusammenarbeit, die vielen schönen Stunden und die, wenn nötig, aufmunternden Worte.

Ihr lieben, übriggebliebenen Mibis- Kerstin, Dorthe, Monika, Giesela, Ulla, Johanna, Roland, Jörg, Petra, Brigitte, Gabi, Sabrina und Vera- ich danke Euch von Herzen für eine tolle Zeit! Kerstin und Dorthe, danke für viele wissenschaftliche Diskussionen, aber auch und vor allem für Eure freundschaftliche Verbundenheit. Monika, Giesela, Johanna und Roland, Euch danke ich besonders für den Beistand in schwereren Stunden. Jörg und Gabi, tausend Dank fürs schnelle und bereitwillige Korrekturlesen, aber auch für hilfreiche Hinweise während meiner Promotion!

Meine lieben Freunde, danke, dass Ihr mich von Zeit zu Zeit daran erinnert habt, dass es noch so viele andere, tolle Dinge auf dieser Welt gibt. Es ist schön zu wissen, dass es Euch gibt!

Mein größter Dank allerdings gilt meiner Familie und natürlich Thomas. Ihr wart stets für mich da, habt mich von Zeit zu Zeit geerdet und auch so manches Mal getröstet und wieder aufgebaut. Mit so tollen Menschen an seiner Seite, hat man das Gefühl, einfach Alles schaffen zu können! Danke!

Thomas, ich danke Dir für Deine uneingeschränkte Liebe!

Lasst mich das, was Ihr alle mir gegeben habt, mit Albert Einstein sagen:

„Ein Freund ist ein Mensch, der die Melodie deines Herzen kennt und sie dir vorspielt, wenn du sie vergessen hast.“

CURRICULUM VITAE

Personal data

Inga Hänelt
Lange Str. 67
49080 Osnabrück

born: 02.10.1980 in Osnabrück
nationality: German
single

Work experience

Since 01/04/2010	Post-doctoral position at the Department of Biochemistry, University of Groningen, The Netherlands
Since 01/05/2006	Doctoral thesis in biological science at the Department of Microbiology in the research group of Prof. Evert P. Bakker, University of Osnabrück Ph.D. thesis: "The role of the M_{2C} region of the K^+ translocating subunit KtrB of the Ktr system of *Vibrio alginolyticus*"

Education

07/2004 – 03/2005	Diploma thesis at the Department of Microbiology, University of Osnabrück with Prof. Dr. E.P. Bakker: "The KtrAB complex of the K^+ uptake system Ktr of *Vibrio alginolyticus"*
10/2000 – 03/2005	Biology studies at the University of Osnabrück, major subjects: microbiology, biochemistry, ecology degree: biologist (diploma)
10/2002 – 09/2005	Mathematic and biology studies to receive a teaching certification at the University of Osnabrück, major subjects: main courses in didactics and mathematics, ecology, zoology and psychology, pree-degree as teacher

College education

08/1994 – 06/2000	Graf-Stauffenberg-Gymnasium Osnabrück, general qualification for university entrance (Abitur)

Erklärung über die Eigenständigkeit der erbrachten wissenschaftlichen Leistung

Ich erkläre hiermit, dass ich die vorliegende Arbeit ohne unzulässige Hilfe Dritter und ohne Benutzung anderer als der angegebenen Hilfsmittel angefertigt habe. Die aus anderen Quellen direkt oder indirekt übernommenen Daten und Konzepte sind unter Angabe der Quelle gekennzeichnet.

Bei der Auswahl und Auswertung folgenden Materials haben mir die nachstehend aufgeführten Personen in der jeweils beschriebenen Weise unentgeltlich geholfen.
1. Die SEC-LS/UV/RI-Messungen wurden in Zusammenarbeit mit Prof. Dr. Dirk-Jan Slotboom in der Abteilung Biochemie, Universität Groningen, Niederlande durchgeführt.
2. Die für KtrB angewandte Rekonstitutionsmethode wurde mir von Gea Schuurman-Wolters und Bert Poolman, Abteilung Biochemie, Universität Groningen, Niederlande gelehrt.
3. Die in dieser Arbeit gezeigten PhoA-, GFP-, und LacZ-Fusionsstudien wurden von Dr. Marc Vor der Brüggen (2007) und Sara Löchte (2008) durchgeführt.
4. Diverse Plasmide wurden wie aufgeführt von Marc Vor der Brüggen (2007), Sara Löchte (2008), Lea Sundermann (2008) und Katharina Elbers (2009) erstellt (alle Abteilung Mikrobiologie, Arbeitsgruppe E. P. Bakker).
4. Lea Sundermann und Katharina Elbers haben im Rahmen ihrer Diplom- bzw. Bachelorarbeit die im Einzelnen in Kapitel III aufgeführten Wachstums- und K^+-Transportversuche durchgeführt, K. Elbers hat desweiteren benannte Co-Reinigungen von KtrAB-Derivaten durchgeführt.
5. Studien an KtrB-Deletionsvarianten wurden von Eva Limpinsel und Prof. Dr. Evert P. Bakker durchgeführt.
6. Die ESR-spektrospkopischen Messungen wurden in Kooperation mit der Arbeitsgruppe von Prof. Dr. H.-J. Steinhoff „Experimentalphysik Makromolekülstruktur“, Fachbereich Physik der Universität Osnabrück von Dr. Meike A. Müller-Trimbusch und insbesondere Dorith Wunnicke durchgeführt. Alle in dieser Arbeit gezeigten Spektren wurden mit Gerätschaften der AG Steinhoff aufgenommen, dokumentiert und anschließend in erster Instanz unentgeltlich bewertet (involvierte Personen: Prof. Dr. H.-J. Steinhoff , Dr. Meike A. Müller Trimbusch und Dorith Wunnicke). Einzelne Spektren entstammen wie in Kapitel IV aufgeführt, der Dissertation von Dr. Marc Vor der Brüggen sowie der Masterarbeit von Inga Kraus.

Weitere Personen waren an der inhaltlichen materiellen Erstellung der vorliegenden Arbeit nicht beteiligt. Insbesondere habe ich hierfür nicht die entgeltliche Hilfe von Vermittlungs- bzw. Beratungsdiensten (Promotionsberater oder andere Personen) in Anspruch genommen. Niemand hat von mir unmittelbar geldwerte Leistungen für Arbeiten erhalten, die im Zusammenhang mit dem Inhalt der vorgelegten Dissertation stehen.

Die Arbeit wurde bisher weder im In- noch im Ausland in gleicher oder ähnlicher Form einer anderen Prüfungsbehörde vorgelegt.

(Ort, Datum) (Unterschrift)